Centre for Ore Deposit and Exploration Studies

Proterozoic sediment-hosted base metal deposits

AMIRA/ARC Project P.384
Report No.1

University of Tasmania

Contents

Introduction

PROJECT OBJECTIVES

1. To determine the primary geological, geochemical and structural controls on the location and timing of base metal mineral deposits in sedimentary basins.
2. To understand the chemical and hydrological evolution of metalliferous brines in selected Proterozoic sedimentary basins of Australia.
3. To develop basin metallogenic models and specific ore deposit models that may be used in the exploration for large-tonnage base-metal ore deposits.

RESEARCH FRAMEWORK

This research project involves a multi-disciplinary approach using regional geological, geophysical and structural studies, brine chemical modelling and geochemical and isotopic halo studies to provide a foundation on which to build a network of exploration criteria and ore deposit models for major sediment-hosted base metal deposits.

The project consists of three research modules as outlined below:

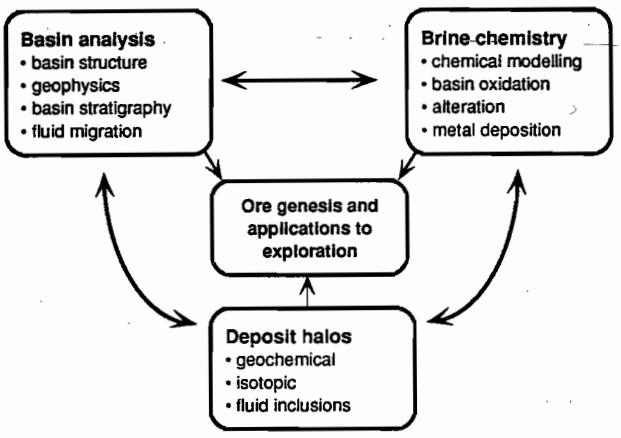

THIS REPORT

This is the first major progress report on the project and covers the six-month period from May to October 1992. Very good progress has been achieved in all three modules.

M1: Basin Analysis

- David Leaman reports on a regional geophysical analysis of basic architecture in the Southern McArthur basin, surrounding the HYC deposit.
- Richard Keele and Jamie Rogers provide a preliminary report on structural mapping in the Southern McArthur Basin.

M2: Deposit Halos

- Peter McGoldrick reports on progress to date in the geochemical study of the Lady Loretta halo.

M3: Brine Chemistry

- David Cooke has undertaken initial computer modelling on fluid geochemistry of sedimentary brines to simulate potential ore-forming conditions for sediment-hosted Pb–Zn deposits.

Important data and conclusions are already emerging from this project which have significant implications for exploration and will be discussed in detail at the November meeting. Progress in the first six months of the project has been very encouraging and I would like to acknowledge the excellent work by the CODES research team and the cooperation provided by the BMR and sponsor companies.

Ross Large
Director

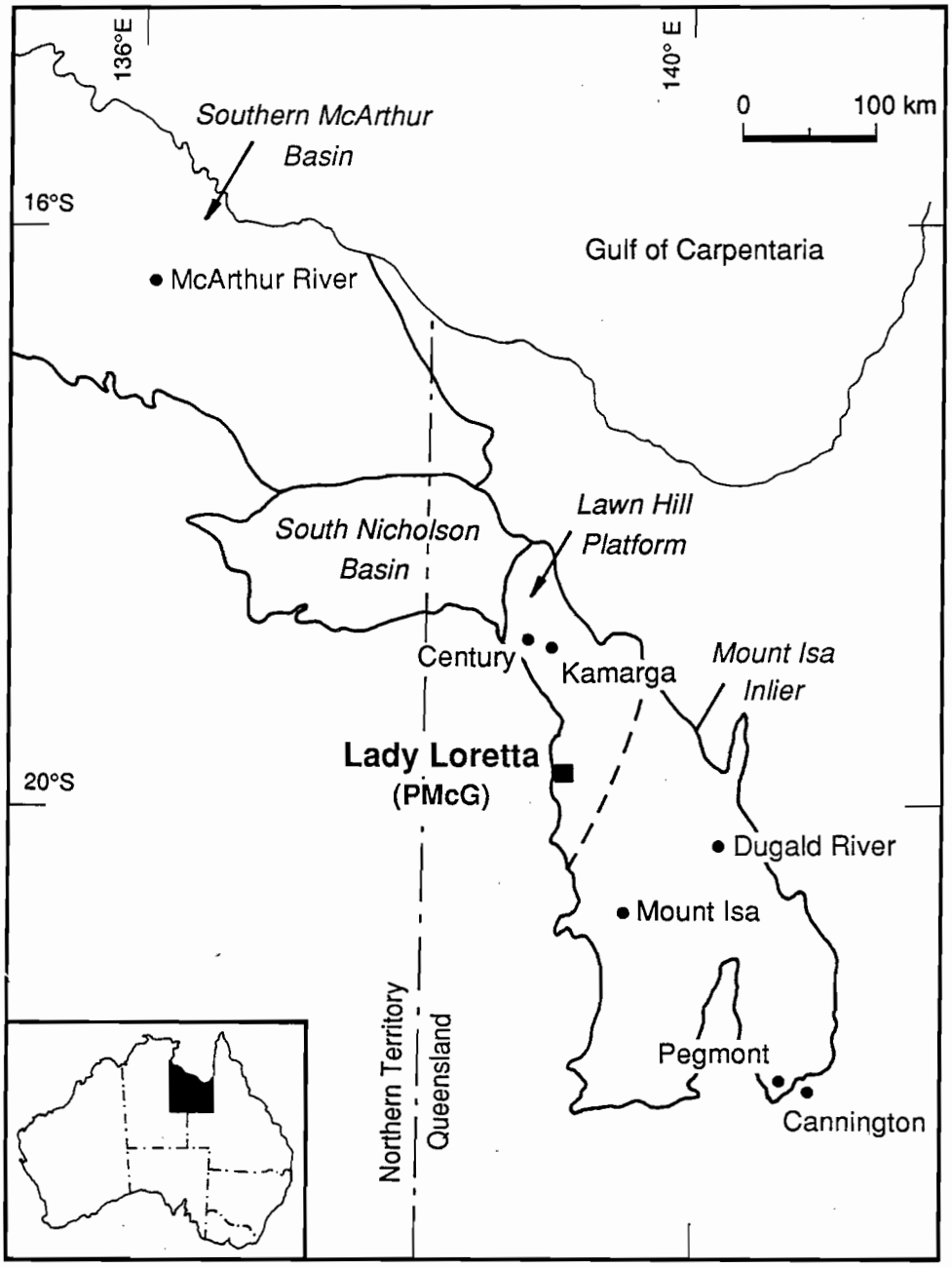
136°E
140° E
0
100 km
Southern McArthur
Basin
16°S
Gulf of Carpentaria
McArthur River
South Nicholson
Basin
Lawn Hill
Platform
Century
Kamarga
Mount Isa
Inlier
Lady Loretta
(PMcG)
20°S
Dugald River
Mount Isa
Pegmont
Cannington
Northern Territory
Queensland

Geologic and structural setting of study areas (from NTGS 1:250 000 metallogenic map series, Calvert Hills, 1989).

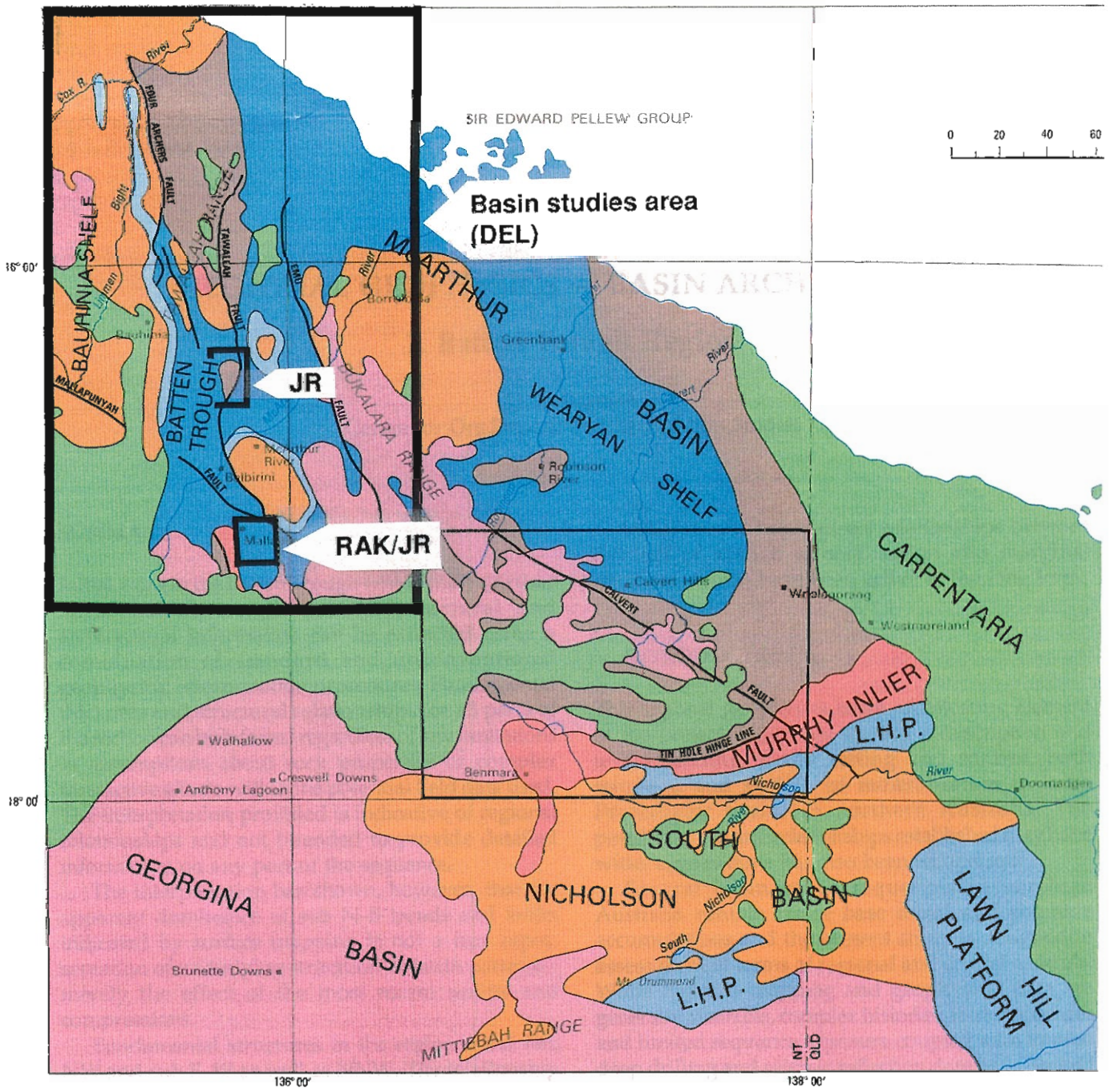

EARLY CRETACEOUS

EARLY CAMBRIAN

PROTEROZOIC

- *Roper and South Nicholson group*
- **Middle**
  - *Nathan Group*
  - *Lawn Hill Platform sequence*
  - *McArthur Group*
  - *Tawallah Group*
- **Early**
  - *Murphy Inlier sequence*

REGIONAL GEOPHYSICS — BASIN ARCHITECTURE

1. Batten Trough Region

D. E. Leaman
Centre for Ore Deposit and Exploration Studies

SUMMARY

Initial work in the Batten Trough within the McArthur Basin has shown that much structural and architectural information can be extracted using a combination of standard and unconventional geophysical interpretation procedures. Fundamental thickness and structural relationships for all parts of the section can be inferred regardless of any limitations in assumptions about rock properties or complex interactive effects within the potential field data used. The interpretation provided is indicative of regional relationships and not intended to provide detailed information on any part of the sequence.

The interpretation has shown, however, that the apparent dominance of sub N–S trends and faults indicated by surface mapping is not a true representation of underlying structural or basin patterns - merely the effect of the most recent uplifts and compressions.

Fundamental structures in the region trend NE, NW and sub E–W as well as NNW. The relationship of deeper volcanic sequences, such as the Scrutton Volcanics, and previously unrecognised variations in mafic units, either deep within the Tawallah Group or a variation of the Scrutton Volcanics, to these fundamental trends has not been described previously.

Growth relationships are evident across many major faults, most of which display reversal of displacements with time. Initial review of the relationships between mineralisation, deep basement trends, deep basin trends, growth patterns and distribution of particular volcanic compositions would seem to suggest that copper shows reflect the presence of thick (>3 km) mafic piles in half grabens while other base metals may be associated with active margins which display substantial thickness variations in units older than the Tawallah Group.

Initial results imply direct relationships between the loci of known mineralisation and marginal structures which have been active in the long term.

INTRODUCTION

The regional geophysics-basin architecture element of the project is directed toward a description and understanding of the setting and control, both temporal and spatial, of mineralisation in large Proterozoic basins in northern Australia. The possibility that any relationships established may have wider applications has also been recognised.

Several basin cover sequences in northern Australia contain major base metal and sulphide accumulations and the present study is designed to assess them in terms of regional and crustal controls. While regional mapping and geophysical data are generally available, complex histories, thick sequences and limited sequence exposure coupled with limited deep drilling and seismic reflection data have limited appraisal of the materials and settings — especially in terms of basin formation and associated deposition information.

The Batten Trough portion of the McArthur River Basin was selected for initial evaluation since data coverage is good, the area has not been previously assessed in the manner proposed, and its mineral potential is high even though the reasons for this are not known. The region centred on McArthur River and the HYC deposit, is considered in this report.

The work reported here represents the first six month period of the project and was initially delayed by belated supply of some data. It is focussed on the Bauhinia Downs 1:250 000 map sheet but extends from the northern part of the Wallhallow sheet to the Mt Young sheet. Much of the preliminary review

CODES: AMIRA/ARC Project P.384 — Proterozoic sediment-hosted base metal deposits. November 1992

time has been directed toward assessment of optimum methods and analysis in order to test options, ambiguity, resolution or limitations of results. The report considers these issues and their impact upon any conclusions in terms of the Batten Trough and similar discussions will not be repeated in future reports.

BASIC DATA

Regional geological, gravity and aeromagnetic data have formed the basis of the present analysis. Geological data include the 1:250 000 mapping by the BMR (Plumb et al., 1962 – Wallhallow; Smith et al., 1963 – Bauhinia Downs; Plumb & Paine, 1964 – Mount Young) and 1: 100 000 mapping of the BMR (Jackson et al., 1987 – S McArthur Basin) and the NT Geological Survey (Pietsch et al., 1991 – McArthur River region).

Principal structural elements are shown in figure 1 (for a simplified geological map see page v).

Regional gravity data, supplied by the BMR in map form (fig. 2), supplemented by extracts from the gravity data base, is based on a coverage with a station spacing of about 11 km. This data base incorporates a handful of more detailed traverses but the data is considered to be only of regional value. Most shallow or small sources are poorly defined. This has not been found to be a serious limitation in terms of the present gross architecture study (below).

Regional aeromagnetic data are of variable age and quality and, at this stage, have only been provided in contour map form for most of the region (BMR data, fig. 1). More detailed coverage of the Bauhinia Downs area (at 1:100 000 scale) has been provided by the NTGS. Digital data for the latter survey has been provided but gridding and imaging is incomplete. This has not seriously limited the present analysis, for the reasons explained below.

No significant problems are posed by use of contoured data for regional applications and the analysis reported here is not limited in any way by such formats. Detailed processing and images may well assist surface mapping projects but do not necessarily convey the quantitative information sought here.

Some seismic data is available (e.g. Collins, 1983) but no full size panels have been supplied for examination. Many published versions are small scale and unclear. Coverage of this information is very limited.

Few previous interpretations of this data have been reported (e.g. Plumb & Wellman, 1987) and none have attempted to describe the entire basin or its architecture in the systematic way which would be accepted by petroleum geologists, for example.

The data types available would not normally be considered suitable for comprehensive basin study and would, if used at all by petroleum or basin explorers, be applied to definition of basin extent, rather than content or internal relationships. The latter tasks usually depend on good seismic data. Rock property data is also virtually non-existent for the McArthur River region.

Some qualitative comments based on gross anomaly character may be noted.

The Bouguer gravity field is generally positive or neutral for much of the area and several gross N–S elements are evident. One of these may be directly correlated with the Roper Group exposures west of Bauhinia Downs. The Batten "Trough" region is generally positive although a marked local negative has been observed in the Batten Range. Large negative anomalies dominate the gravity field within the Wallhallow sheet. A major regional change (trending NW) occurs from south to north within the southern part of the Bauhinia Downs sheet and the anomalies within the Batten Trough region are anomalous in gross terms. A quite different pattern is evident within the Mt Young sheet. The gravity field of the region west of the Yiyintyi Range is comparable with that in the Bauhinia Downs sheet but a positive NNE-trending feature dominates the eastern region. This becomes systematically more positive as the gulf is approached. There is little exposure of rocks older than Cretaceous in this region.

The magnetic field does not obviously correlate with any of these patterns. This is not a result of coverage or detail. There are markedly differing response patterns and several sub N–S and NE–trending elements are more obvious. A large magnetic high dominates the southern half of the Bauhinia Downs sheet. Although it extends across the Emu Fault zone this fault is clearly represented. The magnetic field toward the gulf and across most of the Mt Young sheet is relatively positive but variable. A number of near surface responses are apparent and relate to exposures of the Scrutton Volcanics or mafic volcanics within the Tawallah Group. A belt of anomalies with no mapped surface expression mimics the western side of the syncline containing Roper Group rocks, and extends south beneath them, in the Bauhinia Downs and Wallhallow sheets.

THE GEOPHYSICAL PROBLEM

Basin studies, including definition of unit thickness or compositional changes as well as location of controlling structures, volcanism and unconformities, are normally associated with relatively young basins (post Cambrian) and petroleum exploration. Seismic reflection methods are usually considered essential for acceptable description and resolution of relationships and estimates of scale.

The petroleum exploration industry does not normally consider gravity or magnetic methods able to provide much useful information on a routine basis and rarely acquire adequate data, or apply it, if available. Such data may be used only to provide some gross indication of the location and size of the basin, including some estimates of "basement" depth, in order to focus seismic surveys — although even this cost effective sequence is not universally applied. Thus any data acquired, usually carelessly or incidentally, are rarely interpreted fully and remain underutilised. Many examples could be cited where this forgotten information may provide critical clues about internal volcanism and structural patterns.

This study of mid Proterozoic basins, which have good magnetic and fair gravity coverage but negligible seismic coverage, must fully utilise any data available. The real issue is, can gravity and magnetic data replace seismic data? The work reported here would suggest that they can to a large extent although it must be recognised that different elements of the basin may be assessed. Thus the potential field methods can define igneous components and primary structures (at all levels) while seismic data best describe sedimentary features and internal structures provided the section is not highly structured. Ideally, all three methods should be used but in gross terms the potential field methods coupled can provide as much, but different, information as the reflection method. Unfortunately the seismic methods are not universally workable due to surface or velocity conditions and in such cases the other methods will always yield more information — and certainly at far less cost. This is the condition to be expected in older, or deformed, rocks — including the McArthur Basin.

Some key issues must be declared at outset and appreciated throughout all interpretation stages. The interpretation problems posed by immense basin structures are unlike all other applications. Rock volumes are large, properties tend to integrate broadly and thickness, rather than depth, estimates are important. Most interpretations, especially of magnetic data, tend to focus on depth issues; depth to source, target or basement, while the more complex gravity interpretations must attempt an integration of concealed, deep sources. Thickness is not so readily estimated since it depends on evaluation of paired, often asymmetrical surfaces.

Further, magnetic responses of large sub tabular bodies predominant in basins with width–depth or width–thickness ratios in excess of 15:1 tend to background and only edges, abrupt changes, or systematic variations generate large anomalies. This means that regional studies should treat gross features, not be blinded or dominated by spiky elements, and assess the relative subtleties on a large areal scale. This may also mean that simple two dimensional (2D) methods may not be generally applicable and that three dimensional effects may be common (3D). A further corrollary to these relationships is that it may be almost impossible to define an initial basin concept using 3D methods from genesis and that initial work must be 2D in order to rapidly assess possible conficts and forms.

A more crucial observation in such circumstances is that **every** long wavelength feature is an interference effect and represents an integration of many elements. In a region where the de-spiked magnetic field has a relief of only 100 nT and each large element of the structure can generate 25 or more nT at 50 km distance from a change in form it is easy to see how many effects are complex interactions (fig. 3). Any attempt to separate a single source — without considering the others — will provide a neat, but inevitably incorrect and ultimately, doomed solution. These comments do not apply in any serious manner to high frequency effects related to outcrop, or near outcrop, of sources (depths less than 1 km max.). Gravity responses, especially when based on smoothed or coarsely spaced data, are unquestionably interference patterns and must be treated as such. It is therefore unwise or not possible to use any gradient-based method of interpretation, including popular rules of thumb, or other automated procedures away from any clearly high frequency elements. This does not mean that qualitative derivative or lineament studies cannot be used; simply that quantitative results must be based on forward modelling procedures and testing of geological options comprising ***all*** the geology.

A simple illustration of the dangers of false responses is shown in figure 3. In map form the asterisked response appears real and gradient studies can yield depth estimates. But there is no source and the effect is solely due to larger sources nearby. This risk is enhanced when dealing with thick or large area tabular bodies.

How then can an interpreter, or reviewer of an interpretation, ensure that the solution(s) offered are either feasible or reliable and consistent in such conditions? This confidence is essential given the decidedly original application and demands of these methods reported here.

I apply five rules to all modelling, whether my own, or that of others, which apply regardless of issue or style of interpretation (2D or 3D) (Leaman, 1992). In the 3D case their application forces the solution to the limit of resolution possible with the given methods or data set.

The rules are:

1. Does the solution honour all known geological, drilling or other control? This includes the surface distribution of materials.
2. Does the solution contain discontinuities, in terms of contrasts, properties or geometries, which are

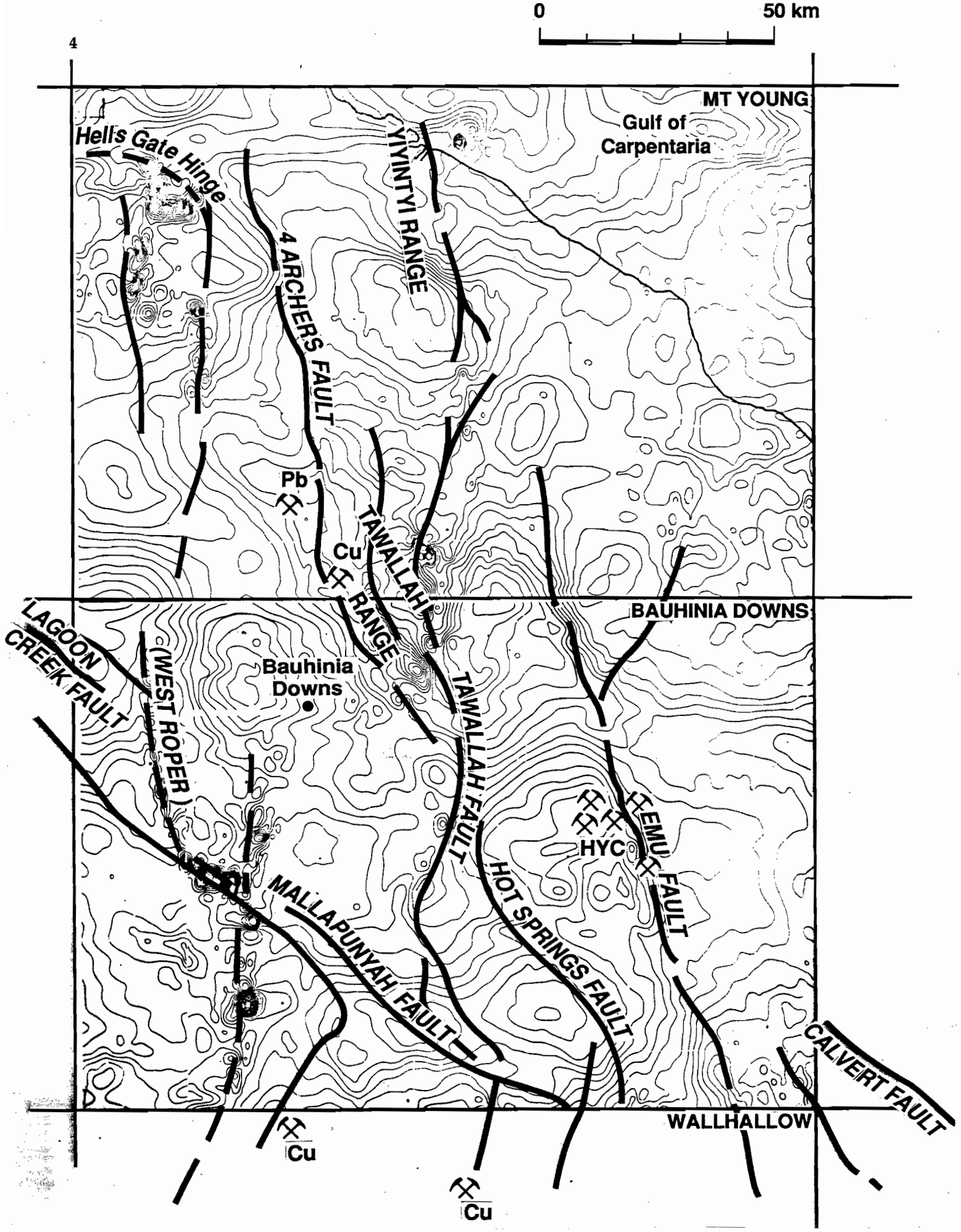

Figure 1 — A basemap drawn from published 250 000 sheets showing selected faults and prospects has been overprinted by the regional magnetic data compilations used (BMR data).

Geological overlay for Figure 1

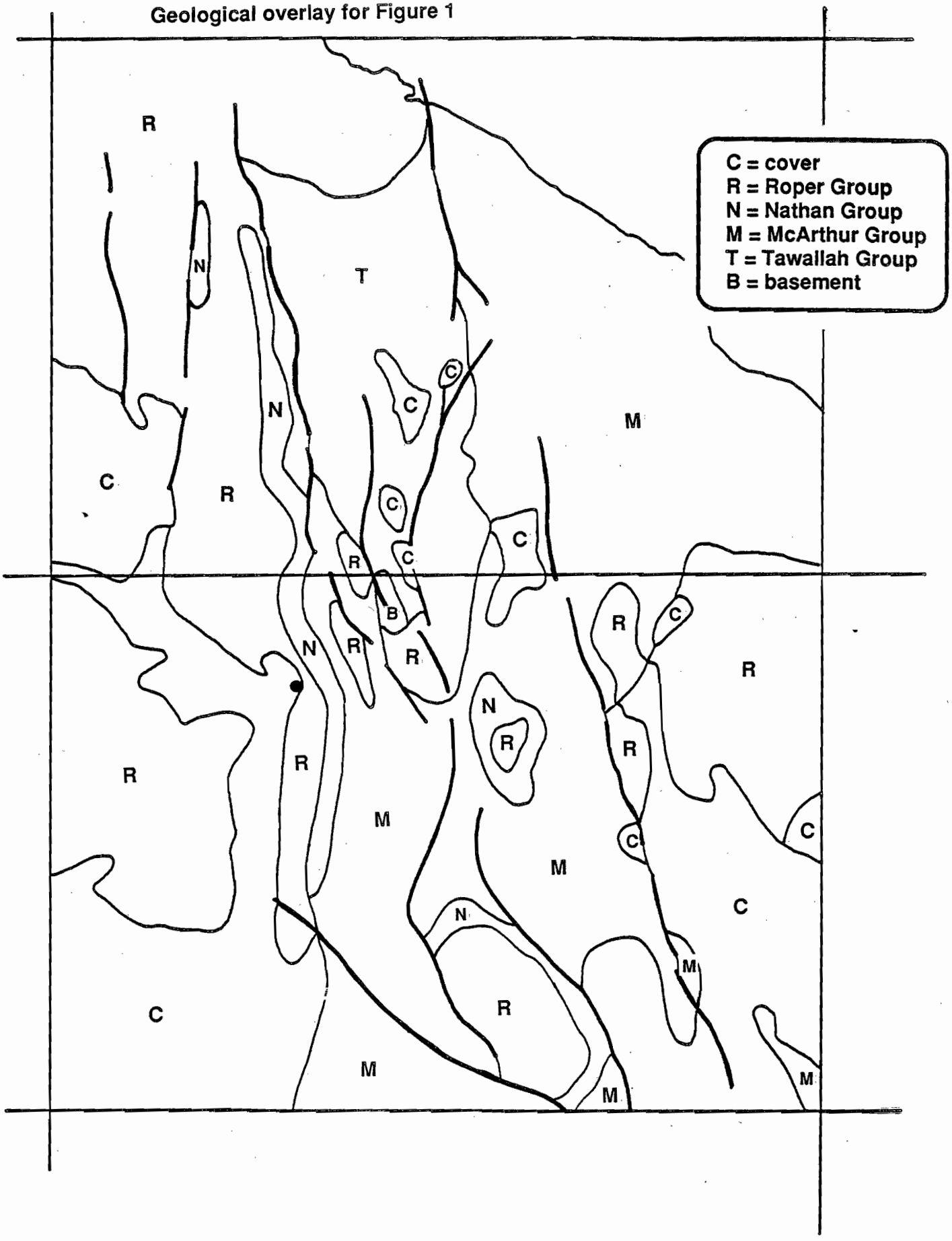

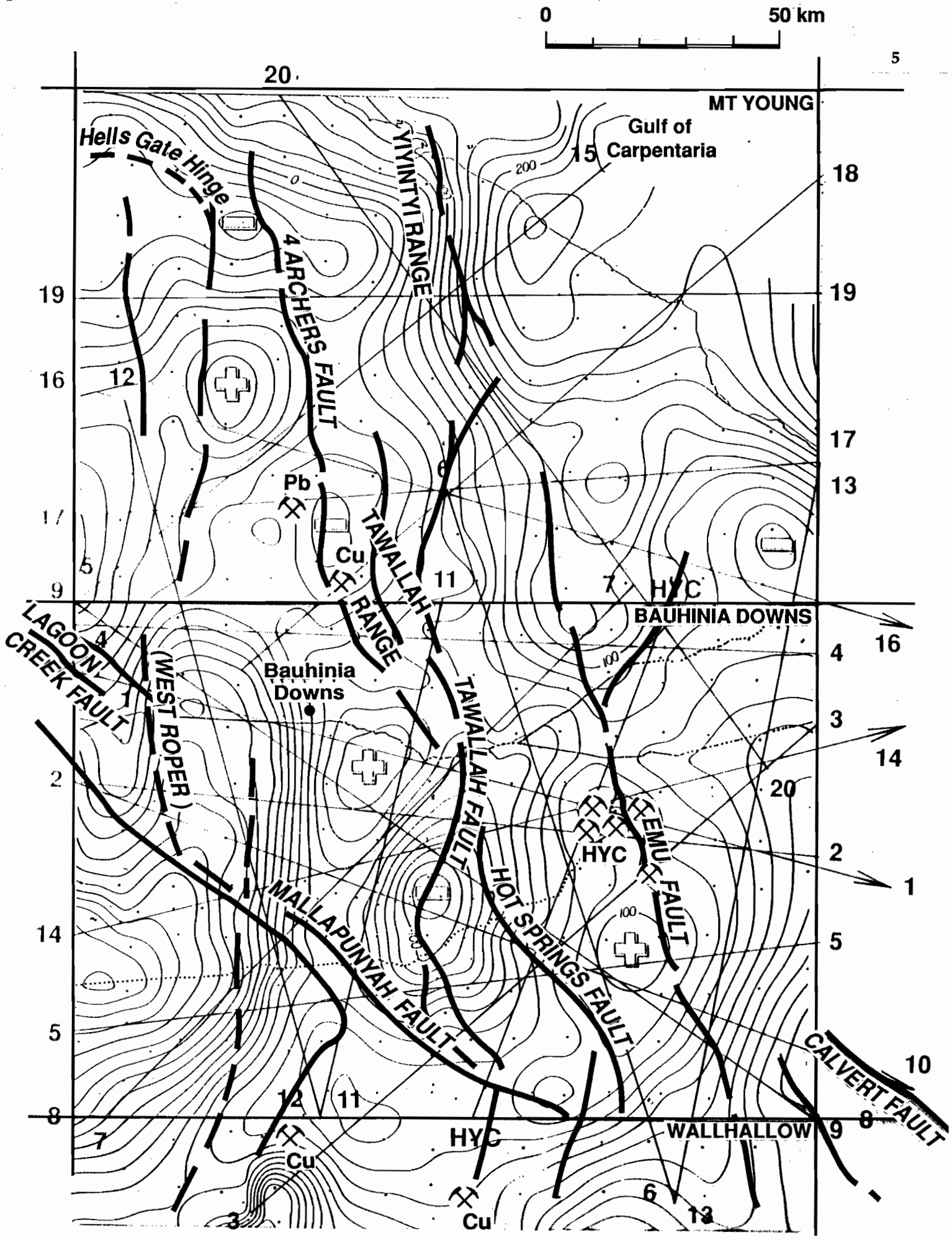

Figure 2 — The simplified geological basemap has been combined with the location of the modelled traverses and is overprinted by the regional gravity data compilations used (BMR data).

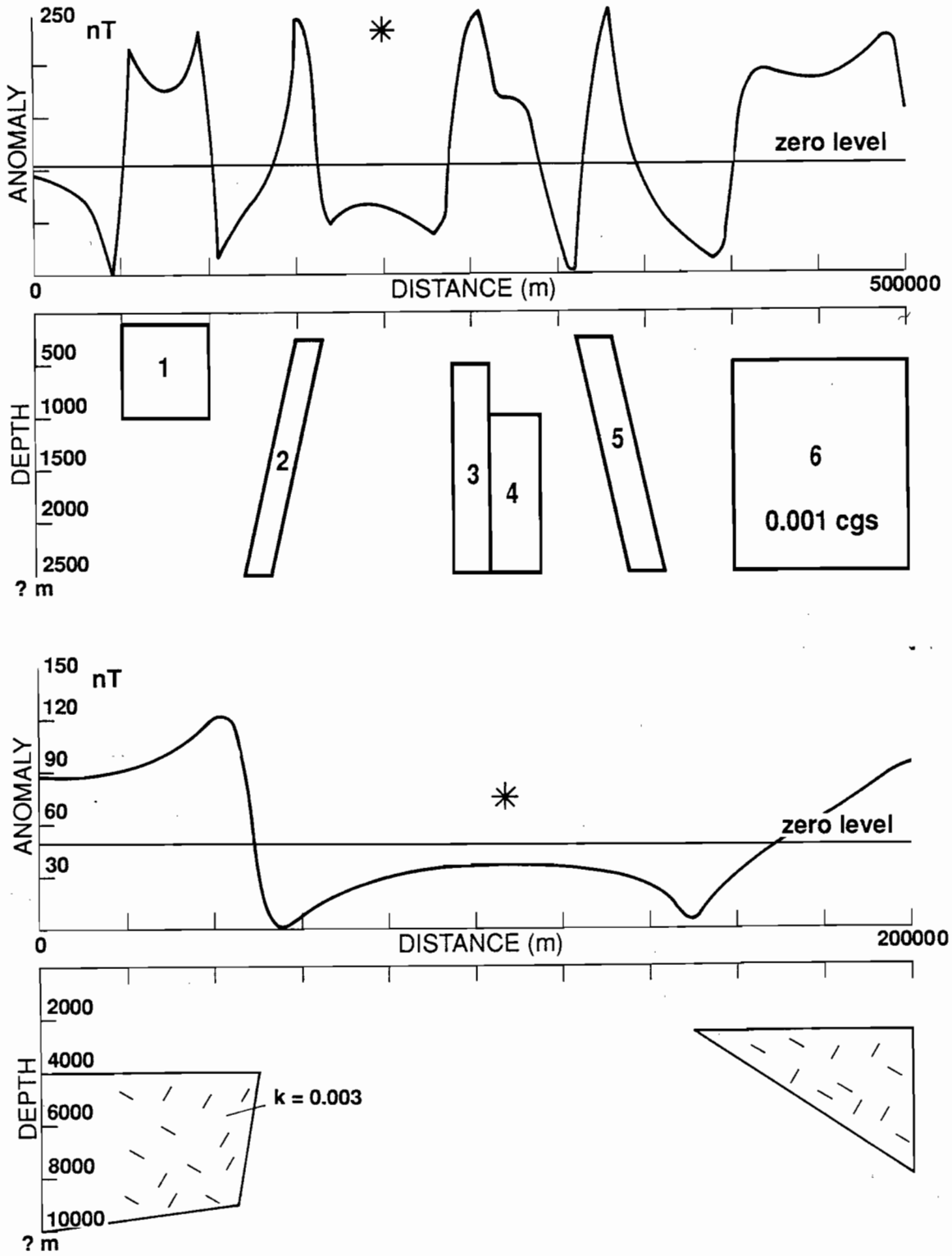

*Figure 3 — Effect of anomaly interference and misleading forms is illustrated. The upper diagram shows how anomalies may diverge from base level when interference occurs and why it is important always to model against the true base level. The lower diagram illustrates how similar forms can arise in regional situations. The offset is a large proportion of the peak effect. In each case the * marks the location of an apparent anomaly. But there is no source, only interference. Any automated approach must be misleading and cause error.*

not reasonably sustainable in view of local geology or possess consistent 3D geometries?

3. Are the rock properties used or implied within observed or tested ranges?
4. Is the regional solution based on several, preferably interlocking, profiles? Any solution based on single or separated profiles is considered interesting but suspect unless this and the following condition are satisfied. This test has the particular value of forcing consideration of many, if not all, aspects of the geology of an area and consequent evaluation of relationships of both sources and generated responses.
5. Does modelling of the individual profiles of the array yield a consistent implied base level for the data sets employed? This base level should be equivalent to that established during observation and processing but is rarely stated on maps. This test is absolutely critical since it is often possible to generate many solutions for a given profile based on the first three criteria. Coupling of base determination and the array test usually leads to denial of most options.

There is only one geology and the methods employed have only seen that. With care an interpreter should be able to approach that unique solution.

In the case of the Batten Trough basin study where there is limited geological control, merely fragments or inferences of information for some areas, the interpretation is faithful to what is either known or is reasonable induction near exposures.

Properties are largely unknown but have been inferred from little data or actual responses in areas where the data is detailed enough (usually magnetics) to provide direct correlations and estimates. This approach is necessarily incomplete when few possible sources can be assessed. In order to impose limits the entire modelling sequence has been based on maximum contrast modelling. This means that if the unit is a basalt, and described as being predominantly basaltic, then the magnetic contrast applied is that of a strongly magnetised basalt and the density that of a basalt sequence. This conservative approach means that depth estimates may be suspect — actually minima — but that the general relationships and relative changes in thickness in and between units are preserved. Where this has led to absurd or inconsistent results within the framework of either the criteria or reasonably inferred properties the maximum supportable contrast has been employed. This approach, based on effective contrasts as inferred from responses or interference integrations incorporates any effects due to remanent magnetisation. These tend to be erratic and only significant when near the source. Induction, or resultant inductive effects, predominate when considering large source distributions or sources distant from the observer or magnetometer. The apparent inductive contrast may, however, be higher or lower than implied by measured susceptibilities depending on the direction of the remanent vector. The maximum contrast view thus allows for this. Clearly any interpretation using property estimates may be suspect but, in terms of the criteria or consistency, this will only affect absolute depth or thickness estimates, not relative estimates which are the over-riding consideration of this study. Geometric variations have been largely evaluated by the line array employed.

The interpretation offered satisfies all the criteria in terms of both data sets, taken independently or combined, and is consistent with any other control known to exist. This should not be taken to mean that it is either perfect or correct. It is offered as a credible outline subject to revisions pending further evaluation of surrounding regions or incorporation of better property information.

2D methods only have been used at this stage. It is clear from this preliminary analysis that any major revision must employ 3D methods. The simpler methods have, however, defined a general view and located all critical areas. 3D refinement, and detailing, may well be beyond the scope of this project and be more appropriate at tenement exploration scale - within the gross framework offered. It should be noted that no 3D detailing of smaller areas can be undertaken without insetting that detail within the regional setting, however crude, in order to define interference effects and resolve local elements. The regional setting in the sense used here means basin wide and must also include the entire relief of the basin (about 15 km) and important basement sources (granites in the gravity case).

THE GEOLOGICAL PROBLEM

A number of geological inferences have been made about the McArthur Basin, and the Batten Trough in particular. These are listed below as elements or assumptions which should be reviewed or tested as part of any basin study. This is done on the basis that most deductions have been based on surface geological relationships and stratigraphic sections, which may not apply far from outcrop or across some hidden discontinuity, and those which have incorporated geophysical information have been based on inspection of anomaly patterns and not extended quantitative analysis. The interference problem, or risk, may have rendered many of these analyses suspect.

Plumb & Paine (1964) made only limited comments which may be relevant to basin history or architecture in so far as it might affect mineralisation.

1. The Scrutton Volcanics seen around Mt Young are felsic but a possible correlation was made to the Cliffdale Volcanics of the Murphy Inlier where the latter are intruded by the Norris Granite. This may be relevant to dating mineralisation if all the links are accepted.
2. The Peters Creek Volcanics are very thin but basaltic. In other areas the Tawallah Volcanics tend to be bimodal.
3. Folding patterns have been linked to basement controls. The N-trending anticlinorium elevating Scrutton Volcanics and Yiyintyi Sandstone is thought to have been controlled in this way.
4. The block east of the Tawallah Range is thought to have been stable over a long period.
5. The block west of the Four Archers Fault is also thought to have been quite stable but domed post Roper Group. A 6 km throw is implied for this fault.
6. Faults within the structure core have introduced Scrutton Volcanics.

Jackson et al. (1987) presented a summary of ideas based on earlier work and some implications from the region studied.

7. The main concept of the Batten Fault zone was that of a zone about 50 km wide previously a syndepositional graben.
8. The eastern margin was proposed near the Emu Fault while the western margin was complex. It was noted that typical graben sedimentation, such as the Westmoreland Conglomerate near a distant SE margin trends anomalously to the SW. This was explained by distance from the Emu Fault.
9. Depocentres shifted westward from McArthur Group to Roper Group times. Main Roper deposition west of Bauhinia Downs property.
10. Up to 7.5 km of vertical displacement was claimed for the Batten Fault Zone (comparable to Four Archers of Plumb & Paine, 1964) which reversed the graben. The shelves were only mildly deformed. (All this assumes stratigraphic assumptions valid across region)
11. The major faults of the area are all part of major lineaments in N Australia.
12. The Calvert–Mallapunyah Fault system was said to be offset by the Batten Trough.
13. A conflict was noted between presumed sinistral offset at the Trough and claimed vertical throws with little displacement post McArthur Group.
14. The Emu Fault varies in dip along strike to both sides. Reversals with time.
15. Many faults curl to the NE.
16. Wrench-related tectonism inferred to the NNW. This yields some NW regional elements and possible NE elements with classic pull-apart relationships.
17. Trace copper mineralisation is widespread south of the Mallapunyah Fault Zone.

Pietsch et al. (1991) attempt some specific and updated comments.

18. Fold axes are noted to be oriented NNW with local ENE and NW–WNW variations.
19. Tawallah Group subsidence appears to have been of the order of 4–5 km on pre-existing basement structures trending regionally to the NW.
20. McArthur basin geometry is dominated by a N–S trough. The Batten (Emu Fault) zone deemed the major zone of subsidence.
21. The McArthur Group was up to 10 km thick.
22. The western margin of the trough was complex and bounded by the Mallapunyah, Hot Springs and Abner Faults with much thinning of the McArthur Group onto lateral shelves (especially Bauhinia Shelf).
23. Umbolooga SubGroup rocks noted as more widespread as cover sequence with no consistent changes across the Emu Fault or at any proposed trough marginal location. Anomalous.
24. Some thickness changes have been noted for the Umbolooga implying activity late in deposition with some faulting? Batten Sub Group shows no changes.
25. Nathan and McArthur Groups are absent south of the Mallapunyah F.
26. The Roper Group differs; thickest on Wearyan Shelf.
27. Noted that claims exist (Plumb & Wellman, 1987) that the rifts widen irregularly to the south.
28. A total section of at least 15 km is implied. Is it all in one place?
29. There is no evidence for deep metamorphism of either the Scrutton Volcanics or older Tawallah formations which would imply that these have not been buried by 15 km of section.
30. Noted that the Mallapunyah–Calvert Hills Fault system was long lived and controlled southern extent of deposition.
31. The major magnetic high observed represents a high in basement.
32. A central gravity low NW of the Abner Range is related to Nathan Group.

It will be noted that most of these comments and notes relate to post Tawallah Formations reflecting available exposure. Plumb & Wellman (1987) have attempted a regional synthesis using the data analysed for this study. They concluded that:

33. The trough was a syn sedimentary half graben basin with shelves about 80 km wide at most and 600 km long with up to 12 km sediments.

34. Mafic volcanics are largely restricted to the Wearyan shelf (E).
35. Magnetic basement was inferred using established rules of thumb to be 4 km on shelves and up to 10 km or more elsewhere in trough.
36. Some NE trends were inferred S of Mallapunyah Fault and then N–S to the Urapunga Zone.
37. Different rifts were active at different times over 200 m.y.

Many of these ideas conflict with surface geological indications. It should, however, be noted that they are based on qualitative inspection of the data and use of guide rules. The effect of interference or limitations imposed by this was not evaluated.

INTERPRETATION

The interpretation described was directed toward a general evaluation of data, issues and methods in order to provide primary conclusions about the unit relationships and structures within the Batten Trough portion of the McArthur Basin. Thus matters such as "can useful information be extracted?", "how ambiguous might the results be?", have been addressed.

All previous workers have downgraded the usefulness of the gravity data set by describing it as too regional in character. But, if the basin or its contents, or basement elements, extend across a depth range of 5 to >15 km then it may provide gross discrimination of any magnetically derived options.

Thus the magnetic data sets have been used to test many alternatives and provide primary concepts. Key to the use of the magnetic data is the nature of the possible magnetic sources.

Inspection of the magnetic field within the Bauhinia Downs–Mt Young region shows that high frequency anomalies are related to exposures of Scrutton Volcanics and volcanic members of the Tawallah Group (including the Seigal, Peters Creek, and Settlement Creek Volcanics). No other units are significantly magnetised and these are shown to be somewhat variable.

Pietsch et al. (1991) have suggested that the large magnetic anomaly which dominates most of Bauhinia Downs map sheet is due to basement variations (relief or contrast). The possibility of large tracts, or entirely, of magnetic basement was assessed but no coherent solution can be found if this is assumed. Gravity data, and basement granitoids which displace any such character if present, show beyond any reasonable doubt that this option may be ignored as most unlikely. This was confirmed by modelling.

The following properties have been inferred for the critical materials based either on local anomaly analysis, lithological descriptions or limited direct measurements available to the project.

Scrutton Volcanics: 0.003 cgs, 2.79 gm/cc
Tawallah Volcanics: 0.004–0.006, 2.84+
(all volcanic members)

The reference density used for near surface rocks, largely dolomitic, was 2.74 gm/cc although this is not critical. Use of this background density leads to credible inferences for both basement granitoids, Roper Group and younger cover rocks. In the case of the Roper Group the anomaly, density, thickness relationship is excellent — density 2.58–2.60 gm/cc. Basement granitoids have a bulk density of about 2.64 gm/cc on this basis.

Cambrian cover rocks have been inferred to possess bulk densities of about 2.45–2.50 gm/cc.

An anomalous response pattern has been observed for certain members of the Bauhinia Downs sub Group of the McArthur group within the Batten Trough west of the Emu Fault. These denser dolomites appear to have densities of at least 2.77 gm/cc and the effect is more regional than simply about the mineralised area.

Initial interpretation to confirm the methods, scope and likely style of any conclusions was based on profiles 1 to 7 (fig. 2). Two of these profiles correspond to published sections (e.g. Smith et al., 1963) and were used to test presented inferences and inferred properties. Other more random orientations were designed to satisfy the criteria defined in the previous section and to check a number of the geological components of the Bauhinia Downs region.

This first analysis suggested that the treatment proposed was indeed workable and would expose the architecture of the basin. It was also clear that 3D methods might be required if detail was sought but that an original 3D concept could not be established on the basis of only seven profiles or direct use of 3D methods from commencement. Many complex and overlaid structures were clearly present and a simpler framework must be derived first. Several other options and issues were also raised by this early work including the possibility of podding or local variation within the volcanics of the Tawallah Group, or variations in composition within the Scrutton Volcanics. This preliminary analysis also suggested that some significant variations might occur near the HYC area and that the orientation of the deeper structures was not N–S — as has always been assumed (above). Such fundamental elements may well have influenced the disruption of, and complex nature of, elements of the Mallapunyah, Tawallah and Emu Faults as seen today. The orientation of modern drainage may also be related.

A second stage review was then undertaken with the assurance that useful results would be forthcoming. An additional fourteen lines were added to the line array and all twenty one lines were calculated

and iterated to consistency within the constraints of 2D methods. During this process a number of possible source options were reviewed and excluded.

An important issue considered at some length relates to the relative contributions of the volcanics within the Tawallah Group and the Scrutton Volcanics. It has been found that these components are separable even where the Scrutton Volcanics are predominantly felsic or acidic due to the nature of responses and geometric factors. Direct linkages to surface show that the Tawallah Volcanics are generally very thin (<500 m) and though of higher contrast generally cannot produce the anomalies of the magnitude or coverage observed. The bulk of the magnetic field response is generated either by the Scrutton Volcanics with the lithologies exposed or by variations of considerable volumetric scale. As noted below this comment can be translated to mean either that the Scrutton Volcanics are bimodal or that the deepest of the Tawallah series volcanics has some local and very thick developments. This stratigraphic uncertainty does not affect implications for basin history or architecture since the inferred relationships are very distinctive.

There has, therefore, been no attempt made to separate individual volcanic members of the Tawallah Group. This could be done in many cases using the best data set available and 3D methods but this type of treatment is not justified at this stage of the project.

The results of the analysis to date are summarised in figures 7 to 14. The overall results, in terms of basin description, are in many ways better than is normally achieved seismically since a much greater depth range has been resolved. Given that volcanic rocks make up a large part of the section, and that these often blind seismic techniques, this is a most satisfactory result.

We may now consider syntheses of elements of the interpretation and structure.

Figures 4 to 6 present samples of modelled profiles in order to illustrate the type of relationships recovered and the reliability or resolution of the interpretation.

Only a few of the profiles analysed are discussed in this report. All are considered to offer preliminary solutions until the entire regional framework has been established and some rock properties confirmed. Of the twenty one profiles examined within the Batten Trough region six are presented here to illustrate various relationships and permit discussion of any limitations within the interpretation. The profile locations are shown in figure 2 and are randomly oriented. Only some aspects of the shallow geology, let alone deeper, concealed elements, can be considered to be treated two dimensionally but at the scale of this analysis this is not a crucial limitation at this stage of interpretation. Data sampling within the data sets has also been coarse, approximately 5 km. This means that many shallow source effects, even if reproduced in the regional compilations, will not be reliably assessed here. The object of the analysis has been solely to define primary relationships across the entire basin. There is ample scope for local detailing within any framework established — provided adequate data exist, and in many regions they do not in public domain.

PROFILE 3 (fig. 4) crosses the SE quadrant of Bauhinia Downs. It illustrates several features.

1. There is a significant variation in the magnetic properties of the principal magnetic source — the Scrutton Volcanics, and in their thickness. Parts of the properties imply felsic or bimodal contents but the remainder can only be due to a predominance of basalts.
2. Any variation within the total Tawallah Group volcanics package, however constituted, generates only minor profile noise with this sampling. It can be expected to create some spikiness in detailed coverage or analyses. The total effect is less than about 15% of total amplitudes even assuming massive, magnetised basalts.
3. The large spike near the Emu Fault is due to a step in the Scrutton, not Tawallah Volcanics.
4. Systematic changes in composition occur within the Scrutton Volcanics near the Emu, Hot Springs and Tawallah/Mallapunyah Faults. Detailed work would be needed to define exactly what happens near each fault but the changes amount to 1–3 km of lithological thickness change. This section is not able to clearly discriminate the relative effects of the Mallapunyah or Tawallah Faults due to their proximity.
5. The thick volcanic section to the SW is either predominantly or totally mafic; that to the NE is predominantly felsic.
6. Any implied thinning of Tawallah Volcanic units is less certain. The section implies an upper mafic sequence capping the Scrutton series but this does not disallow the possibility that the volcanics indicated are equivalent to Seigal or Peters Creek Volcanics other than the fact, that within Bauhinia Downs, these units are either absent — where mapping permits — or lack the properties inferred or required. The felsic-mafic interpretation does make considerable demands on any gravity interpretation but these are easily met.
7. Gravity analysis stresses the effect of the Roper Group section which is sampled at the SW end of the profile and across the Abner Range.
8. The regional elements, with a scale greater than the width of a 1:250 000 map sheet, stress another negative source to SE and SW within Wallhallow. A granite of some relief and contrast is required. This conclusion is supported by other profiles. In

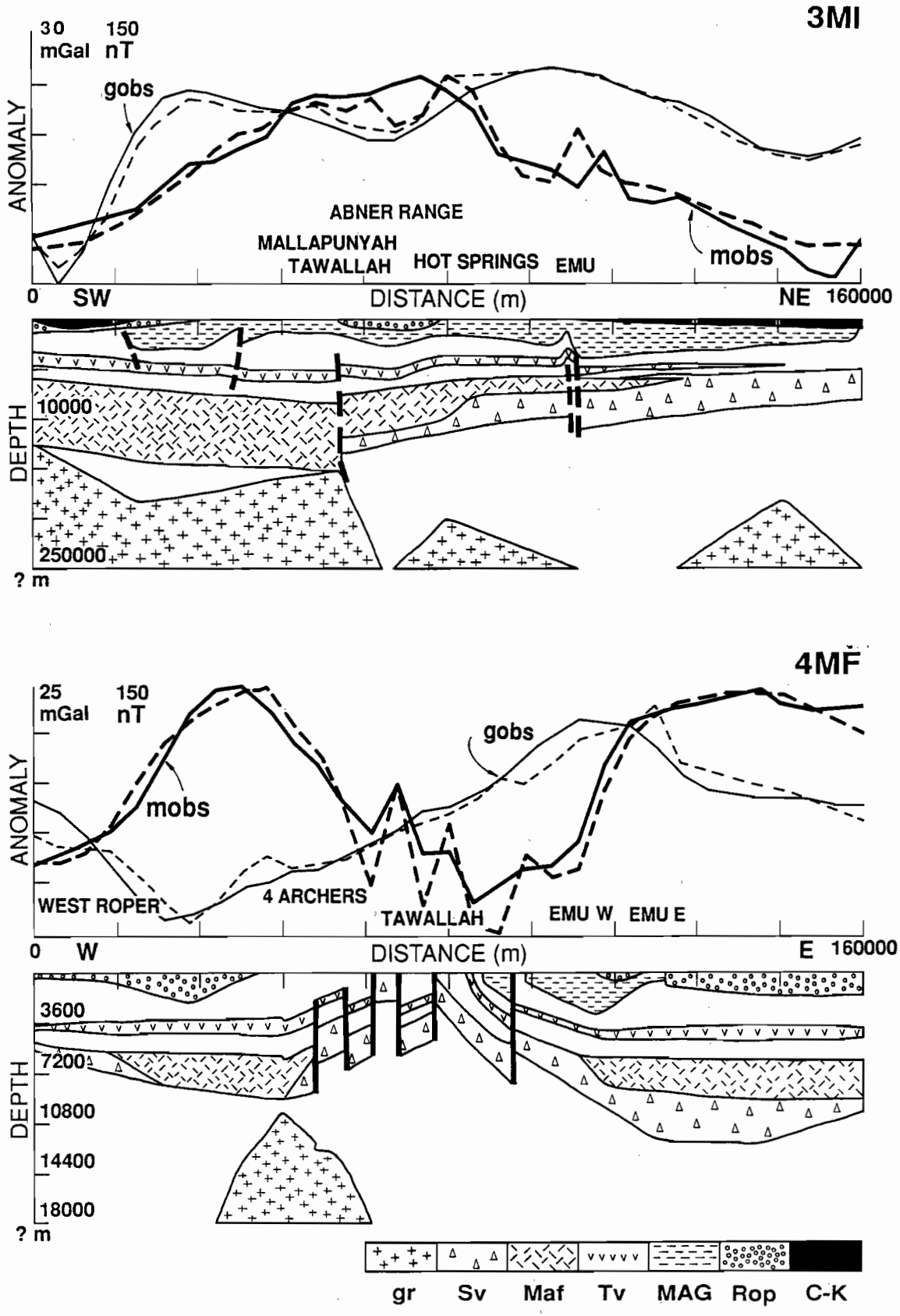

Figure 4 — Modelled solutions for lines 3 and 4. The fits are constrained within the limitations of the data set and the scale of the models. Note that a neutral shift pattern has been recovered.

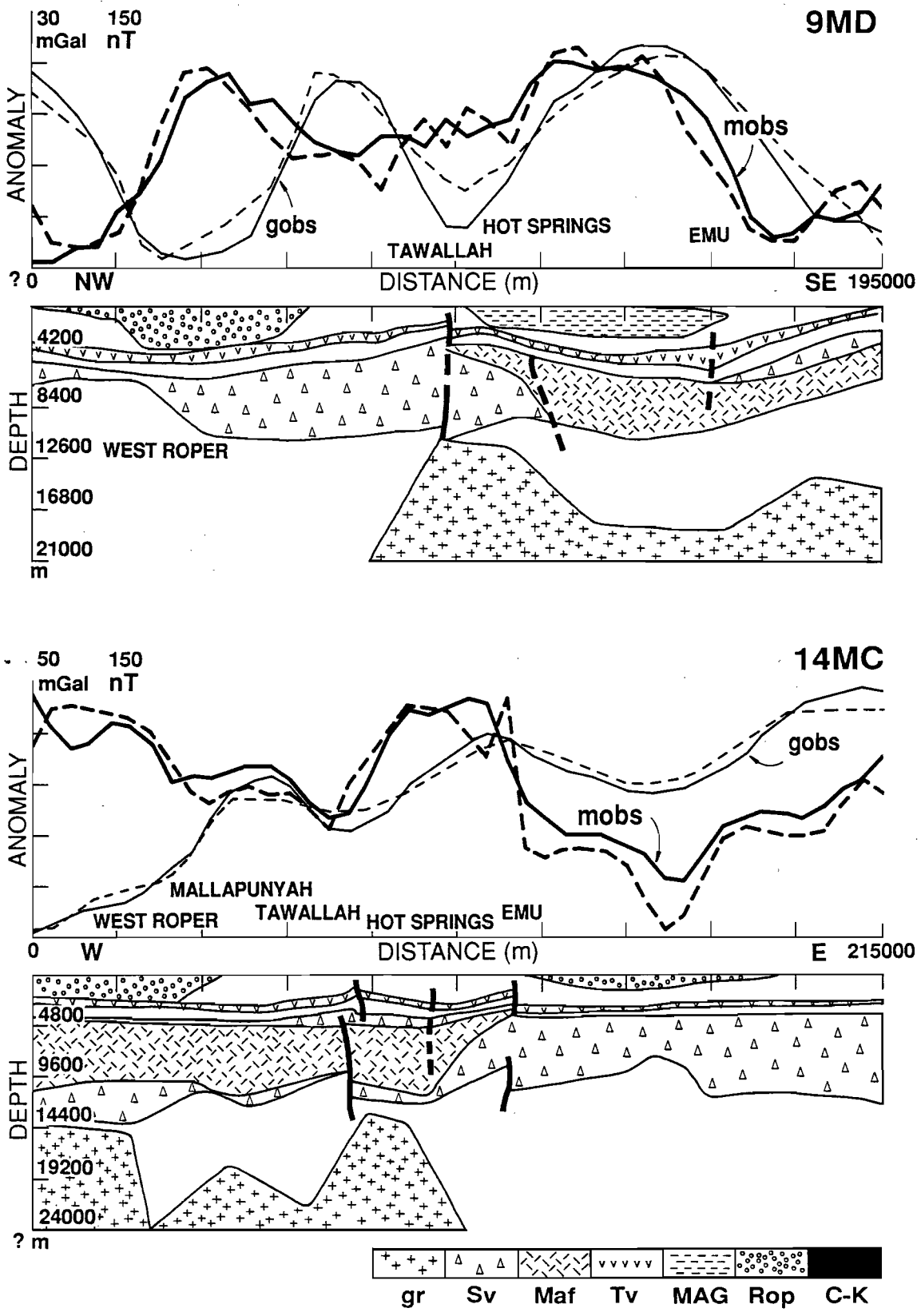

Figure 5 — Modelled solutions for lines 9 and 14.

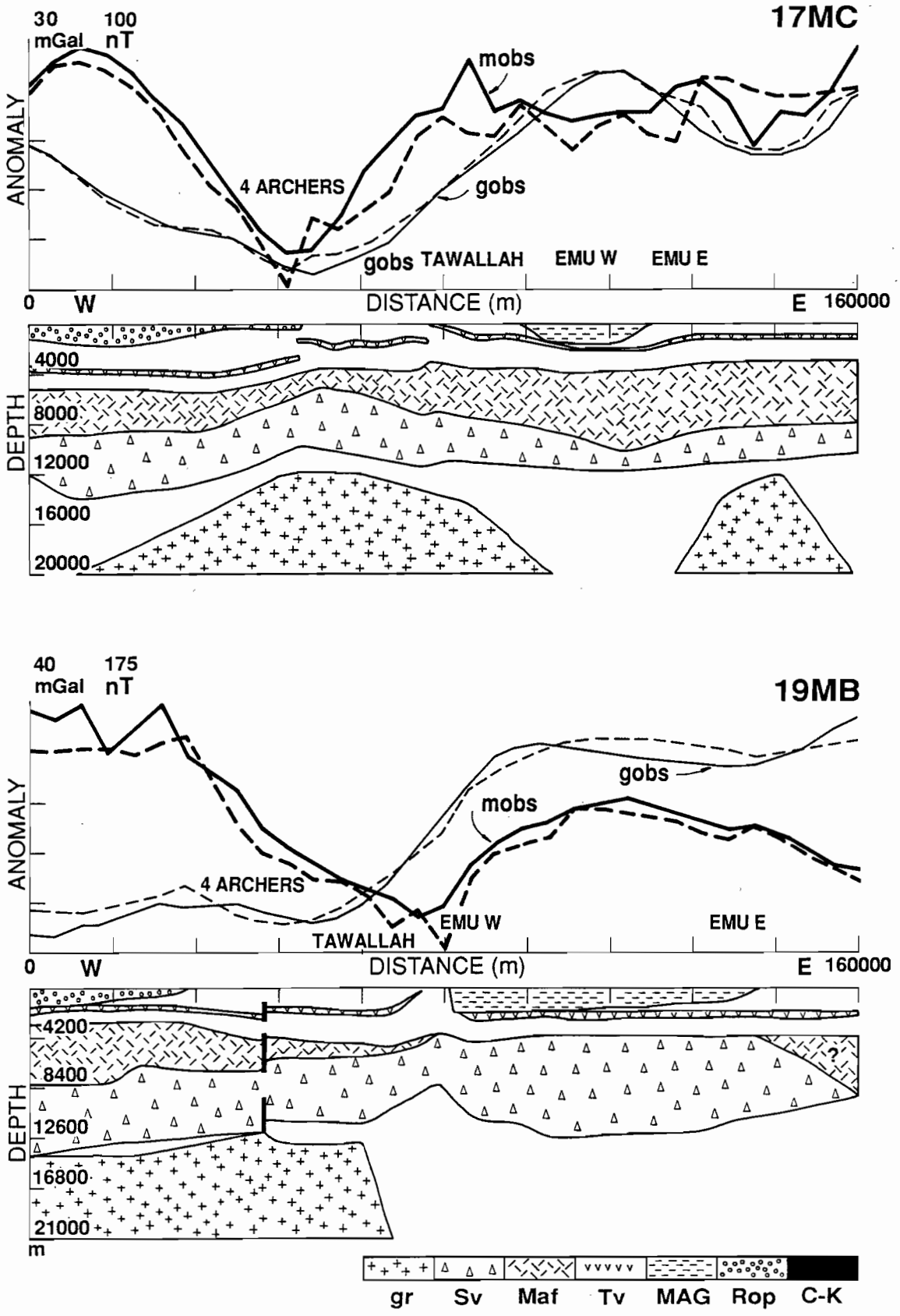

Figure 6 — Modelled solutions for lines 17 and 19.

all cases a pluton with maximum relief of about 11 km has been modelled. In my experience neither granite plutons nor their property contrast relief exceeds 8 to 12 km. The base position or depth is not critical in any event since small, still credible contrast adjustments to background are feasible and can not be resolved.

9. The McArthur Group is also included in the model in terms of its denser elements. These are crucial to the mass balance of the line array - and deposits extend far to the east beneath the Cretaceous and Cambrian cover. The distribution suggests that less than 1.5 km underlies the Abner Range and that the greatest thickness is preserved east of the Emu Fault and south of Umbolooga Creek. Thinning is clearly implied between the Hot Springs and Tawallah Faults in pre Roper times which implies some uplift if the cover had been complete.
10. Both magnetic and gravity data indicate that any major property changes, to magnetic and dense material, occur near or at the top of the Scrutton series, not deep within it.

PROFILE 4 (fig. 4) samples the northern part of Bauhinia Downs and the Tawallah Range.

1. Analysis shows that the thickest section of Scrutton Volcanics occurs east of the Emu Fault. In this section the modelling can be tied to Scrutton outcrop.
2. Mafic volcanic sections in the Tawallah Volcanics thin to the range on both sides although the actual site of termination is not easily defined at this scale.
3. Major changes in Scrutton Volcanics are fault bounded; Emu Fault in the east and at the Tawallah and West Roper in the west. I have defined the West Roper Fault as the feature marked by high frequency magnetic responses along the western side of the Roper trough or syncline (fig. 1).
4. The mafic piles do not extend onto the range zone which implies that it was uplifted before or during formation of these units. Note that the Scrutton sequence also thins.
5. The McArthur Group shows its greatest retained thicknesses near the Emu Fault but it continues far to the east under cover. The Emu Fault posed no fundamental limiting control on this deposition.
6. The effect of the Roper Group is apparent in gravity gradients and the interpreted syncline depth and scale is consistent with known thicknesses and reasonable properties. The latter can be considered among the most reliable inferred from observed responses.
7. The maximum thickness of Tawallah Group, given the gap between Roper and Scrutton sections can not exceed 6 km. This thickness must also include the lower formations of the McArthur Group even though there has clearly been some removal of these beneath the Roper syncline.
8. The negative gravity balance required west of the Tawallah axis presents some intriguing issues. No exposed materials can be used to remove the effect, such as additional Roper Group — since it is absent. It is almost impossible to explain unless a spine boss is added to the granite crest near 47 km. But this would mean that this granitoid intruded at least the Scrutton Volcanics. (see further discussion below)

PROFILE 9 (figure 5) provides a NW–SE transect of the Bauhinia Downs sheet and samples most structures. This sampling is very similar to that provided by sections presented on both 1:250 000 and 1:500 000 map sheets of the region (actually tested as profiles 1 and 2).

1. Modelling shows that the thickest Scrutton Volcanics occur near the Tawallah Fault axis. This may be contrasted with the conclusion drawn near the Tawallah Range to the north (#4) and the pattern here is more like profile #3.
2. Major changes are implied near the West Roper Fault zone at Scrutton level.
3. The Tawallah Volcanics are more variable but thinner near the Tawallah Fault and thickest near the Emu Fault.
4. Felsic components within the Scrutton series are predominant west of the Tawallah Fault but the situation is more variable to the east and massive basalts are indicated. There are suggestions that the mafic components thin east of the Emu Fault and west of the Hot Springs Fault.
5. The gravitational effect of the Roper Group is clear and erosion/removal of most of the Tawallah Group and all McArthur Group is indicated at the West Roper Fault.
6. A thick pod about 3.5 km thick of McArthur Group is preserved which thins SE of the Emu Fault. This is a preserved, not necessarily original or cover, thickness.
7. A regional granitoid underlies the SE zone into the Calvert Hills region.
8. The central gravity negative is related to a granite boss and the issue raised for the previous profile applies here. Does some of this pluton penetrate the Scrutton Volcanics? Although control is limited, it seems that the regional implications demand such penetration. This means, of course, that part of the underlying granitic mass, hardly likely to be uniform or a single age, may well postdate the Scrutton Volcanics and possibly the Tawallah Group. Proper assessment of this

inference and its implications requires more detailed profiling and links to surface materials.

PROFILE 14 (fig. 5) also reviews the key central elements of Bauhinia Downs although a number of 3D effects are inevitable along this profile.

1. Changes in composition of the Scrutton Volcanics occur at the Mallapunyah, Tawallah and west Emu Faults.
2. The thickest felsic volcanics occur to the east of the Emu Fault and thin rapidly westward. The volanics are anomalous to the east but the thickest mafics occur near the Tawallah Fault and rapidly thin east.
3. The Roper Group appears to have been deposited on a much thinned section (primary or erosional thinning) such that the Tawallah Group is much reduced and the McArthur Group is probably entirely absent.
4. The regional response of the western granitoid is undoubted.
5. The central gravity low is glanced by this profile near the Tawallah Fault and granite penetration may again be implied.
6. The McArthur Group is not well defined by this profile.

PROFILE 17 (fig. 6) samples the northern part of the Tawallah Range within Mt Young.

1. Major structural and depositional changes occur across the Four Archers Fault. This zone was uplifted after Scrutton times.
2. There is no major displacement across the Four Archers Fault (1.5 km max).
3. The Tawallah Fault is a similar size.
4. There are very modest changes in all sections between the faults making up the Emu Fault couplet.
5. A link has been established between the Four Archers Fault, thinning of the volcanics and the crest of the underlying pluton.
6. The McArthur Group between the parts of the Emu Fault, is thickest near the western fault arm (the main Emu Fault trend).
7. There is a complex mix of relationships near the Tawallah Fault.
8. Some variations in Yiyintyi Sandstone thickness are implied near some faults. This is essential if the data is to be fitted.

PROFILE 19 (fig. 6) also considers the northern part of the Tawallah and Yiyintyi Ranges within Mt Young.

1. Modelling shows that most, if not all, of the Scrutton section is felsic.
2. The Tawallah Fault zone is marked in the region of the Yiyintyi Range. Not only are displacements not as predicted in explanatory notes but a pronounced local thickening of the Yiyintyi Sandstone is essential if any reasonable geophysical fit is to be obtained. This may reflect the smoothed nature of the available data but there is no indication of any high relief, high frequency variations within the observations which might be consistent with normal thickness and larger fault displacements.
3. This interpretation raises the question as to the nature of the Scrutton Volcanics. Are these mafics really part of the Scrutton, or a subsequent sequence? It should be noted that it is possible to model this section with some minor variations in both thickness and mafic-felsic compositions but great increases in thickness cannot be supported.
4. The shelf zone to the east is very consistent and few changes of any type are indicated.
5. The Scrutton section is very thick centrally.
6. This profile also shows that the throw on the Four Archers Fault is strictly limited and that a greater displacement occurs on the Tawallah Fault.
7. The entire sequence rests on a granitoid basement in the west but there is no evidence of any penetration.
8. Some McArthur Group rocks are indicated east of the Yiyintyi Range.
9. The gravity response at the eastern end of the profile, in the region of the Sir Edward Pellew Group Islands is abnormally positive. This is taken to imply more, or more dense, basalts than normally presumed throughout this interpretation. No member of the defined geology of this part of the Northern Territory can account for this large, relatively local anomaly (see regional gravity compilation, fig. 2). The inferred presence of a thick mafic sequence provides a feasible basic explanation.

A number of important relationships are raised by these examples:

(a) There is erosion of much section, if ever present, beneath the Roper Group in the region of the syncline in the west of Bauhinia Downs.
(b) There is thinning of most units onto the Tawallah Fault zone north of the Mallapunyah and Hot Springs Faults.
(c) There is much variability within the Scrutton Volcanics in the southern part of Mt Young and the northern half of Bauhinia Downs. The rocks are very mafic far to the north east, and within the Wallhallow region.
(d) The Yiyintyi Sandstone thickens onto the the Tawallah Fault axis in the north.
(e) The Emu Fault zone has been very active throughout the entire history of the region,

including during McArthur Group deposition and after.

(f) The previously unmapped and largely concealed West Roper Fault zone has also been critical and has controlled many elements of deposition.

(g) Granitoids appear generally confined to the pre-Scrutton basement volume but there are at least two sites where this confinement appears most uncertain. Given that a younger granite intrudes older granitoids (Ahmad & Wygralak, 1989) and perhaps Scrutton equivalents within Calvert Hills to the SE of the Batten Trough it is not impossible that this has also occurred here. Any such penetration of the pre-McArthur section would appear to lie near the Tawallah Fault axis.

(h) Relatively small throws are indicated on both the Four Archers and Tawallah Faults in the north of the trough. The displacements of 5–7 km implied by earlier workers can not be sustained. This means, since those estimates were based on stratigraphic assumptions, that many units are absent or locally much thinner.

The results of profile analysis have been compiled into a series of structural contour or isopach maps. These have been presented in order to indicate the nature of any systematic relationships interpreted while noting that the actual values quoted must be regarded as approximate. Thus only the general order of magnitude, or relative thickness factors are considered significant.

Figure 7 presents the implied distribution of basement granitoids. This diagram does not distinguish between possible variations in composition or age and shows only the cross sectional extent of the material. The Figure shows that much of the basement is granitic and this limits its ability to be considered as a source of large scale magnetic anomalies or be regarded as a magnetic basement. A granite relief of about 10 km is typical within the middle crust beneath the inferred base of the magnetic, volcanic series. Scrutton Volcanics or Tawallah Group rocks directly overlie these granitoids in many areas but it is only locally that any body may penetrate the cover. The densities assumed for the granitoids provide for the highest feasible contrast compatible with granite–adamellite compositions. This means that any misfit related to granitoids must be explained by greater relief and shallower depths to roof than currently modelled.

Figure 8 presents structure contours of the base of the magnetic volcanic pile here presumed to be the felsic Scrutton Volcanics. There is a 10 km relief on this surface with its shallowest expression underlying the exposed materials of the Tawallah Range. There is general thickening in all directions, but especially to north and south. The diagram, diffuse as it must be given the 15 km depth range, suggests a major NW–SE trend across Bauhinia Downs which has either offset or controlled deposition. A gross NE–SW sense is also suggested as an axis of deposition as are E–W trends. The dense volcanics implied beneath the Pellew Group Islands lie on the NE trend. The obvious NW–SE trend can be traced as an extension of the Calvert Fault and Lagoon Creek Fault system. Although not mapped, or considered significant within Bauhinia Downs, it is clearly an old and major structure.

There is a considerable variation in depth of the base of the volcanics within the HYC region.

Some of the relationships between modern structure and mineralisation are clarified by considering isopachs of the primary magnetic units — whether felsic or mafic. Figure 9 treats the Scrutton felsic series. This diagram reinforces comments about extensions of the Calvert Fault and the NE–SW depositional axes. There is a major change across the Calvert Fault extension. The Mallapunyah Fault is presumably a sympathetic fracture. This diagram stresses the abnormality of the HYC area. Nowhere else are the variations in thickness of these rocks so great. This indicates some very active volcanism and margins in this zone. The diagram also, for the first time, provides a clear suggestion of a proto-Emu Fault. Thus an Emu, Mallapunyah–Calvert and NE–SW fault system was active during formation of the thick basal volcanic sequences.

These comments are supported by consideration of only the mafic component of the volcanic sequences (fig. 10). Many elements of the previous diagrams are evident, particularly the variations in thickness and, clearly, composition near the HYC mineralised area. Of most interest, however, is not the clear suggestion of an Emu Fault, but the presence of a major sub E–W axis at the northing of HYC. This is an astonishing and surprising find and clearly very important.

It forces the question, why is an E–W structure present? However, if we consider the geology of the western gulf in its broadest terms it is hardly surprising. For example, the Murphy Inlier and the Urapunga Fault zones to south and north of this region respectively trend approximately E–W. Could it not be that the ruling basement grain is actually sub E–W and that another constituent of this grain has now been defined beneath the Batten Trough? It is argued here that the really grand structures trend either E–W, NW or ENE. We have a modern, but biassed view of N–S structuring due to exposed features.

Figures 11 and 12 present the current interpretation of the depth of the uppermost volcanics within the Tawallah Group and their thickness. There is almost certainly some integration of the various volcanics of the group and these rocks are not well defined by the

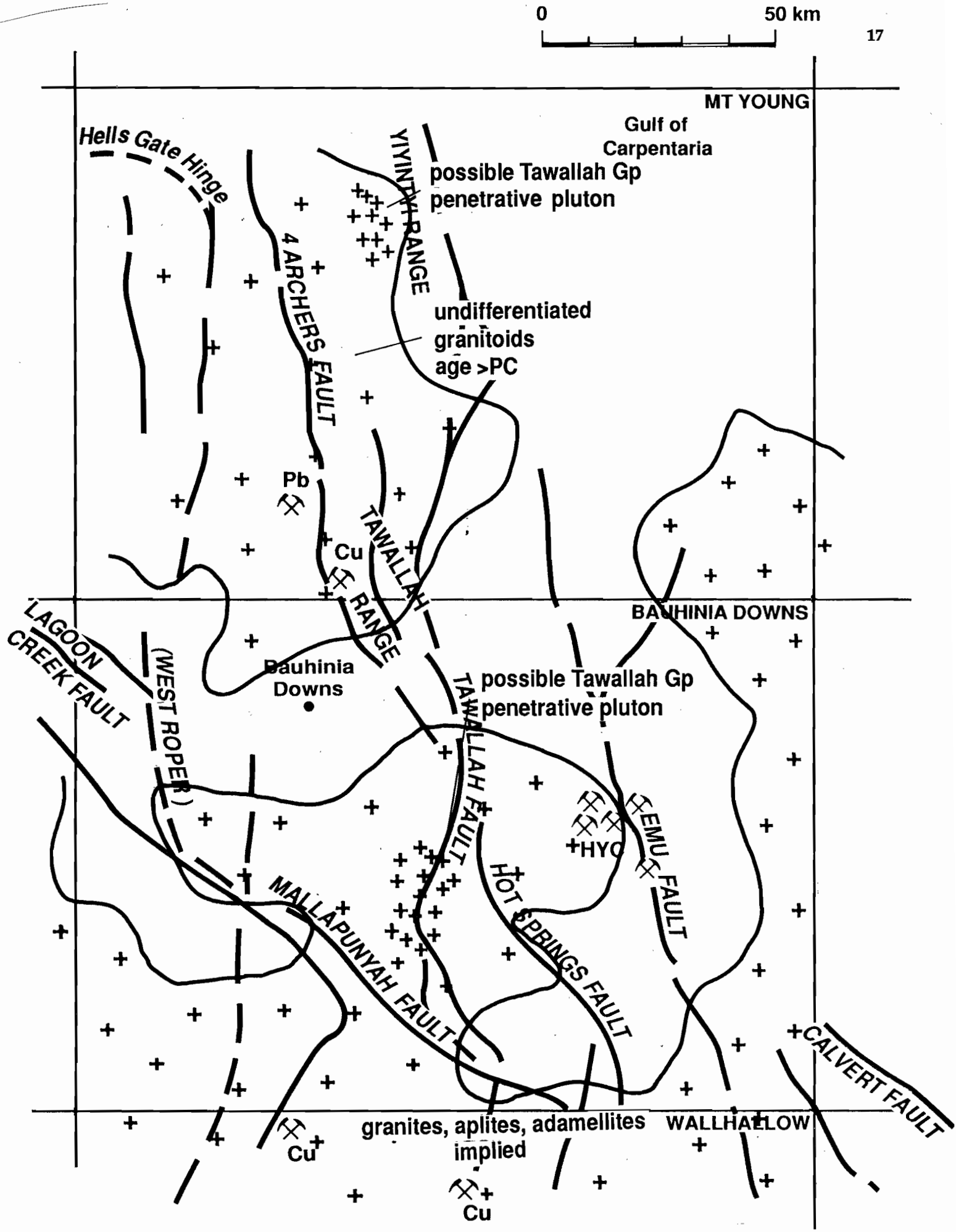

Figure 7 — Distribution of basement granitoids. Largely based on gravity data. The outline suggests the coverage. The diagram does not suggest the axes of local relief. The finer pattern locates those portions of this mass, or diapiric plutons, which possibly penetrate Scrutton Volcanics and Tawallah Group.

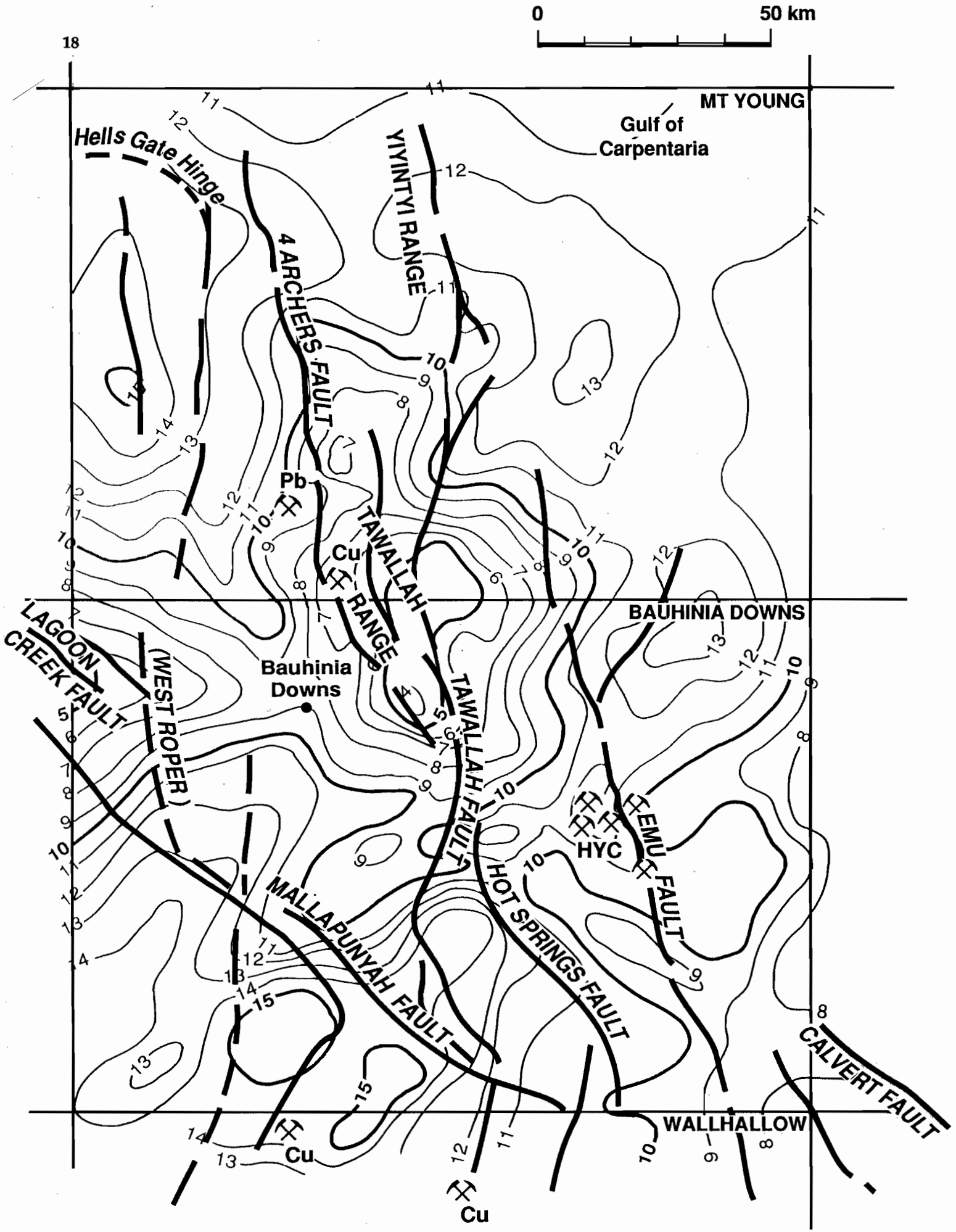

Figure 8 — Interpretation of depth to base of Scrutton Volcanics. Contours in km. Note the general disturbance along the Calvert–Lagoon Creek–Mallaypunyah axis and the general elevation of the unit in the Tawallah Range.

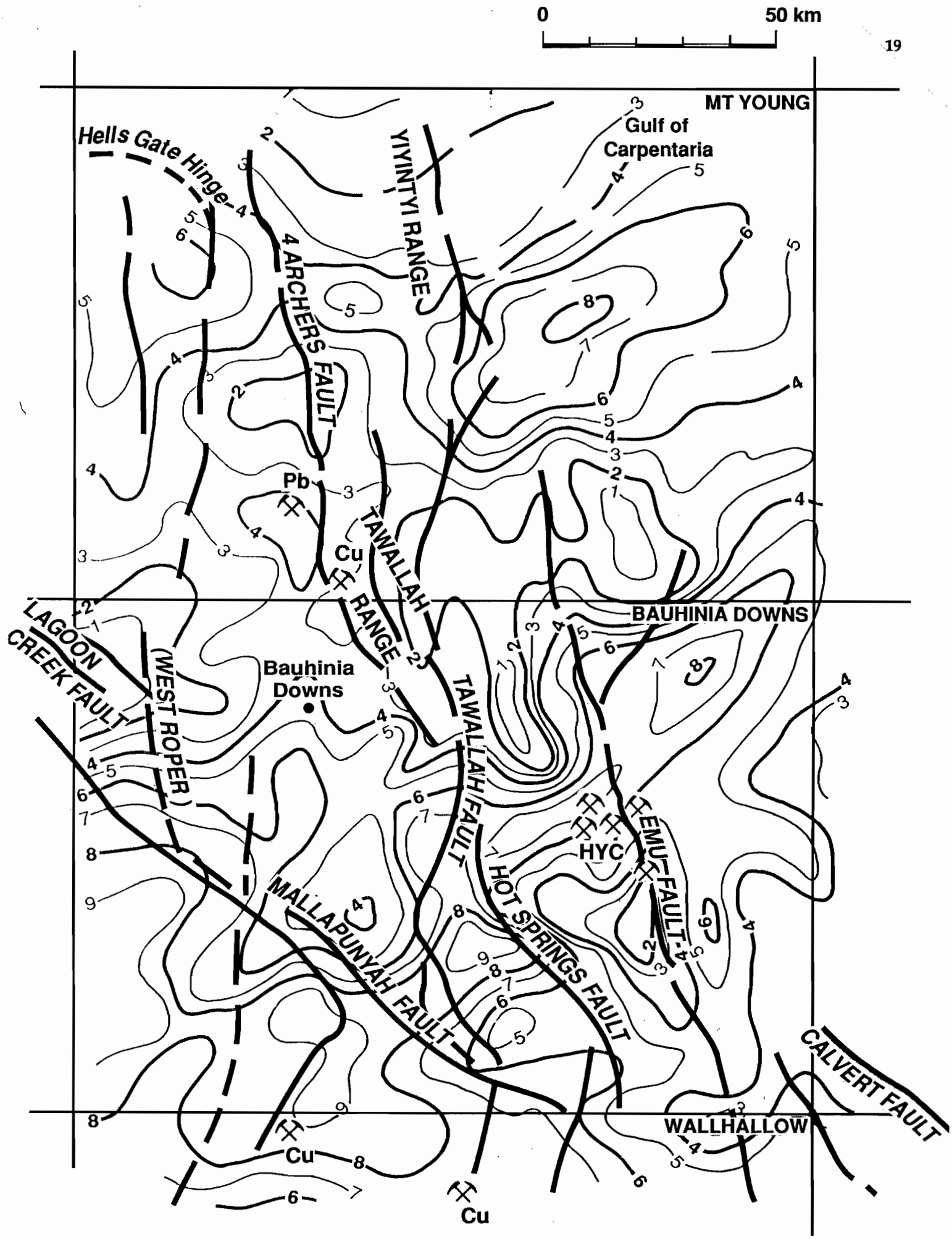

Figure 9 — Interpreted thickness of felsic Scrutton Volcanics. Note the general E-W and NE–SW trends of the formative rifts and the general thinness of the unit near the Tawallah Range.

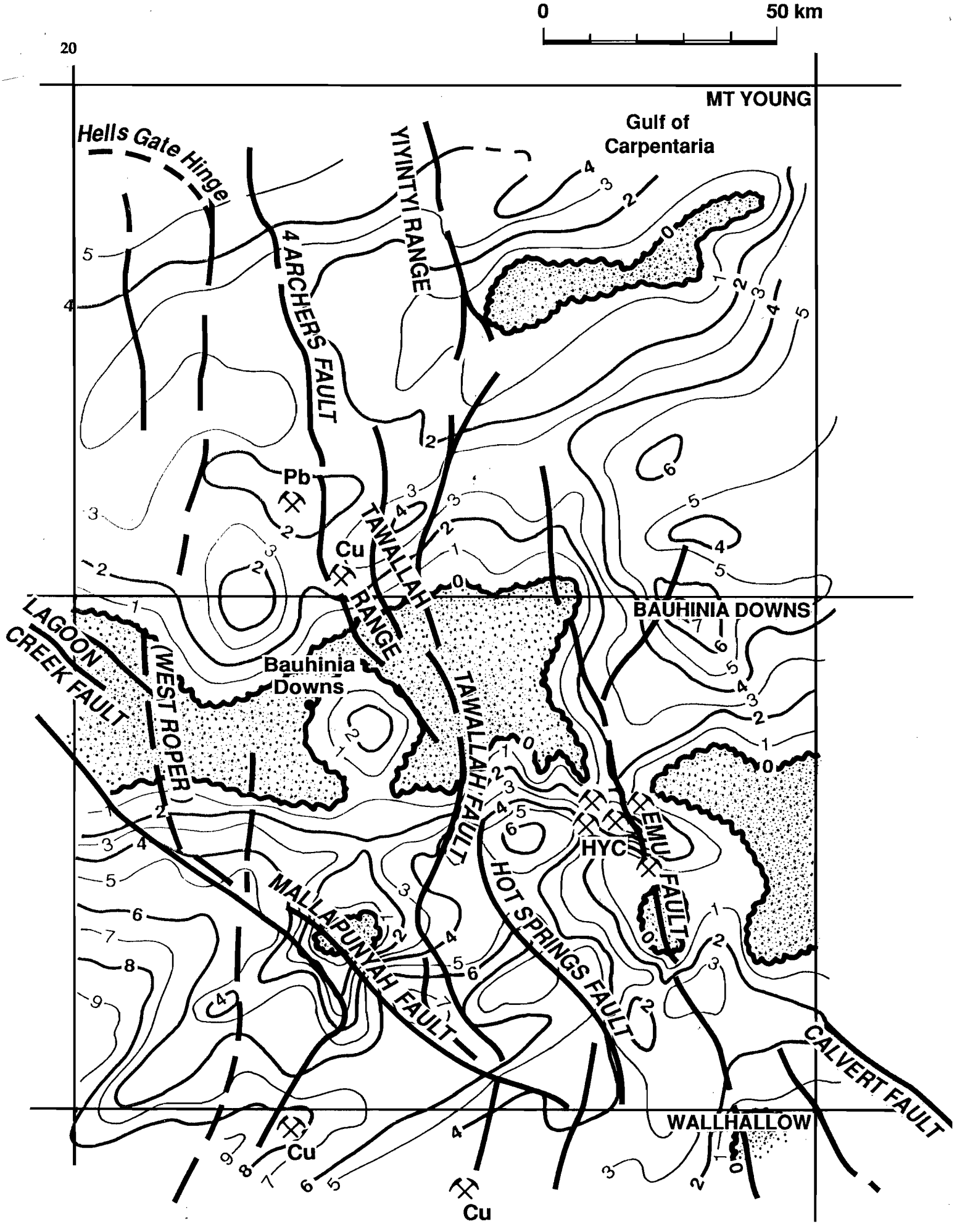

Figure 10 — Interpreted thickness of major mafic volcanic units which post date the Scrutton Volcanics. These rocks my correlate with the Seigal or Eastern Creek Volcanics of other regions. Note the strong E–W and NE bias in the deposition and the clear presence of a proto-Emu Fault. The Tawallah Range region was high during formation.

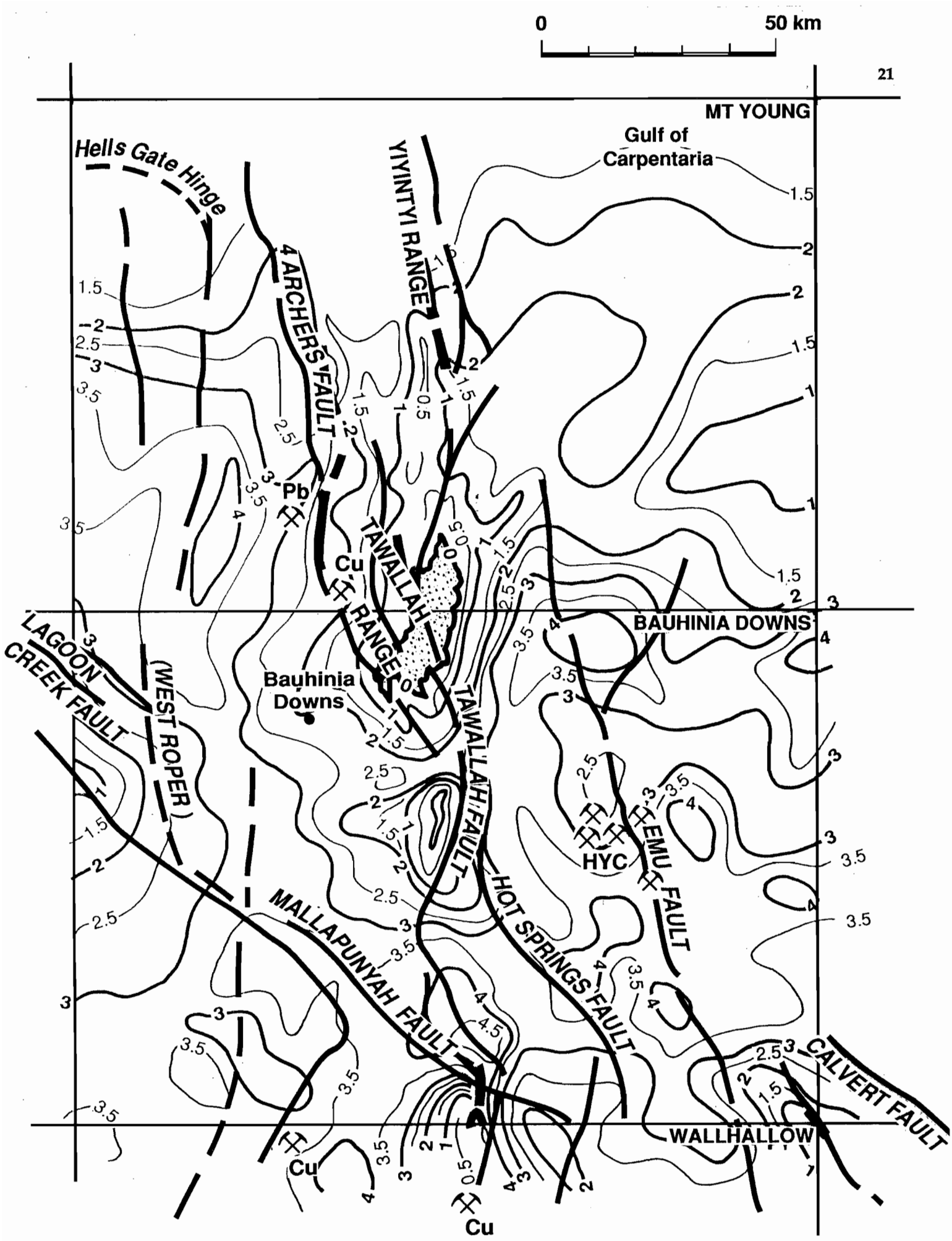

Figure 11 — Interpreted depths to upper Tawallah mafic volcanics. This diagram may integrate the effects of several units, if more than one is present, or locate the mean depth. The figure should be used as an indication of distribution and form. The Tawallah axis is strongly defined but no eastern margin of any trough has been found.
Contours in km.

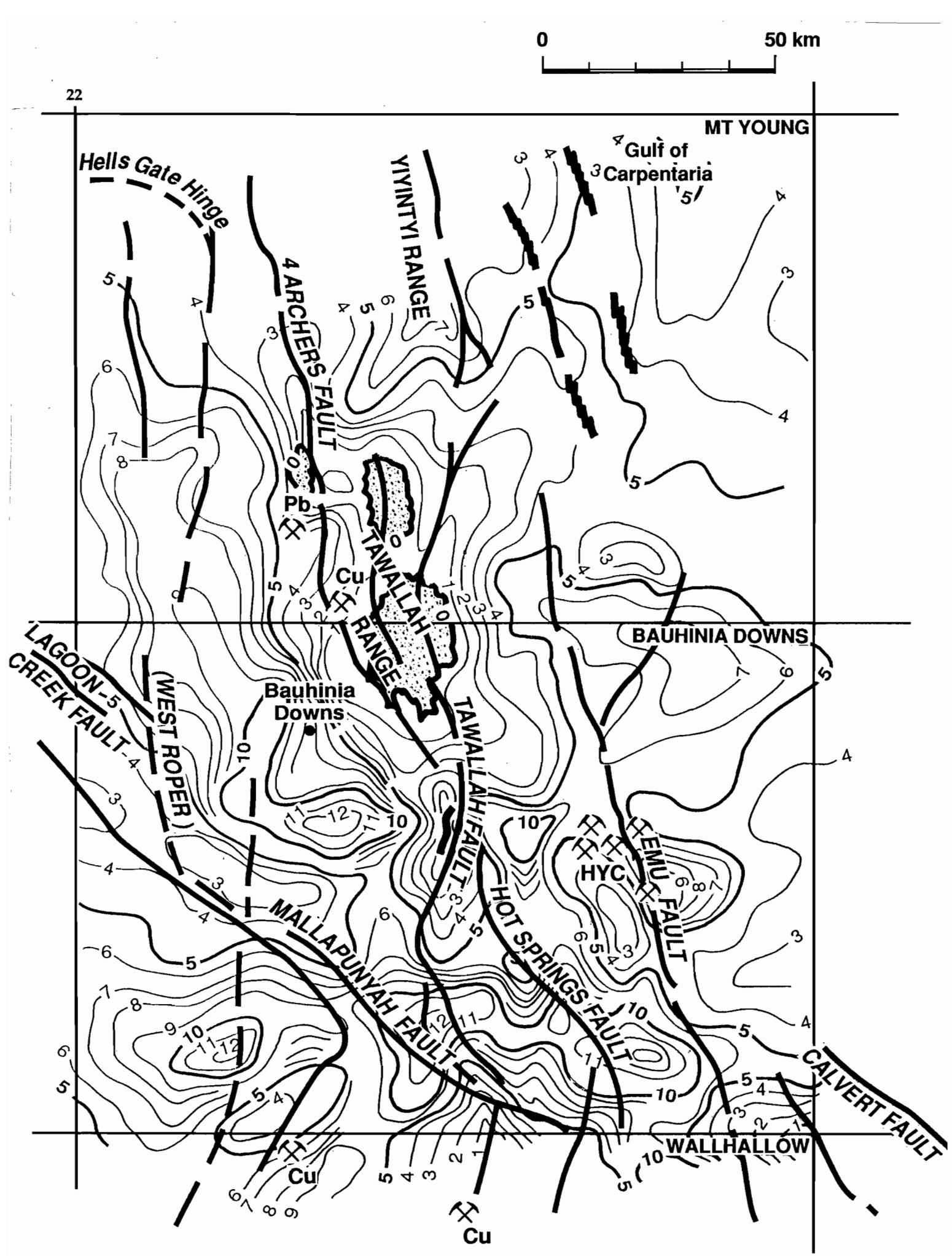

Figure 12 — Interpreted thickness of upper Tawallah mafic volcanics. This interpretation must be considered approximate since many variables may interfere with the conclusions and the analysis completed is limited in terms of these units. The figure does stress the disturbed and variable nature of the units in the region of the Mallapunyah and southern Emu Faults. Contours are in hundreds of metres.

present work. Thus the thickness shown may be a summation of two or three units separated by sedimentary thicknessess not much greater that those of the volcanics while the top depth may be a depth pick on the dominant local volcanic if more than one member is present. It is not thought that these ambiguities are particularly critical since all evidence indicates that only parts of the Tawallah Volcanics are magnetic and that only one member offers substantial magnetic contrasts in any given section or locality.

The depth to volcanics largely mirrors modern surface geology but there are suggestions of the Emu and Calvert Fault systems. Apart from a zone which corresponds to the concealed E–W change in underlying basement, discussed above, the units are elevated in the region of the Tawallah Fault and range axis. Thickness variations appear less systematic but there is a clear relationship between this axis and that of the Calvert–Mallapunyah Fault systems. Some local pods occur along the Emu Fault zone. The HYC zone appears to have retained its local activity in these terms on the northern side of a broad E-W axis just south of the centre of the Bauhinia Downs sheet.

A final compilation is offered for the McArthur Group (figure 13). This incomplete diagram, based largely on gravity interpretation, can only show what now remains of these units. It does show some interesting features,however. It indicates that the group once extended very widely and has now been truncated or removed by subsequent erosion and deposition well to the east of the Emu Fault except in the area near HYC. This implies much activity subsequent to, or during, deposition in this central area. Similar cut outs occur beneath the Abner Range and along the Tawallah Range implying activity pre Roper Group deposition. The diagram also suggests that some of the modern distribution has been influenced by the underlying Calvert Fault system. If this material was deposited in a "Batten Trough" then its location is not as previously described.

Trend information, from raw data plots and interpretation, are shown in a weighted form in figure 14. Greatest weight is given to features which are structurally now well defined. This stresses the relative roles of particular features and relationships to exposed features.

The interpretation, as indicated by the sections and diagrams included, suggests some very complex growth and inherited relationships within the Batten Trough region. An attempt has been made to quantify these in the table 1. The table presents results from each of the sections modelled in terms of the major faults in each part of the trough. Table 2 summarises these results.

COMMENTS ON INTERPRETATION

A number of assumptions are implicit in the analysis described. These include a presumption that the Scrutton Volcanics are magnetised in bulk, even if variably, and that some elements of the mafic volcanics within the Tawallah Group are also magnetic. Both assumptions may be verified from inspection of both analysis and direct correlations to exposures although it is clear that the thickness and contrast combinations offered by the Tawallah Volcanic members are both variable and patchy. It is also very likely that the various members, such as the Settlement Creek, Peters Creek and Seigal Volcanics are absent in parts of the region or locally thickened in others.

The influence of any "magnetic basement" other than the Scrutton Volcanics may be discounted following extensive review in combination with the assessment of granitoid distribution.

Maximum contrasts have been employed throughout in order to allow for remanence and regional integration effects. These contrasts coupled with a presumption that interference effects are ubiquitous (also verified) and use of interlocking profile arrays for both gravity and magnetic data have ensured some consistency and increased confidence in the general reliability of any conclusions.

The inferred magnetic contrasts directly reflect the mafic content in any volcanic sequence.

The analysis has demonstrated that there are variations in depositional patterns of Scrutton Volcanics and other volcanics and that it does not much matter whether the magnetically effective Tawallah Volcanic member is a single member of the sequence or some local combination (or in some cases, absent). The level of this treatment designed to define gross elements of stratigraphic continuity and basin architecture is unaffected by minor variations within the Tawallah section. This is not to say that these are unimportant, or unable to be resolved, simply that they have been beyond the scope of this review. It is clear, however, that the Tawallah Volcanic members are relatively insignificant when compared with the bulk of the Scrutton Volcanics but that they are podded and variable. The review has shown that systematic variations can be defined which are interpretable in terms of basin history with direct links to mineralised province patterns.

The need to deal with very large volumes and long sections yields quite different response patterns from those normally expected in potential field analysis. These patterns, at all scales, turn out to be quite sensitive and relatively unambiguous when combined with rigorous interpretation and profile fit criteria. This unusual application of potential methods for basin architecture study is clearly workable.

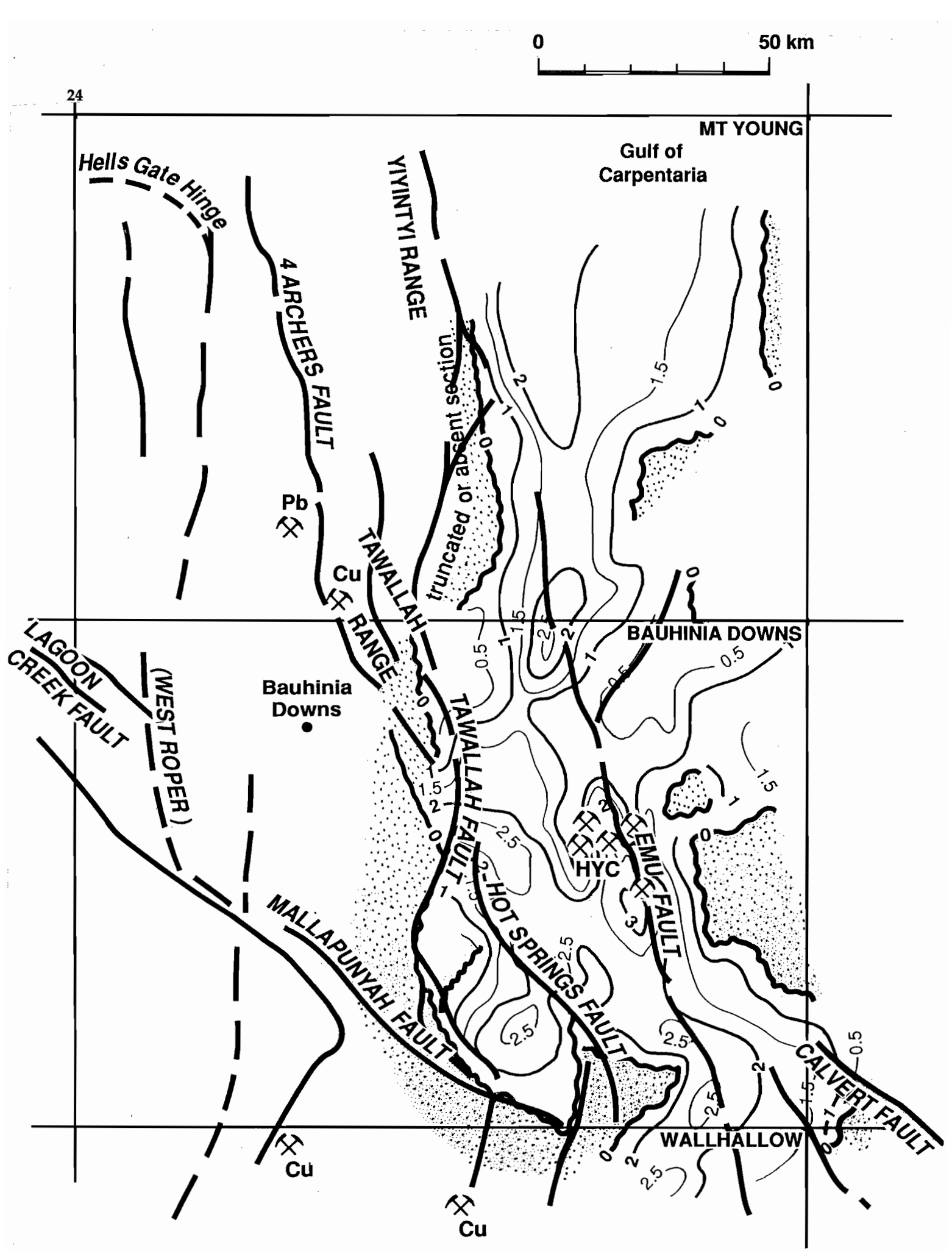

Figure 13. — Interpreted distribution of more massive sequences in the eastern McArthur Group. Structural and depositional truncations indicate the present distribution and suggest it was once more widespread, especially to the east. There are only localised indications of control by the Emu Fault system. Contours in km show residual present day thicknesses.

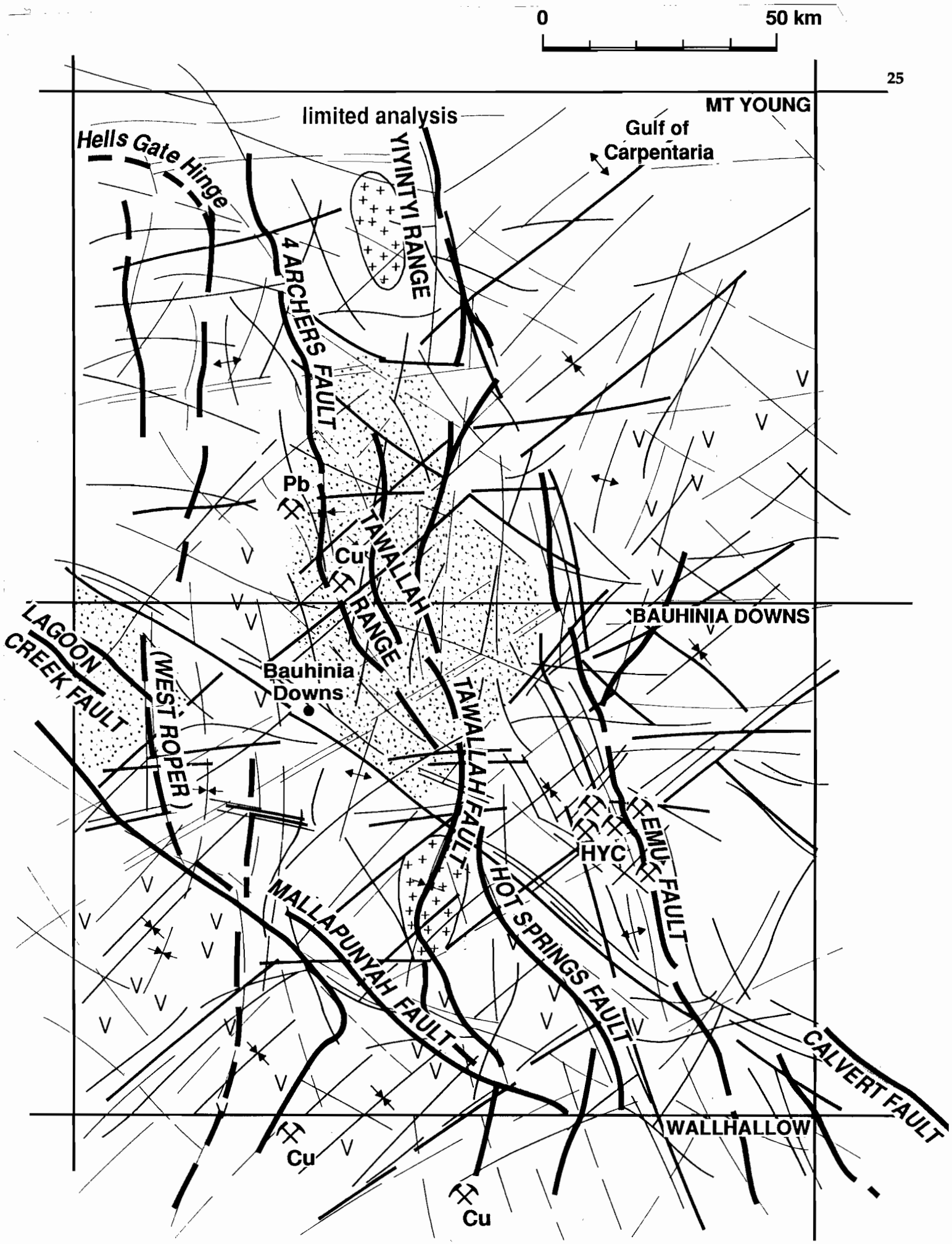

Figure 14 — Principal trend patterns recognisable in both raw data and interpreted structures. Lighest line weights refer to trends seen in regional gravity and magnetic compilations. Heaviest weights apply to structures and trends interpreted. Inferred granitic diapirs are also indicated.

Table 1
Results from each of the sections modelled in terms of the major faults in each part of the trough.

Profile	Unit	Lagoon Ck	West Roper	Tawallah	Emu	Mallapunyah
1MH	Sv	0	≤ 6	2.5GDW	≤2-4GDE	see LCF
	Mf	0	0	3GDE	≤6GDW	
	Tv	0	0.5-1	<0.5	<0.5GDW	
	MAG	0	<1	>2.5	>1	
	ROP	1	3.5	0?	>0.2	
2MFrev	Sv	≤5	≤5	3.5G~ >	3.5GDE	-
	Mf	0	0	>1.5GDE 2	.3GDW	
	Tv	<0.3	?	<0.3DW	0.3-1G~	
	MAG	0	0	<<1	>3DE	
	ROP	0?	>=3	0?	0?	
3MI	Sv	-	4 0	-1.5GDE	2-4GDE	1-2 DW
	Mf		>5	3-6GDW	~1.5GDW	>5~
	Tv	>1	1 ~	0.3-1GDE?	>1~	
	MAG		>3	>1.5	2-3+GDE	
	ROP	0?	>1	0?		
4MF	Sv	~1	2DW	3	2-4GDE	see LCF
	Mf	0	0-1GDE	0$	0-2+GDE@	
	Tv	<0.5	1	0.5	0.3-1GDE	
	MAG	?	?	0?	>3GDE	
	ROP	~0?	>2.5DW	0?	0+	
$ DW/Fault W	@ scissor from lines 3/4					
5MD	Sv	0	0-1GDW	0-11GDE	1	
	Mf		9GDE	9-10GDE	0-6GDW	11
	Tv		<1	1+	0.3-1GDW	~1
	MAG		0	?	>2.5	?
	ROP		3.5GDW	1+GDE	?	(3.5GDW)
6MH	Sv	-	-	thins to unclear -		
	Mf		"	"		
	Tv		"	"		
	MAG		"	"		
	ROP		?	"		
7MH	Sv	-	11GDW	4-7GDE	5-8GDE	~9DW
	Mf	~0	0-3DE	2-3GDW	~0	
	Tv	>1	0.3-0.6GDE	0.5+GDE	0.5-1+GDE	
	MAG	>2?	0-2GDE	2-3GDE	?	
	ROP	3	?	?	0-3GDW	
8ME	Sv	0-1GDE	?	1-3GDW	<1-5GDE	2-5GDE
	Mf	9DW?	?	4-5GDE	0-5GDW	3-5GDW
	Tv	<1		0.5	0.5	0.3
	MAG	?		?	?	?
	ROP	1-3GDW	?	?	?	

Table 1 cont.

Profile	Unit	Lagoon Ck	West Roper	Tawallah	Emu	Mallapunyah
9MD	Sv	1-2GDW	1-5GDE	0-9GDW	0-1GDE	-
	Mf	0	0	0->2GDE@	3-4GDW	
	Tv	0.6-1GDE	?	0.4	0.3-1.5at	
	MAG	?	<1?	0-2.5+GDE	0-3GDW	
	ROP	0-0.5GDE	1-4GDE	?	?GDE	
@ split fault						
10MD	Sv	-	4-6GDW	0-2GDE	<1+GDE/W	3-5GDE
	Mf	0-1GDE	3-5GDW	3-5GDW	0	
	Tv	0.3	0.3	0.3-1GDW	0.3GDW	
	MAG	0?	0?Hi	>2.5	?	
	ROP	1-3GDE	0	?	?	
11MC	Sv	-	-	0-1.5GDW	-	5-7GDW
	Mf		0		0-1GDW	
	Tv		0-0.3		0.5	
	MAG		?		?	
	ROP		?		?	
12MA	Sv	see Malla	-	-	-	1-3GDW
	Mf				1-2.5GDW	
	Tv				0.4	
	MAG				?	
	ROP				0-2.5GDE	
13MA	Sv	-	-	-	1-2.5GDW	2-4.5GDW
	Mf			3-4GDE	1-2.5GDE	
	Tv			0.3	0.3	
	MAG			?	?	
	ROP			2-3GDE	2- 3GDW	
14MC	Sv	-	3GDW	0-1GDE	5-7GDE	0-2GDW
	Mf		5.5?	4-6GDE	0->2GDW	4-6GDE
	Tv		0.3	0.3?	0.5	0.4
	MAG		0	?	2+?	?
	ROP		>2.5	0?	>1GDE	0-3GDW
HYC	Sv	-	-	1.5-2.5GDE	2.5	0.5-1.5GDE
	Mf		2-3.5GDW	2.5	4-6GDW	
	Tv		0.3-0.5GDW	0.2-0.6GDW	0.3-0.8GDW	
	MAG		?	0-3GDW	?	
	ROP		?	?	0-1GDE	
Situation at Hot Springs Fault						
Profile		HYC	3	5	10	9
	Sv	2.5-3.5GDW	1-3GDE	?	3*	6*
	Mf	1-2.5GDW	1.5-3.5GDW	4-6GDW	4-6GDE	0-1.5GDE
	Tv	0.3-0.8GDW	0.5-1GDW	0.7-1.2GDW	0.3-0.6GDE	0.5
	MAG	?	?	2-3GD?W	0-3GDE	0-2.5GDE
	ROP	0-1GDW	0-1.5GDW	0-1.5GDW	?	?

Table 1 cont.

Profile	Unit	West Roper	4 Archers	Tawallah	Emu W	Emu E
15MC	Sv	4=	6=	-	5*	-
	Mf	3-4GDE	2-4GDE/W$		1.5-2.5GDE	
	Yiy	?	2-4GDE		?	
	Tv	?	0.3-0GDW		0-0.3GDE	
	MAG	?	?		?	
	ROP	1.5-3GDW	0-2.5GDW		?	
$ two faults indicated; one at Four Archers, one 10 km to west.						
16MB	Sv	1-1.5GDE	2	2-4GDE	1#	1-2GDW
	Mf	4	4	4-6GDE	5-6GDW?	5-6GDE
	Yiy	?	2-3GDE	1-2GW	-	-
	Tv	0.3-0.5#	0-0.3GDW	0-0.3GE	0.3-0.5GDE?	0.4
	MAG	?	?	?	?	?
	ROP	0.6-2.5GDW	?	?	?	?
17MC	Sv	3-5GDE	4-5GDE	4-5GDW	3-4	1-3*
	Mf	4	2-3*	3-4GDE	5GDE?	7#
	Yiy	?	1.5-2.5GDE	2-3GDE	?	?
	Tv	0.3	0.2-0.3GDW	0-0.3GDW	0.4	0.4
	MAG	?	?	?	0-2GDE	0-2GDW
	ROP	0.5-1GDW	?	?	?	?
18MC	Sv	-	0.5-3GDE	2-4*	6-8GDE	6-7GDE
	Mf		3-4GDE	5#	1.5-3GDW	0-1GDW
	Yiy		1.5-3GDE	1.5-2.5GDE*	? ?	
	Tv		0.2-0.3GDW?	0-0.8GDW	0.3-0.5GDE	0.6
	MAG	?		0-1.5GDE	1-2.5GDW	
	ROP	0-1GDW		?	?	
19MB	Sv	6-7GDW	5	3-6*	7	4-7GDW
	Mf	3-4GDW	2-3GDW	0-1GDW	-	0-5GDE
	Yiy	?	?	2-4GDW	?	?
	Tv	0.4	0.	0-0.8GDE	0.3-0.6GDE	0.3-0.7GDE
	MAG	?	?	0-2GDE	?	?0-1GDW
	ROP	0-2GDW	?	?	?	?
20MB	Sv	-	-	4-6#	2-3GDW	1*
	Mf		0-2+GDE	3-5GDE	8#	
	Yiy		?	?	?	
	Tv		0.4?	0.4?	0.4?	
	MAG		0-1.5GDE	2	2-3GDE	
	ROP		?	?	?	

The following abbreviations have been used:

Sv	Scrutton Volcanics	Mf	mafic volcanic component
Tv	Tawallah Volcanics	MAG	McArthur Group
ROP	Roper Group	G	growth fault at this stage
Yiy	Yiyintyi Sandstone	E/W	to east or west
*	thickens at	#	thins to
=	no change at fault	D	down or thickening

Values given are approximate thickness changes in km.

Table 2: Summary

Unit	Fault	Lagoon Creek	W Roper	4 Archers	Tawallah	Hot Spr	Emu W/Emu E	Mallap
Scrutton	DW	9	7,10,14,19		1,5,8,9,11, 17	HYC	13 20 /16,19	3,9,11,12, 13,14
	DE	8	9,16,17	17,18	3,7,10,14 16,HYC	3	1,2,3,4,5,7,8, 9,(10),14 18/18	8,10, HYC
	AT				16,18,19,20	9,10	15 –/17,20	
Mafics Late Sv or Seigal?	DW	8	17,19	17,19	3,10,19, HYC	HYC 3,5	1,2,3,5,8,9, 10,14 16,18 /18	8,12, HYC
	DE		4,10,15	17,18	1,2,5,8,9, 16,17,20	9,10, 14	4,7,13 15,20/19	13,14, 16
	AT			15,17	18		–/17,20	
Yiyintyi	DW				16,19			
	DE			15,16,17, 18	17,18			
Tawal Volcs	DW		16	15,16,17 18	2,17,18 HYC	3,5 HYC	1,5,10 HYC	HYC
	DE	9			7,16,19	10	3,4,7,15 18/16,19	
Mag	DW					5	9,HYC 18 /17,18,19	
	DE				7,9,19,20	9,10	2,3,4,7 17/20	
Rop	DW	8	4,5,15,16, 17,19	15,18		3,5,HYC		5,7,13, 14
	DE	9	9,10		5		9?,13,14	12,HYC

Note that the Lagoon Creek Fault reverses character after the Scrutton Volcanics while the West Roper which responds similarly is affected by the Mallapunyah differentially from N to S. The Tawallah Fault is variable throughout its history and from N to S. The Emu Fault shows all motions to east or south to north at Scrutton stage but the southern zone switches with the mafics and this character is then maintained through to McArthur Group deposition but the central section is active throughout this deposition. The Mallapunyah Fault shows a main reversal at the end of Scrutton deposition but is subsequently reversed prior to Roper Group deposition — during late McArthur Group times?
DW, DE indicate sense of change/fault; AT implies changes localised near fault only.

There are some elements which require further review.

Not all materials in the McArthur Basin or surrounds have yet been sampled by profiles or analysis, including true basement inliers such as the Murphy Tectonic Ridge. Complete linking of these elements and the present study area will ensure and test the validity of the curve fit criteria and verify continental scale relativities in the models. Some revision is to be expected as analysis extends regionally.

CONCLUSIONS

The present work has shown that useful results can be obtained from quite crude data sets using simple potential field methods very rigorously applied. Enough systematic and credible relationships have been established to show that the style, if not absolute magnitudes, of significant elements of the basin architecture relevant to exploration, mineralisation control and fluid system studies can be derived. Detailing to prospect or target scale is feasible but requires some improved rock property data and use of three dimensional procedures within the regional skeleton provided here.

Analysis has shown that:

1. The volcanics of the Tawallah Group are relatively thin, commonly basaltic and often patchily developed. There is little evidence that all members are regionally continuous. Systematic changes occur near particular faults.
2. There are quite variable relationships between unit thicknesses and faults, including some not previously named or regarded as significant in their near surface expression. There has clearly been a long history of movement and sediment/volcanism control. The most important event resetting and inverting motions occurred following deposition of the Scrutton Volcanics and prior to mafic cover. Most faults have behaved consistently since that time although local hinges and scissors are implied across the basin. Some clear wrench movements are also indicated in association with such variations.
3. The fault patterns deep in the basin are very different from those now exposed. The fundamental deep grain is sub E–W with an evolution to ENE and finally N–S with persistent NW–SE elements. One of the more important of the latter is an extension of the Calvert Fault.
4. Mapping of the base of the Scrutton Volcanics, apparently very deep and which might be expected to be insensitive to treatment — but is not, shows that these primary controls have long been active. The central doming which has resulted in modern exposure of this unit is also an old feature. A central rift uplift belt would be consistent with this evolution since it must be active throughout the entire history of the region. Thickness estimates of the Scrutton Volcanics stress the regional sub E–W control and local ENE rifting of the period.
5. These changes are clearly defined by the overlying mafic volcanics. Plots of inferred thickness reveal both E–W and ENE trends with general absence of these materials along E–W axes. But, for the first time, the influence of an Emu Fault is apparent, possibly as a sinistral shear or transform, while the influence of the Calvert Fault system is much diminished. The HYC mineralisation and associated prospects all lie close to a primary triple point involving these structures and these thick mafic volcanics. Note that this is second stage basin development since all indicators show that an inversion was effected prior to this activity.

   A fundamental question is, just what are these mafic volcanics? There is no evidence to suggest that they are connected with any of the upper volcanic members of the Tawallah Group. They may well be basal, however, and perhaps correlates of the Seigal or Eastern Creek Volcanics of other parts of the Isa — Carpentaria region. This may be resolved by expansion of the analysis to the SE to, and across, the Murphy Inlier. There is no doubt, though, that these volcanics are present, are often very thick, strongly magnetised, certainly mafic and were deposited in their own sub basins unconformably above the Scrutton Volcanics.

   A substantial, persistent extensional regime is indicated.
6. Consideration of the upper Tawallah Volcanics and the McArthur Group shows that many of the modern elements of exposed structure have become dominant although basically controlled by the concealed deep seated structures. Activity is variable and localised with continuity and deformation distortions imposed by older features. Structures such as the Emu Fault, in its two parts as they fan toward the gulf north of HYC, have remained active throughout sedimentation. This is demonstrated by the thickness changes associated with such structures. Most of these changes cannot be confirmed by surface mapping or shallow drilling since the information base, or exposure, does not permit it. Such variations can be inferred from the potential field data.
7. The Roper Group sedimentation has been controlled by different elements of the deep structure and this has affected its distribution

and overlaps with the McArthur Group. The structural bias was now very much N–S. Many faults with this orientation have been mapped or inferred in the Mt Young sheet and many of these are more important than might seem to be the case. The Four Archers Fault is an example. This named fault is considered important, rightly, but it has companions to east and west, which at various times have been more significant.

8. This preliminary work has several important implications for exploration as well as evaluation of controls and emplacement of mineralisation.

   It has been shown that the total sediment and volcanic pile within the basin is up to 14 km thick; about half of which may be composed of volcanics of various compositions. This thickness represents the preserved thickness and excludes some removed portions of Roper or McArthur Group sequences. All known mineralisation occurs in areas where the thickness of the pre-Roper section exceeded 10–12 km. At least half of this section is comprised of acid and mafic volcanics older that lower Tawallah Group or basal to it.

   If it is argued that fluid circulation is from the top down then these rich sources of mineral nutrients are not only thick but deep. Alternatively any passage of fluids upward through the section will pass some very important source assemblages, but the paths will be long. The proportions of particular compositions available at any given location, coupled with the fracture controls available, may well have governed much of the result in terms of ore blend. All mineralised sites compiled to date seem to bear some relationship either to thick volcanic sections or structures marginal to thick sections, as well as intersections of crustal scale structures.

   The relative rarity of the HYC region is stressed by even the present crude regional analysis. Other zones approaching comparable complexity are presently concealed by post Roper Group sedimentation.

   Copper mineralisation appears to be associated with the thickened side of half grabens containing much mafic volcanics while other base metals are associated with persistently active zones rather than any predominance of rock type. This inference depends upon the current compilation of mineralised sites and review of both this area and others may well change the conclusion.

9. The heat engine required to drive any circulation mechanism may be related to granitoids or the disturbed thermal conditions within a complex and evolved and deep extensional basin. The present analysis cannot exclude the possibility that at least two granitoids within the apparent basement have intruded high into the Scrutton Volcanics. This appears to have occurred within the Tawallah-Yiyintyi axis and nowhere else. This zone contains thin sequences generally and elevated basement within the basin core which must have been continually rising during extension. The nearest interpreted granitoid of this type lies no more than 30 km from HYC. The age of this body cannot be defined with certainty from this analysis but may, given correlations with the nearby Calvert Hills area, be contemporaneous with at least part of the McArthur Group. This possibility must also be considered in any evaluation of fluid transfers.

10. This interpretation shows that many previous published inferences made about the Batten Trough relate to shallow components and that a very different history and structural control pattern exists at depth. The evolution of the HYC region cannot be understood without this crustal overview. A corrollary to this conclusion poses the question, just what and where is the Batten Trough? Should the term be associated only with the McArthur Group? Concepts of a N–S axis can only apply to the younger parts of this basin and its evolution.

Some comments may also be offered on previously published conclusions such as summarised in the section "The Geological Problem". Comment numbers refer to the original statements.

1. A granitoid, possibly equivalent to the Norris Granite, may intrude to Tawallah level within the Batten Trough region also.
3. There is no question that deep basement controls have persistently elevated the Tawallah Range anticlinorium zone.
4. The block east of the Tawallah Range has ***not*** been passive, but very active.
5. The zone west of the Four Archers Fault has ***not*** been very stable and ***no*** 6 km throw is possible. Thickness changes implicit.

7, 8, 20, 22, 33

The Batten Trough is a late conception (compare figs 8, 9, 10 and 13). The Emu Fault is a complex feature which has ***not*** confined the McArthur Group sedimentation.

9, 10, 26

It is established that depocentres shifted westward between McArthur Group and Roper Group times.

10. 7.5 km of vertical movement is ***not*** sustainable in the Batten Zone.

11, 18

All major faults ***are*** part of major north Australian grain and it is sub EW or NW–SE.

12. The Calvert Hills-Mallapunyah Fault system is

persistent through time and has offset and hinged motions on both Emu and Tawallah Faults.

14. The Emu Fault *does* have different hinged motions in time and space.
15. Modern fault expressions are controlled by deeper forms.
17. Trace copper south of the Mallapunyah Fault zone reflects the presence of thick, concealed mafic sequences in this region.
19. Tawallah Group subsidence occurred more to the NE than NW.
21. There is no evidence that the McArthur Group ever exceeded 4.5 km in total.
23. Activity of the Emu Fault during McArthur Group time is regionally supported.
27. There is no evidence of rift widening to the south — unless one refers to pre-Tawallah Group times.
28. A total sedimentary section up to 15 km thick does exist but *not* in any one place. Simple section totalling is invalid due to complex overlaps. Post Scrutton sections rarely exceed 5 or 6 km.
29. No deep metamorphism has been recorded anywhere, and especially not in the exposed Scrutton (supposedly once very deeply buried) simply because the exposed Scrutton zone has *always* been high and thinly covered. No such metamorphism should be expected there.
30. The Tawallah Fault has been long-lived.
31. The major magnetic high in the HYC region is **not** a high in basement. It is a function of mafic distribution and section geometry but this cannot be determined without the array analysis reported here.

1, 32 The central gravity low in the Abner Range region is **not** related to any exposed rocks or sub groups of the Tawallah or McArthur Groups. It is related to a penetrative granitoid (= Norris?).

34. Mafic volcanics are *not* restricted to Wearyan Shelf.
35. Any magnetic basement judged on simple analysis represents either top Seigal (?) or top Scrutton and their equivalents.
36. NE trend patterns have been verified.
37. There is absolutely no doubt that different rifts in different periods have evolved in different places and with different orientations in the time covered by the base Scrutton to top Roper Group.

RECOMMENDATIONS AND FURTHER WORK

It is now intended that the methodology described in this report be applied to adjacent areas. The next stage of analysis will consider the shelf zone SE to the Murphy Inlier. Subsequent study will extend to the Century area and the Kamarga Dome. A continuous linked analysis is proposed in order to incorporate all known major geological elements and allow review and revision under increasingly constrained and tested assumptions. The feasibility of basin analysis by these means is now considered established in this region.

The aim of this analysis is to derive a family of architectural relationships for each major mineralised site and to inspect these for ruling patterns which might assist target selection elsewhere as well as constrain fluid-dynamic and geochemical concepts and experiments. Many high level, or exposed, structures may well be re-interpreted in terms of concealed basin forms as a result.

There is a need to inspect such seismic data as does exist in order to provide independent tests of any implications. One such test has already been attempted using published reflection seismic panels (Collins, 1983). Although the soundings provide limited coverage and the published diagrams are difficult to examine reflections at about 1, 2, 2.5, 5, 6, 7.5 seconds at HYC can be converted to depths of about 2.5, 5, 6, 12, 15 and 19 km respectively. The first four of these can be recognised in the present interpretation; base McArthur Group, base Tawallah Group (?) mafics, top Scrutton volcanics, base Scrutton volcanics.

While the style of analysis reported here does not require detailed or modern data, or data in digital formats — whether images or profiles, more detailed work within the present regional framework would benefit from such data. This has been considered beyond the scope of this phase or this element of the project. It should also be noted that image analysis will not reveal the information extracted and reported here which requires comprehensive quantitative analysis of the data set.

REFERENCES

Ahmad, M. & Wygralak, A.S., 1989. *Calvert Hills* (SE53-8) 1:250 000 metallogenic map series, explanatory notes. Northern Territory Geological Survey, Darwin.

Collins, C.D.N., 1983. Crustal structure of the southern McArthur Basin from deep seismic sounding. *BMR Journal Geology & Geophysics* 8, 19-34.

Jackson, M.J., Muir, M.D. & Plumb, K.A., 1987. Geology of the southern McArthur Basin Northern Territory. *BMR Bulletin* 220.

Leaman, D.E., 1992. Criteria for evaluation of potential field interpretations. *Ext. Abs. Vol., 54th Annual meeting EAEG Paris, June.*

Pietsch, B.A., Wyche, S., Rawlings, D.J., Creaser, P.M. & Findhammer, T.L.R., 1991. *McArthur Region* (6065-6165) 1: 100 000 map series, explanatory notes. Northern Territory Geological Survey, Darwin.

Plumb, K.A. & Paine, A.G.L., 1964. *Mount Young* (SD 53-3) explanatory notes and map. Bureau of Mineral Resources, Canberra.

Plumb, K.A. & Wellman, P., 1987. McArthur Basin Northern Territory. Mapping of deep troughs using gravity and magnetic anomalies. *BMR Journal Geology & Geophysics* 10: 243-252.

Plumb, K.A., Rhodes, J.M., Randal, M.A., & Nichols., 1962. *Wallhallow* (SE 53-7) 1: 250 000 geological map sheet. Bureau of Mineral Resources, Canberra.

Smith, J.W., Roberts, H.G., Plumb, K.A. & Webb, A.W., 1963. *Bauhinia Downs* (SE 53-3) 1: 250 000 geological map sheet. Bureau of Mineral Resources, Canberra.

Structures in the Southern McArthur Basin

R. A. Keele and J. Rogers
Centre for Ore Deposit and Exploration Studies

INTRODUCTION AND PRIMARY AIMS

The regional geological setting of sediment-hosted base metal deposits within Australian Proterozoic sedimentary basins is at present, poorly understood. Those studies which have been undertaken have placed minimal emphasis on regional basin structure.

In the southern McArthur Basin, deposition of sediments that host base metal mineralisation has primarily been structurally controlled. Furthermore, mineralising fluids have been focussed along major structures at many localities. In consequence, the primary aims of the present research are to investigate:

- the structural evolution of the basin.
- relationships between basin structure and sedimentation.
- relationships between basin structure and the generation and movement of Pb-Zn mineralising fluids.

Understanding these factors will result in the determination of a set of criteria that can be used to recognise faults which acted as conduits for fluid flow. This could ultimately lead to the establishment of possible fluid pathways for mineralising fluids within the southern McArthur Basin.

These problems are being addressed by mapping selected fault structures within the southern McArthur Basin. Particular attention is being paid to fault attitudes, kinematics and any evidence for fault rotations and reactivations.

The areas chosen for detailed regional investigation this season were the Batten Ranges and the Mallapunyah Dome. The Tawallah Ranges were also targeted for investigation, however access to the area was denied by the local property owners (Billengarah Station). Mapping was conducted at 1:25 000 and 1:10 000 respectively using a topographic base of 1:25 000 air photographs.

Batten Range

The Batten Range region contains basal Tawallah Group and McArthur Group sediments which are juxtaposed against younger McArthur Group sediments on the eastern margin of the range by the N–S trending Tawallah Fault. The stratigraphy generally youngs westward from the Tawallah Fault.

Over 100 minor faults have been observed within the Batten Range region (fig. 1). Their attitudes and kinematic histories are easily discerned by the measurement of quartz and/or hematite fault stria in outcrop. The total displacement on each of these minor faults is minimal. In contrast, three major faults are recognised in the area that do show a marked total displacement. These are the Tawallah Fault, an east–west trending fault and a NW–SE trending fault.

The west dipping Tawallah Fault shows an oblique dextral sense of movement and appears as the major structure within the region. The north dipping east–west trending fault displays an oblique sinistral sense of movement, is orthogonal to and appears to precede the Tawallah Fault movements. The NW-SE trending structure shows oblique sinistral movement and is possibly the continuation of the Calvert Fault system which has been suggested, by the geophysics, to transect the Batten Trough and Batten Ranges.

Mallapunyah Dome

Up to 60 fault striae were measured in a 15 km^2 area at the northern end of the Mallapunyah Dome; in addition, rock types, with or without alteration, were noted and magnetic susceptibilities were recorded at each location. Some of the results, subject to revision, are briefly discussed here and a preliminary map of the region will be presented at the meeting.

CODES: AMIRA/ARC Project P.384 — Proterozoic sediment-hosted base metal deposits. November 1992

The following structural features were noted:

- The NW trending Mallapunyah Fault has been re-activated at least twice during its history.
- The presence of E–W trending faults within the dome which predate the main phase of basin inversion (E–W compression) imply vertical movements of at least several hundreds of metres during an early phase of N-S extension.
- Thinned Masterton sandstone (10-15 m thick) adjacent to the Mallapunyah Fault implies the existence of a horst of volcanics at the beginning of McArthur Group times.
- N–S folds with a weak axial plane cleavage and overturning in the Gold Creek volcanics within 100 m of the Mallapunyah Fault, provides evidence that the main regional deformation is fault-related.
- The following timing relationships were observed:
  - Strike-slip sinistral was followed by dip-slip reverse.
  - West-directed thrusts were followed by east-directed thrusts.
  - Sinistral movement was followed by dextral movement.

Stress Orientations

At least three temporally distinct stress orientations are required for the generation of the three distinct fault systems during the structural evolution of the Batten Range and Mallapunyah Dome region. Further work is being conducted to quantify palaeostress orientations and timing of deformation for the region. These results will be presented at the November meeting.

Evidence for Fluid Movements

On first inspection, it is obvious that there has been a great deal of fluid flow along fault structures within the Batten Range region, although the amounts of fluids in the Mallapunyah Dome were much less. For many of these structures, this has resulted in intense silicification of adjacent sediments. This is particularly evident within the Sly Creek Sandstone (Tawallah Group). In addition to silicification, fault structures within the Sly Creek Sandstone have also channelled Fe-rich fluids which are represented by hematite breccias, as hematitic stockwork vein systems and as massive hematite. Iron mineralisation appears to be concentrated along the NNW-SSE trending faults within the Sly Creek Sandstone and is absent south of the major east-west trending fault.

Magnetic Susceptibility

A magnetic susceptibility survey was carried out over the northern Mallapunyah Dome. Two main points arise from this survey.

1. As well as the more usual criteria of texture, composition and degree of alteration, it should be possible to distinguish between the Gold Creek and Settlement Creek volcanics on the basis of magnetic susceptibility alone. The Gold Creek volcanics have susceptibilities which are at least an order of magnitude less than the Settlement Creek volcanics. This may be due to their extensive alteration .

2. The Sly Creek sandstones have marginally, but statistically significant, higher, magnetic suceptibility values than the Masterton sandstones, despite their being the cleaner looking and more silicified of the two sansdtone units. This may reflect the presence of glauconite in the Sly Creek sandsrone.

Note: Field work for the structural module of the AMIRA project has only recently been completed and all interpretations and quantitative analytical work being undertaken is still at in the preliminary stages.

Structure of the north Batten Range Region-Preliminary Map

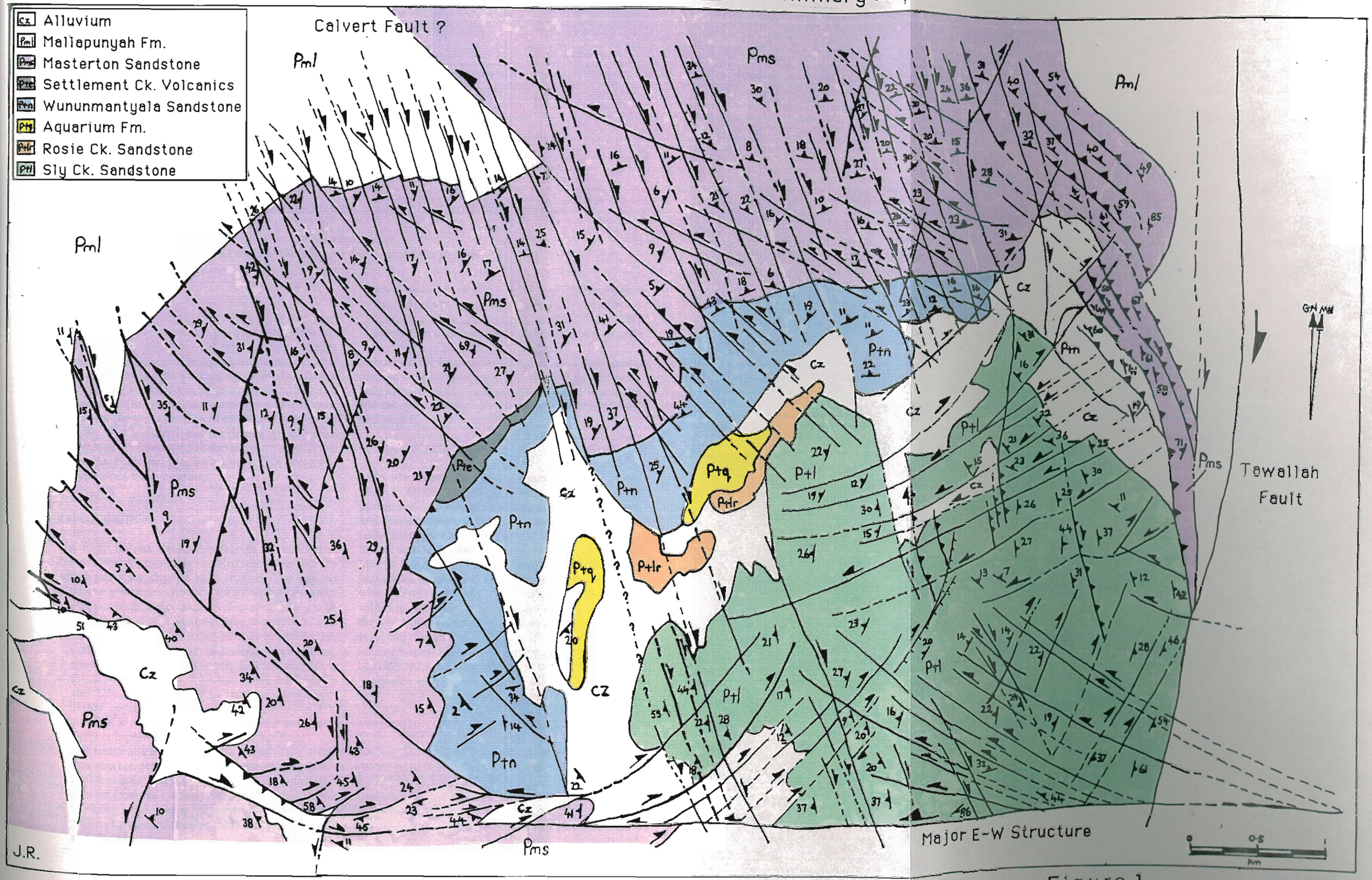

Figure 1.

back of fig. 1

DEPOSIT HALOS

1. Lady Loretta geochemical studies: preliminary results

Peter McGoldrick
Centre for Ore Deposit and Exploration Studies

SUMMARY

Work at Lady Loretta commenced in May this year. This report summarises progress to date on documenting geochemical and isotopic halos associated with the Zn-Pb-Ag mineralisation. A brief review of Lady Loretta geology is provided and some new geological observations are presented and discussed. The sampling strategy and planned analytical program are described. A preliminary set of over one hundred multi-element geochemical analyses of siltstones and shales are presented. Some preliminary discussion of these data will be presented at the forthcoming meeting.

INTRODUCTION

The Lady Loretta Zn-Pb-Ag deposit (Hancock and Purvis, 1990 & references therein) was selected a the initial focus for deposit halo studies. The deposit makes an excellent case study for a number of reason:

- a 20-year exploration and development history with extensive drill core material from the orebody and its environs; this comprises over 24 km of surface drilling and about 14 km of underground drilling, most of which is stored on site and still accessible
- the deposit is a small (8.3 Mt at 18.4% Zn, 8.5% Pb and 125g/t Ag) example of the larger stratiform SHBM deposits of north Queensland; hence, it is possible to sample the deposit and host sediments fairly comprehensively in three dimensions
- the mineralisation and host rocks have been described in detail by previous workers (esp. Carr, 1981 & subsequent papers), and a large geochemical data set from the underground drilling is available
- the host rocks are an (apparently) monotonous group of grey-black pyritic, carbonaceous siltstones and shales
- previous chemical (Zn, Pb, Cu, Ag, Cd, Hg, Fe and Ba) and mineralogical dispersion studies of samples from the surface drilling program (Carr, 1981, 1984) provide an excellent framework for further multi-element and isotopic halo studies

This report briefly describes the geology of the deposit, discusses the sampling strategy used for geochemical halo samples, and presents a preliminary data set of 104 partial analyses of Lady Loretta host siltstones and shales.

GEOLOGICAL SETTING

The Lady Loretta Zn–Pb–Ag deposit is about 120 km north of Mount Isa (fig. 1). The host rocks (variably pyritic and carbonaceous, shales, dolomitic siltstones and fine sandstones) are of low metamorphic grade (sub-greenschist to lower greenschists facies) and are folded into a double syncline structure (the Lady Loretta Syncline — Hutton, Derrick and Gallagher - Mammoth Mines Area 1:100 000 geology map, 1985) which trends north east (fig. 2). The main base metal sulphide resource forms a canoe-shaped mass near the hinge of the northernmost and smaller of the two synclines ('Small Syncline'). Locally the effects of this folding on the sulphide ores can be quite pronounced, but elsewhere the mineralisation is stratabound and stratiform and the ore horizon (OH) is a mappable unit in the Small Syncline and can be recognised to the south in the 'Big Syncline' (only a single intersection of ore-grade mineralisation was drilled in the Big Syncline). A major fault structure (the Carlton Fault) truncates the western limb of the synclines and the OH to the north and separates the Lady Loretta Formation from stratigraphically lower units of the McNamara Group. To the east the Lady Loretta Syncline is cut by the Western Border Fault and further east Lady Loretta Formation is covered by younger (Cambrian and Mesozoic) sediments and

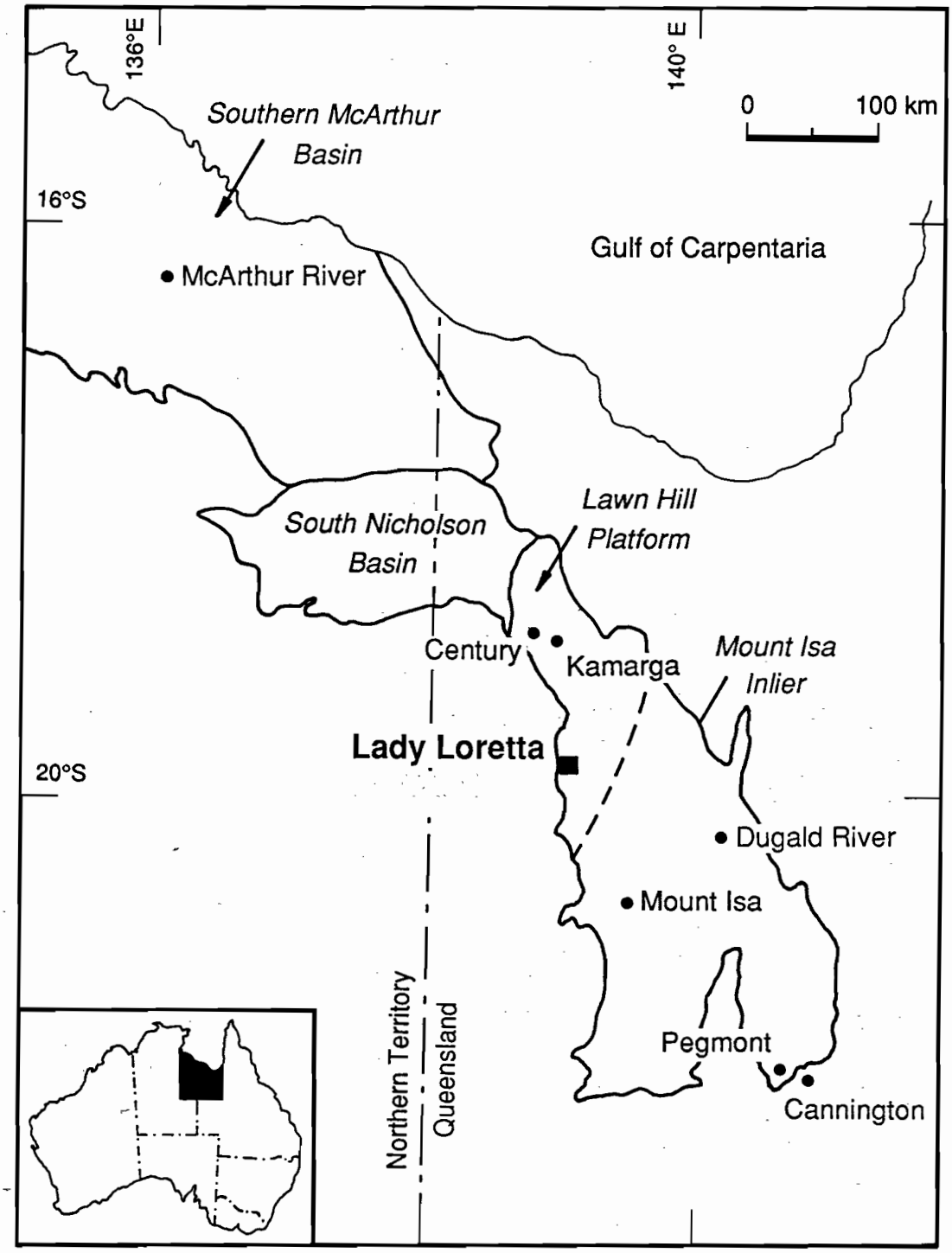

Figure 1 – Major geological subdivision of north west Queensland and eastern Northern Territory with the location of important lead-zinc deposits.

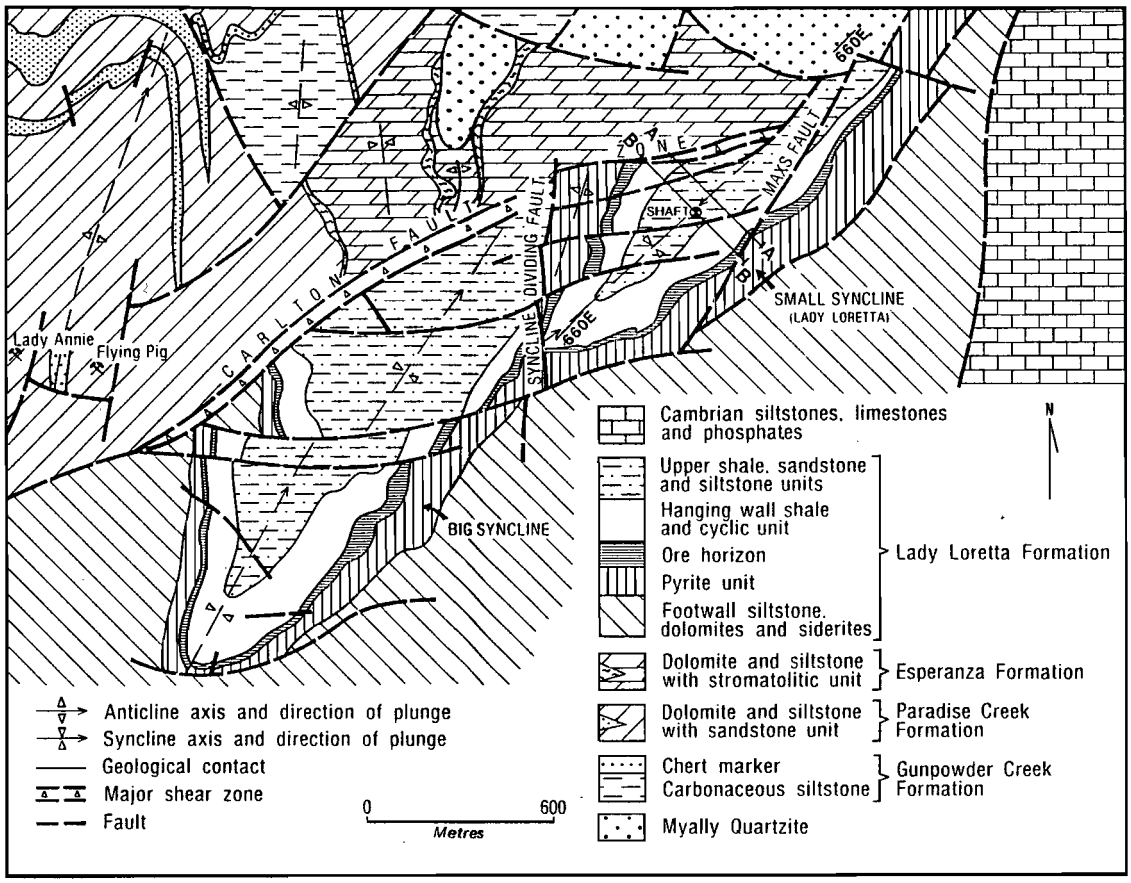

Figure 2 – Geological plan of the Lady Loretta deposit (from Hancock and Purvis, 1990).

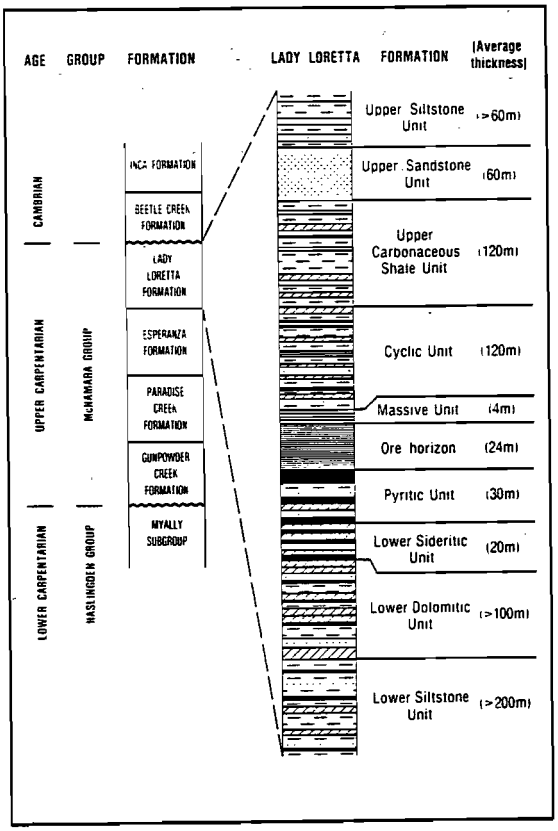

Figure 3– Stratigraphic column, Lady Loretta area (from Hancock and Purvis, 1990)..

obscured by Mesozoic laterite.

Carr's (1981) subdivision of the host succession was adopted during subsequent mine development, and is summarised here on figure 3. He used chemical and mineralogical features of the host rocks to infer a deposition in shallow alkaline, saline marine basin. During times of low terrigenous sediment input pyrite-rich layers formed at the expense of decaying algal matter. He suggested water depths of only 10 m for the footwall rocks and no more than 200 m for the Cyclic Unit in the hangingwall. Recent sedimentological work (Neudert, 1987) and observations made by the author suggest some modification and refinement of this scenario. Neudert (ibid.) recognised components of Bouma sequences at Lady Loretta and argued that the majority of sediments (including Ore Horizon sediments!) were deposited from turbulent suspension currents and pelagic deposition was of minor importance.

During logging for geochemical sampling last May, three common types of pyritic lithologies can be distinguished in the Lady Loretta host rocks. Neudert (ibid.) recognised that one important occurrence is at the base of current deposited units (often carbonaceous siltstones). A second, less common occurrence is in black, carbonaceous, papery shales at the top of graded units. The third important occurrence is subcentimetre to decimetre thick bands separating fine siltstone or shale from overlying coarse siltstone or siltstone. This latter pyrite is the major pyrite type in the Cyclic Unit above the ores. It usually has a planar base and a more irregular top, and displays a 'crinkly' internal layering. Carr (ibid.) suggested this pyrite was 'deposited under quiet conditions and with an abundant supply of decaying algae'.

Another important observation made during geochemical sampling was the recognition of stromatolites and related cryptalgal features in the OH (drill holes 245EI22 & 233ED30).

DISCUSSION

If the Lady Loretta hosts were deposited from turbulent suspension currents then depositional processes must have been fast with periodic sudden influxes of large amounts of sediment (Neudert, ibid.). The pyrite in the base of siltstone units must either be 'clastic' pyrite, hydrodynamically equivalent to the silt grains, carried in turbulent suspension by the current, or the pyrite formed after deposition of the siltstone. The former explanation is considered unlikely given the fine grained nature of much of the pyrite. Furthermore, the carbonaceous matter/pyrite association (also observed in the black, papery shales) suggests a link between organic matter and pyrite. Diagenetic formation of pyrite in the silts after sedimentation is indicated. The third type of pyrite is interpreted to be an *in situ* product of bacterial mat accumulation. Pyritisation may have occurred during accumulation of dead bacterial matter below the living mat, and/or subsequent to burial of the mat by later current deposits.

The relationship of these pyrite types to pyrite in the ores and in the Pyrite Unit in the immediate footwall of the OH is more problematical and will be the focus of further work. A number of scenarios and their implications will be considered. These include:

(i) the 'ore pyrite' is a very extensively developed third pyrite variety and mineralising fluids have used it (or its FeS precursors) as a sulphur source — therefore, a pyrite-rich sediment package ***doesn't*** imply nearby base metal mineralisation

(ii) the 'ore pyrite' is of direct hydrothermal origin (i.e., formed from ore fluids) and ***is*** related to the Cyclic Unit pyrite, i.e., the mineralising system provides heat and mass conducive to a 'cyanobacterial oasis' at the site of ore formation — pyrite-rich sediment package ***might*** indicate nearby base metal mineralisation)

(iii) the 'ore pyrite' is of direct hydrothermal origin ***but*** the Cyclic Unit pyrite is not — if hydrothermal pyrite has a distinctive chemical and/or isotopic signature then this pyrite ***might*** indicate nearby base metal mineralisation).

SAMPLING STRATEGY

A collection of over 300 samples was made during partial re-logging of selected surface and underground drill-core. About 290 of these were from the Small Syncline (n = 292) collected from underground development and ore-reserves drilling (mine sections 2210mN, 23330mN and 2450mN; figs 4, 5 & 6), and from surface holes (sections 2120mN, 2210mN and 2450mN). Surface hole P155 (near 2250mN provided samples from deep into the footwall of the mineralisation. For comparative purposes a smaller number of samples were obtained from core from the Big Syncline (fig. 7). All samples are tabulated in Appendix I.

The precise location of all the samples was recorded and it is hoped that enough samples were collected to create a 3D geochemical picture of the rocks around the folded orebody.

To date, over 100 sub-samples of siltstone and shale have been carefully cleaned and pulped in a tungsten-carbide ring mill at the University of Tasmania. It is planned to crush a further 20 or 30 bedded pyrite samples, and about a dozen ore-grade samples to complete the Lady Loretta sample set.

The original pulps from the underground drilling

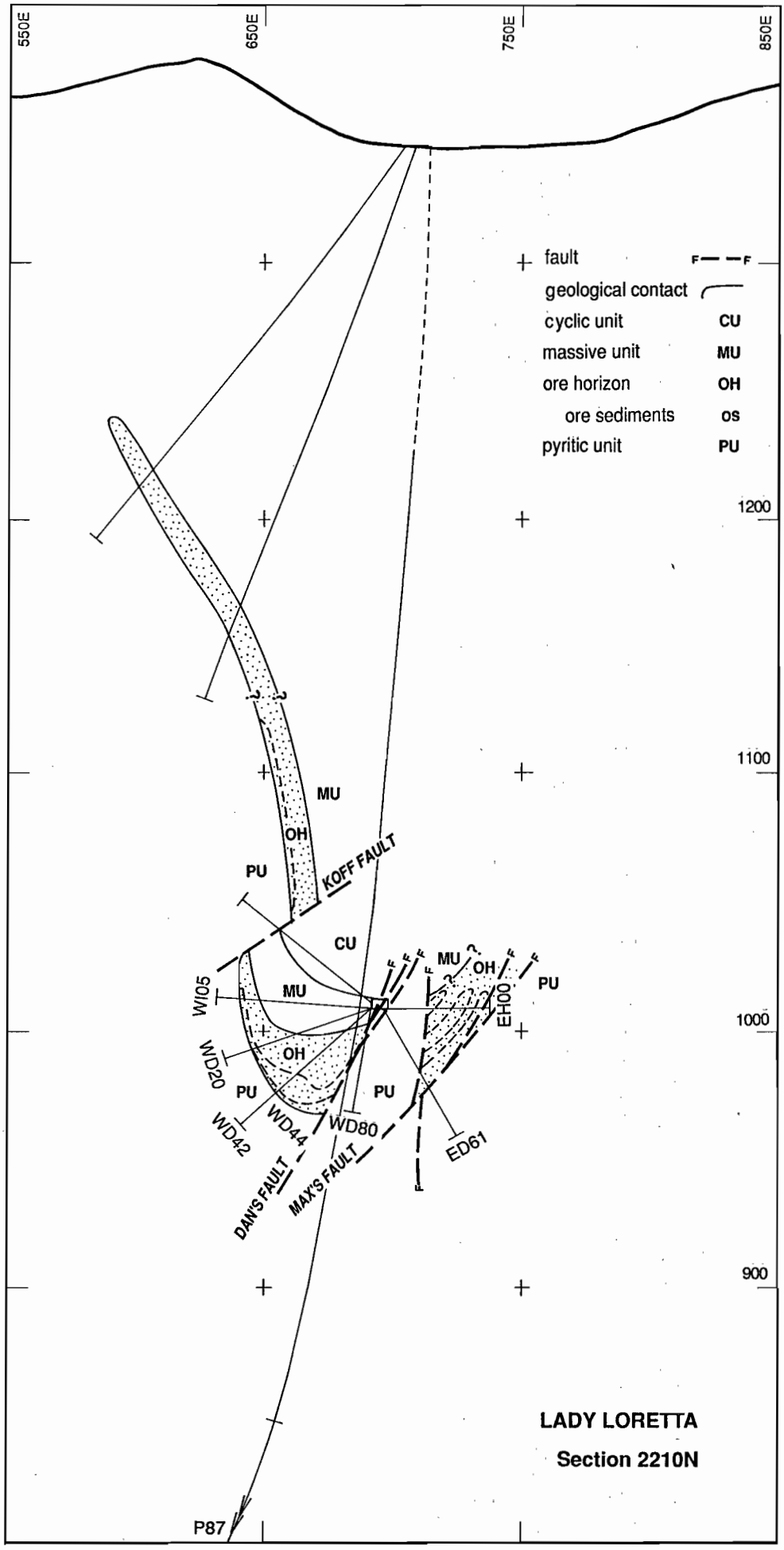

Figure 4– Simplified section through the Lady Loretta deposit (2210 mN - mine grid), showing the location of sampled diamond drill holes.

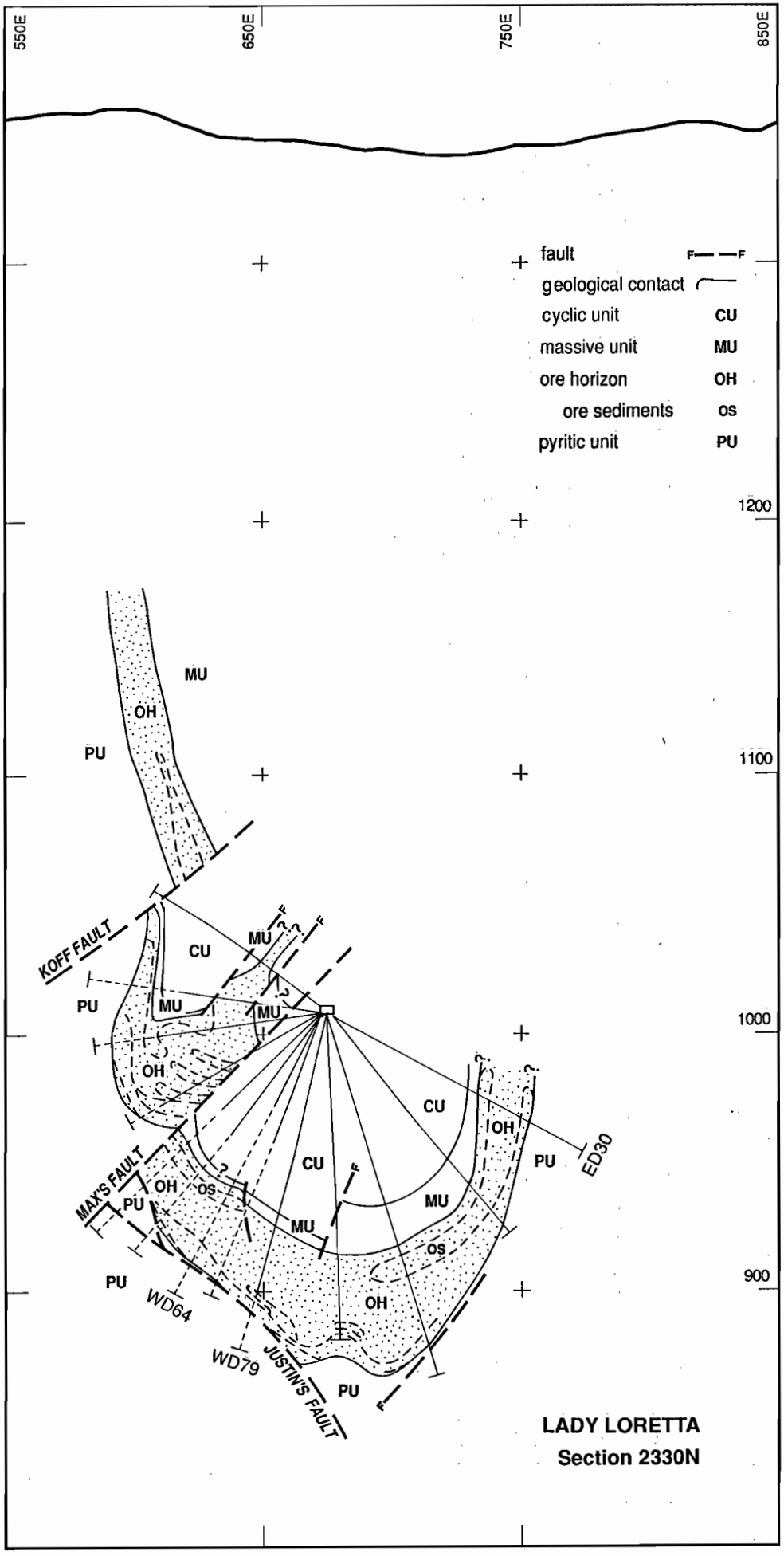

Figure 5– Simplified section through the Lady Loretta deposit (2330 mN - mine grid), showing the location of sampled diamond drill holes.

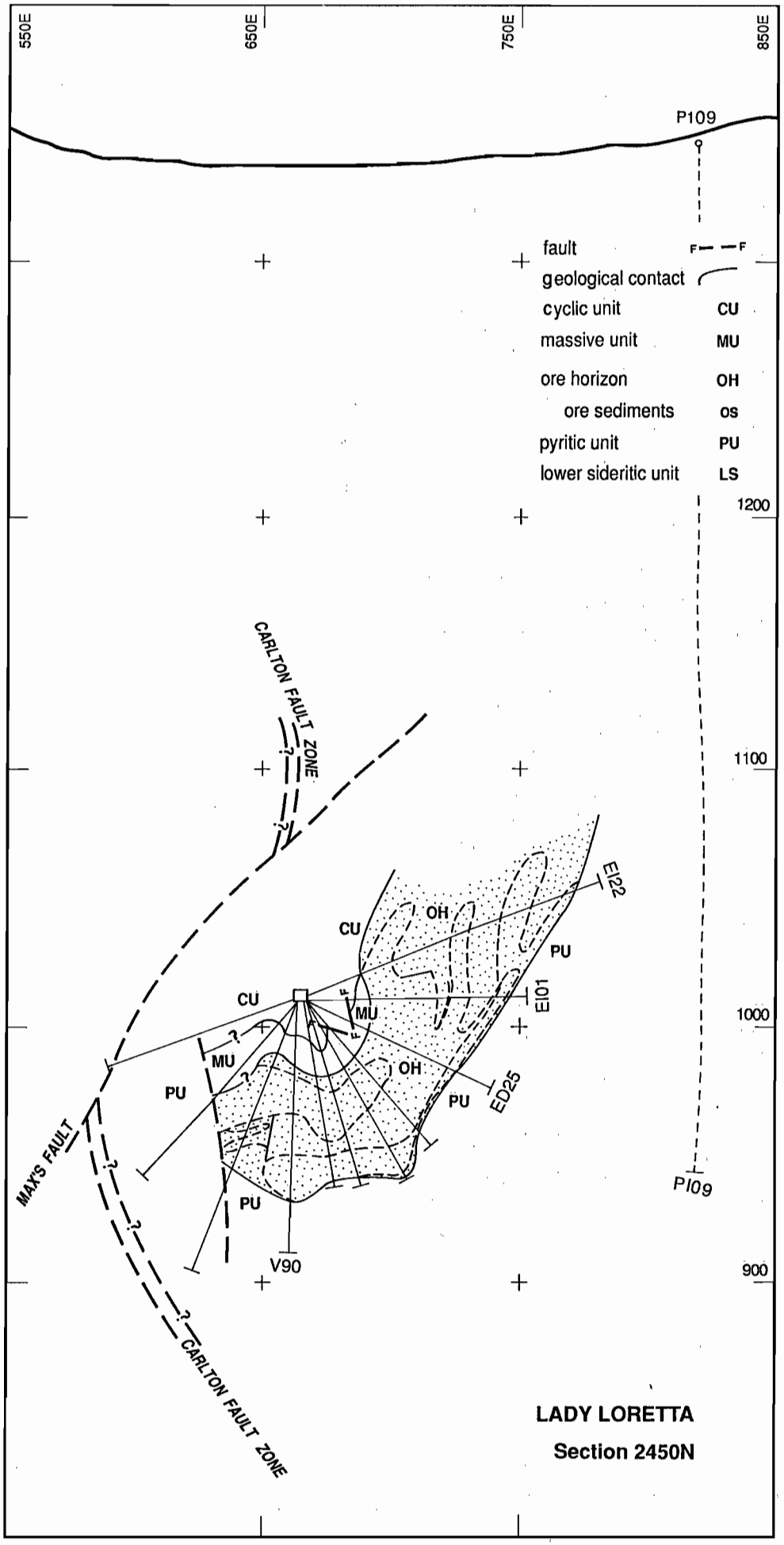

Figure 6– Simplified section through the Lady Loretta deposit (2450mN - mine grid), showing the location of sampled diamond drill holes.

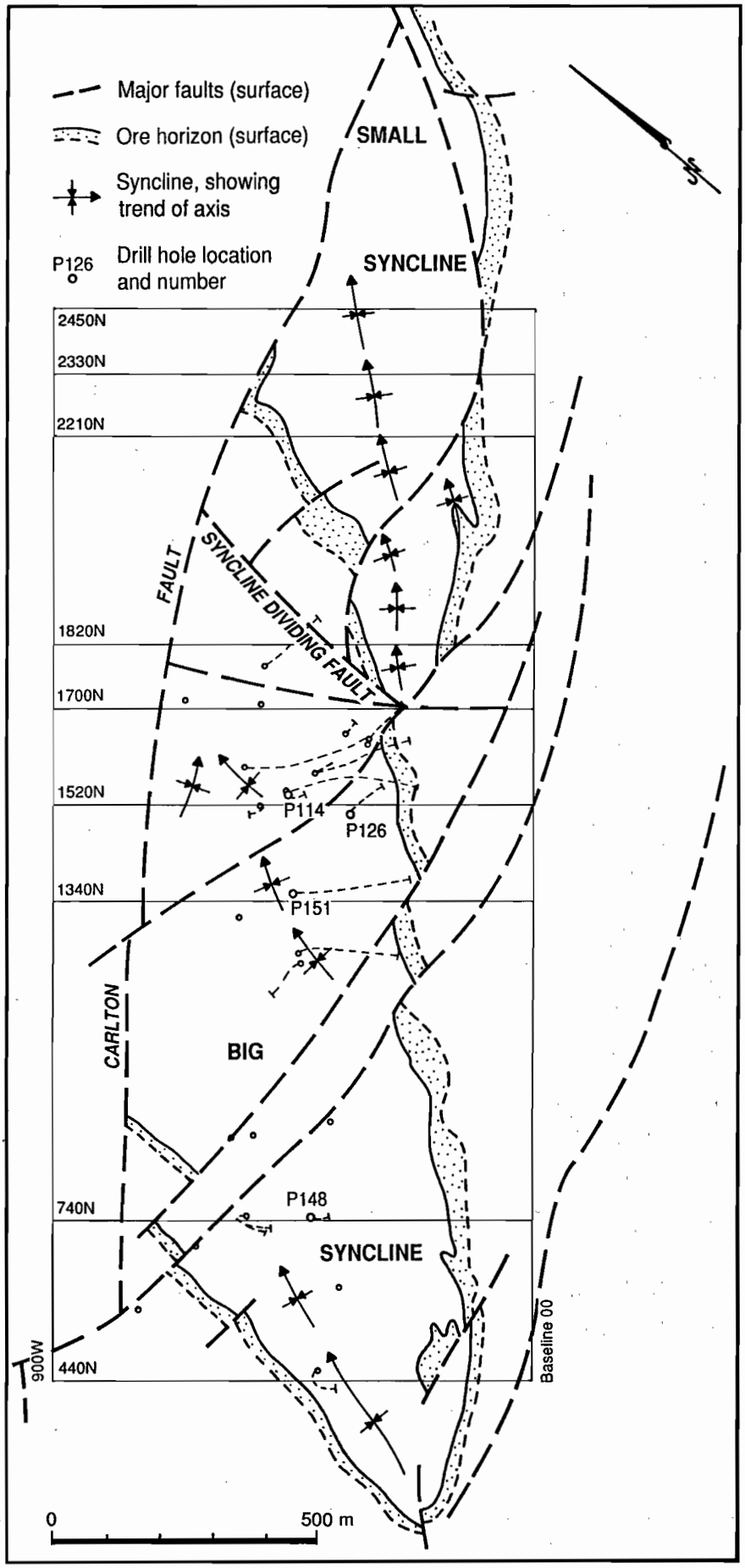

Figure 7– Simplified surface plan of the Lady Loretta Syncline showing the mine grid and the location of sampled diamond drill holes from the Big Syncline.

are also available for multi-element analysis if required.

ANALYTICAL STRATEGY

High quality (and often expensive) geochemical analyses that are both accurate and precise are required for research purposes if the data are to be published. In contrast, routine commercial assays, while comparatively cheap, are often neither very precise nor very accurate (e.g. Appendix III). However, recent developments in rapid multi-element services offered by commercial laboratories offer the pontential for better quality results at quite low cost (see *Journal of Geochemical Exploration* 44, 1992 for an up to date review of 'geoanalysis').

Where possible, analyses for the Lady Loretta study will be carried out 'in house' using the Geology Department's new XFR facility. However, it was decided that the first group of samples for analysis would be run at a commercial lab for two reasons:

(i) commissioning of the XRF meant unacceptable delays in obtaining data (at the time of writing commissioning is complete and the facility is now available for routine analysis of major and a variety of common trace elements; programs to handle more esoteric trace elements are being developed)

(ii) if results from this study are to be applied in exploration then analyses must be obtained at an acceptable cost; commercial multi-element (ICP-ES or ICP-MS) would probably be the cost-effective option

RESULTS

Commercial analyses of 104 siltstone and shales by ICP-ES for the following 26 elements Ag, Al, Ba, Bi, Ca, Cd, Co, Cr, Cu, Fe, K, Mg, Mn, Mo, Na, Ni, P, Pb, S, Sb, Sn, Sr, Ti, V, Zn, Zr, were obtained. The cost was less than $0.50c per element per sample. Thallium was determined separately by graphite furnace-AAS at a cost of about $5 per sample. The results are tabulated in Appendix II and Appendix III summarises the quality of these data.

All these data are preliminary and will be confirmed pending further analytical work over the next few months. At the meeting on 5 November graphical summaries of the data will be presented and discussed. Comparisons with existing data (e.g. Mount Isa and McArthur River) will be made.

UNDERGROUND DEVELOPMENT ASSAYS

Access to the mine development assays has been made available for research purposes. These data comprise very large set of analyses of mineralised samples for Pb, Zn, Ag, and often Ba, Fe and S. A smaller subset of these have been analysed for other elements.

It is planned to use a small subset of analyses from the three sampled mine sections (2210mN, 23330mN and 2450mN) to produce contours of metal and metal ratio distributions in the orebody. Pulps of these samples been obtained and will be analysed for Cu and Ba where neccessary. Systematic variations in metal ratios and distributions may indicate a direction to the source of the ore fluids and thus help interpret any spatial elemental variations in the unmineralised host rocks. Some of this work will be presented at the November meeting.

REFERENCES

Carr, G.R., 1981. Mineralogy, petrology and geochemistry of the Zn-Pb-Ag ores and host sedimentary rocks at Lady Loretta, NW Queensland. Unpubl. PhD thesis, University of Wollongong.

Carr, G.R., 1984. Primary geochemical and mineralogical dispersion in the vicinity of the Lady Loretta Zn-Pb-Ag deposit, NW Queensland. *J.Geochem Expl* 22: 217–238.

Carr, G.R. and Andrew, A.S., 1986. Preliminary studies of the S isotope variations within sedimentary cycles in the Lady Loretta Zn-Pb-Ag deposit. *GSA Abstracts* 15: 41–42.

Hancock, M.C. and Purvis, A.H., 1990. Lady Loretta Ag-Pb-Zn deposit. *In GEOLOGY AND MINERAL DEPOSITS OF AUSTRALIA AND PNG*. AusIMM, Melbourne: 943–948.

Neudert,M.K., 1987. Internal report to Lady Loretta JV.

Appendix I: Lady Loretta sample list

Lady Loretta Samples 2120 mN Section

Sample Code	Drill Hole	Depth (m)	Lithology
T 1	P138	202.0	sh with py bed @ base
T 2	P138	203.4	pyritic ?slst
T 3	P138	210.8	slst
T 4	P138	220.0	sh
T 5	P138	243.5	slst
T 6	P138	245.0	py/dolostone interbeds
T 7	P138	256.0	'mass.' lam. py
T 8	P138	257.5	sh/py/sh interbeds
T 9	P138	258.2	'mass.' lam. py
W 1	P84	177.0	decomposed py
W 2	P84	196.8	grey & black sh
W 3	P84	202.0	brown dolostone
W 4	P84	211.0	slst/py
W 5	P84	222.6	slst with py bands
W 6	P84	226.2	py
W 7	P84	227.5	mst
W 8	P84	232.0	slst
W 9	P84	232.2	mst
W 10	P84	235.0	grey & black sh
W 11	P84	242.4	py/mst interbeds
W 12	P84	248.6	sideritic? slst
W 13	P84	250.0	lam. "mass" py
W 14	P84	252.0	partly decomp. lam. py
W 15	P84	254.2	decomp. shaley lam. py
W 16	P84	259.7	mst
W 17	P84	265.7	slst
W 18	P84	266.5	py x2/slst/mst
W 19	P84	273.3	slst cycle
X 1	P96	238.0	sh
X 2	P96	259.6	folded lam. py
X 3	P96	276.0	mass lam. py
X 4	P96	288.5	lam. py in sh
X 5	P96	298.8	lam. py in mst
X 6	P96	314.5	mass lam. py
X 7	P96	317.0	slst
X 8	P96	317.2	slst

Lady Loretta Samples 2210 mN Section

Sample Code	Drill Hole	Depth (m)	Lithology
A 1	221 EH00	3.0	'shale'
A 2	221 EH00	7.3	siltstone
A 3	221 EH00	13.3	?sideritic siltstone
B 1	221 ED61	40.1	laminated pyrite
B 2	221 ED61	47.5	pale ?dolomitic siltstone
B 3	221 ED61	49.4	sh/slts/pyslts
C 1	221 WD80	4.7	laminated pyrite
C 2	221 WD80	7.7	grit with py bands
C 3	221 WD80	11.7	slts
D 1	221 WD44	7.0	weak min sh/slts
D 2	221 WD44	18.0	weak bms/py/sh/dol
D 3	221 WD44	19.0	weak bms/py/sh/dol
D 4	221 WD44	23.0	weak bms/py/sh/dol
D 5	221 WD44	42.8	'ink blot' f.g. py in bms
D 6	221 WD44	48.1	decomposed 'massive' py
D 7	221 WD44	49.3	layered py, minor sp
E 1	221 WD20	0.1	mst
E 2	221 WD20	2.5	slts
E 3	221 WD20	8.5	lam py
E 4	221 WD20	21.0	weak min grit/sh
E 5	221 WD20	27.0	dolomitic slts
E 6	221 WD20	32.8	lam/cren bms&py
E 7	221 WD20	44.0	decomp lam py (mnr bms)
E 8	221 WD20	49.8	decomp lam py
F 1	221 WI05	0.3	crs slt-sst
F 2	221 WI05	1.8	grey sh
F 3	221 WI05	6.0	slts
F 4	221 WI05	17.4	slts
F 5	221 WI05	19.7	
F 6	221 WI05	26.7	
F 7	221 WI05	36.7	
F 8	221 WI05	41.5	py sh
F 9	221 WI05	45.1	layered py & mnr bms
F 10	221 WI05	45.8	layered py & mnr bms
F 11	221 WI05	49.3	sh
F 12	221 WI05	51.2	layered py
F 13	221 WI05	53.2	layered py
F 14	221 WI05	53.5	brown ?sideritic mst
F 15	221 WI05	57.2	reactive py (decomp.)
F 16	221 WI05	58.0	py
G 1	221 WI40	1.0	slts
G 2	221 WI40	2.2	slts/sh
G 3	221 WI40	9.7	py/slts/sh
G 4	221 WI40	23.7	slts
G 5	221 WI40	47.6	layered py
G 6	221 WI40	60.2	py slts
Y 1	P87	295.8	py
Y 2	P87	296.6	slst
Y 3	P87	297.0	sh
Y 4	P87	297.3	sh
Y 5	P87	301.6	slst
Y 6	P87	506.0	slst/sh
Y 7	P87	571.5	pyritic? slst
Y 8	P87	574.5	pyritic slst
Y 9	P87	579.5	'mass' lam. py
Y 10	P87	581.7	lam. py
Y 11	P87	590.0	crs mass py
Y 12	P87	592.0	mass py

Lady Loretta Samples 2260 mN Section

Sample Code	Drill Hole	From (m)	Lithology
P155 - 1	P155	302.7	dk grey/black sh
P155 - 2	P155	338.0	lam carbc slst with minor mst
P155 - 3	P155	365.6	lam carbc slst (no mst)
P155 - 4	P155	395.3	f.g. slst/mst (partly lam)
P155 - 5	P155	528.9	f.g. more 'massive' slst than 155-2
P155 - 6	P155	165.0	decomposed py

Appendix I: Lady Loretta sample list — cont.

Lady Loretta Samples 2310 mN Section

Sample Code	Drill Hole	From (m)	Lithology
N 1	231 ED62	6	py & mst
N 2	231 ED62	16.8	mst
N 3	231 ED62	20.3	py
N 4	231 ED62	24.8	slts & py
N 5	231 ED62	29.4	slst/mst
N 6	231 ED62	32.1	slts
N 7	231 ED62	38.2	slts
N 8	231 ED62	57.0	py
N 9	231 ED62	64.5	slts
N 10	231 ED62	69.6	sh/slts
N 11	231 ED62	70.1	slts/py/sh
N 12	231 ED62	71.9	sh CU
N 13	231 ED62	76.8	slst
N 14	231 ED62	78.4	sh/mst
N 15	231 ED62	90.6	sulfide-bearing fragmental
N 16	231 ED62	93.0	sulfide-bearing fragmental
N 17	231 ED62	100.8	replacement sp/ slts/sh ±veins
N 18	231 ED62	104.5	py/sh
N 19	231 ED62	111.2	py/ sideritic? dolostone
N 20	231 ED62	135.1	slts
N 21	231 ED62	137.5	lam. py
N 22	231 ED62	139.8	slts
N 23	231 ED62	150.5	mst/slts
N 24	231 ED62	154.8	py/sh
N 25	231 ED62	155.4	slts - py CU
N 26	231 ED62	157.7	slts

Lady Loretta Samples 2330 mN Section

Sample Code	Drill Hole	From (m)	Lithology
M 1	233 ED30	13.3	sh
M 2	233 ED30	19.5	slt/ms/sh
M 3	233 ED30	39.1	
M 4	233 ED30	46.1	slts
M 5	233 ED30	48	slts
M 6	233 ED30	58.8	
M 7	233 ED30	61.4	sh
M 8	233 ED30	66	py
M 9	233 ED30	68.9	
M 10	233 ED30	75.4	
M 11	233 ED30	76.4	
M 12	233 ED30	85.4	py
M 13	233 ED30	95.4	slts
M 14	233 ED30	96	slts
M 15	233 ED30	103.4	slts
M 16	233 ED30	108.2	slts
O 1	233 WD79	24.3	sh py x3 slts
O 2	233 WD79	29.8	sideritic? slts
O 3	233 WD79	37.5	sideritic? slts
O 4	233 WD79	38.5	grey sh
O 5	233 WD79	72.3	slst/sh
O 6	233 WD79	74.0	slst/sh
O 7	233 WD79	87.8	frag. unit (?sulphides)
O 8	233 WD79	120.5	sp repl. lam. py
O 9	233 WD79	121.4	sideritic? dolostone
O 10	233 WD79	125.0	lam. py
O 11	233 WD79	133.1	lam. py
P 1	233 WD64	47.1	slst/mst/py
P 2	233 WD64	74.1	sh/slst
P 3	233 WD64	78.4	py/sh?
P 4	233 WD64	79.4	sh/slts CU
P 5	233 WD64	80.8	sed. bx

Lady Loretta Samples 2340 mN Section

Sample Code	Drill Hole	From (m)	Lithology
L 1	234 ED30	3.4	cycle
L 2	234 ED30	10.8	
L 3	234 ED30	16.7	py
L 4	234 ED30	30.3	mst
L 5	234 ED30	34.8	slts
L 6	234 ED30	51	slts
L 7	234 ED30	54.4	mst
L 8	234 ED30	56.5	py/sp/ga
L 9	234 ED30	59.8	
L 10	234 ED30	68	
L 11	234 ED30	71.3	
L 12	234 ED30	73.3	
L 13	234 ED30	79.7	
L 14	234 ED30	104.1	py
L 15	234 ED30	106	sh/py
L 16	234 ED30	111.9	py
L 17	234 ED30	118.2	
L 18	234 ED30	124.4	sltst
L 19	234 ED30	124.9	
L 20	234 ED30	133	
L 21	234 ED30	135.1	
L 22	234 ED30	140	
L 23	234 ED30	143.6	
L 24	234 ED30	155	mst/slts
L 25	234 ED30	173	mst
L 26	234 ED30	177.4	
L 27	234 ED30	182	slts
L 28	234 ED30	184.8	
L 29	234 ED30	186.5	
L 30	234 ED30	188.8	slts
L 31	234 ED30	189.1	mst

Lady Loretta Samples 2420 mN Section

Sample Code	Drill Hole	From (m)	Lithology
Z 1	242 ED72	8.7	slst/sh/carb sh cycles
Z 2	242 ED72	12.4	slst/sh/carb sh cycles
Z 3	242 ED72	18.0	sh
Z 4	242 ED72	23.2	sh/slst
Z 5	242 ED72	24.2	sh/slst
Z 6	242 ED72	28.0	carb. sh/py
Z 7	242 ED72	28.8	sh/slst
Z 8	242 ED72	33.0	slst sed. structures
Z 9	242 ED72	36.8	low grade bms
Z 10	242 ED72	39.3	low grade bms
Z 11	242 ED72	47.6	slst/mst
Z 12	242 ED72	48.6	
Z 13	242 ED72	54.2	slst/mst
Z 14	242 ED72	56.8	
Z 15	242 ED72	66.5	pyritic bms
Z 16	242 ED72	68.5	pyritic bms
Z 17	242 ED72	76.1	bms (DSO)
Z 18	242 ED72	77.0	bms (DSO)
Z 19	242 ED72	77.1	bms (DSO)
Z 20	242 ED72	80.9	bms/py contact
Z 21	242 ED72	85.0	reactive pyrite
Z 22	242 ED72	90.1	concretions? in bms?
Z 23	242 ED72	101.3	py
Z 24	242 ED72	102.1	py
Z 25	242 ED72	102.5	grey dolomite + carb. veins
Z 26	242 ED72	103.5	grey dolomite + carb. veins
Z 27	242 ED72	104.7	carb. black sh
Z 28	242 ED72	106.9	py/black sh interbeds

Appendix I: Lady Loretta sample list — cont.

Lady Loretta Samples 2450 mN Section

Sample Code	Drill Hole	From (m)	Lithology
H 1	245 EI22	1.0	slts
H 2	245 EI22	4.9	lam py & slts
H 3	245 EI22	7.0	mst
H 4	245 EI22	16.5	slts
H 5	245 EI22	25.0	massive ?banded py
H 6	245 EI22	26.0	py/bar/bms (porous)
H 7	245 EI22	31.9	py/sp/ba
H 8	245 EI22	35.8	py/sp/ba
H 9	245 EI22	40.2	slts
H 10	245 EI22	42.2	mst/sh
H 11	245 EI22	46.0	sed. bx (?sp clasts)
H 12	245 EI22	47.6	bms/py/?ba ?green clay min.
H 13	245 EI22	61.3	sp repl. py & sed. layers
H 14	245 EI22	86.1	bms
H 15	245 EI22	90.7	bms
H 16	245 EI22	96.6	spongy sp/cert
H 17	245 EI22	96.9	sil. wk min. spotty rock
H 18	245 EI22	96.7	stromatolites
H 19	245 EI22	105.4	
H 20	245 EI22	106.2	
H 21	245 EI22	114.8	decomp. mass py & bms
H 22	245 EI22	116.3	black/grey carb. sh
H 23	245 EI22	117.2	black/grey carb. sh
H 24	245 EI22	119.2	py. carb. sh
I 1	245 EI01	8.5	slts
I 2	245 EI01	11.1	sh
I 3	245 EI01	12.2	slts/sh cycle
I 4	245 EI01	21.0	pale (?dol) slts
I 5	245 EI01	25.8	ba-sp (±py) ore
I 6	245 EI01	33.4	fragmental? bms
I 7	245 EI01	59.8	siliceous bms
I 8	245 EI01	59.8	cherty patches/ bms
I 9	245 EI01	57.8	blobby/stringery bms
I 10	245 EI01	62.0	typical i6-i10 material!
I 11	245 EI01	67.0	pyritic/ disturbed bms
I 12	245 EI01	73.6	(stylolitic) sp-rich bms
I 13	245 EI01	78.5	py
I 14	245 EI01	85.9	dol/?sid rock
J 1	245 ED25	4.8	grey mst
J 2	245 ED25	11.5	slst
J 3	245 ED25	18.0	f.g. slts
J 4	245 ED25	19.7	f.g. slts
J 5	245 ED25	36.5	ba-sp-py bms
J 6	245 ED25	48.4	ba-sp-py bms
J 7	245 ED25	63.3	sp-rich bms (DSO) with sil. patches
J 8	245 ED25	71.0	layered pyrite
J 9	245 ED25	72.2	grey sh
J 10	245 ED25	74.6	finely lam. py
J 11	245 ED25	78.5	light brown mst
K 1	245 V90	3.4	slst
K 2	245 V90	4.0	slst with sed. structures
K 3	245 V90	4.9	slst/sh cycle
K 4	245 V90	11.9	slst/sh cycle
K 5	245 V90	17.2	f.g. slst
K 6	245 V90	20.0	mst/sh
K 7	245 V90	22.5	carb sh/ ?red min
K 8	245 V90	27.7	layered low grade bms
K 9	245 V90	28.5	layered bms with py vein
K 10	245 V90	33.5	grey slts
K 11	245 V90	35.0	grey/brown slts
K 12	245 V90	41.4	brown stained mst
K 13	245 V90	42.0	slst/sh sed. structures
K 14	245 V90	56.5	layered bms
K 15	245 V90	60.0	pyritic bms
K 16	245 V90	63.0	high grade bms (DSO)
K 17	245 V90	84.0	lam. py
K 18	245 V90	97.0	carb. veined grey mst/sh
V 1	P109	131.2	grey sh/slst
V 2	P109	139.4	grey sh
V 3	P109	149.1	bms & lam. py
V 4	P109	153.5	sil? seds
V 5	P109	157.5	py/sh
V 6	P109	158.1	sh
V 7	P109	172.6	py/sh
V 8	P109	177.3	py/sh
V 9	P109	185.0	py/sh
V 10	P109	196.5	py/sh
V 11	P109	200.0	py/sh
V 12	P109	160.3	py
V 13	P109	201.8	py/sh
V 14	P109	124.0	

Lady Loretta Samples - Big Syncline

Sample Code	Drill Hole	From (m)	Lithology
Q 1	P148	57.5	reactive py
Q 2	P148	77.5	sh/mst
Q 3	P148	81.5	slst
Q 4	P148	81.6	sh/mst
Q 5	P148	93.6	slst
Q 6	P148	97.8	slst/sh
Q 7	P148	130.2	'mass.' py
Q 8	P148	134.4	mst/slst
Q 9	P148	135.5	slst
Q 10	P148	150.9	slst/pyritic base
Q 11	P148	158.5	py/slst/sh CU
Q 12	P148	162.0	py bands x3
Q 13	P148	162.5	CU with pyritic band
Q 14	P148	169.0	decomp. py
Q 15	P148	177.8	sugary py from OH
Q 16	P148	200.0	grey ?mst
Q 17	P148	207.0	pyritic sed
Q 18	P148	207.2	lam. slst
Q 19	P148	209.4	lam. mass. py
Q 20	P148	215.5	slst/py x2
Q 21	P148	220.2	thin slst/mst CU py base
Q 22	P148	232.2	pyritic slst
Q 23	P148	239.0	v. pyritic slst
Q 24	P148	240.4	py. slst/sh/barren slst
Q 25	P148	248.5	pale slst/sh/pyritic slst
Q 26	P148	260.8	fine slst
Q 27	P148	266.2	grey slst/dark f. lam. slst
R 1	P126	191.5	grey sh
R 2	P126	197.8	slst/py CU
R 3	P126	232.1	slst
R 4	P126	247.6	slst/sh CU
R 5	P126	262.8	slst/sh py bands
R 6	P126	270.5	slst/py
R 7	P126	300.2	thick py band & slst/sh/py units
R 8	P126	312.7	slsts
R 9	P126	314.0	slsts & py band
R 10	P126	341.5	crs dol. & recrys. py rocks
R 11	P126	345.8	crs dol. & recrys. py rocks
R 12	P126	347.5	crs dol. & recrys. py rocks
R 13	P126	355.5	crs dol. & recrys. py rocks
R 14	P126	360.0	as above with f.g. py relics
R 15	P126	391.0	crs 'brassy' py & 'cherty' sed
R 16	P126	392.3	'cherty' black sed.
R 17	P126	416.8	sil. looking dol/py bed
S 1	P151	444.0	slst/sh/py
S 2	P151	431.2	slst
S 3	P151	409.6	'mass.' py
S 4	P151	370.1	crs mass. py
S 5	P151	428.9	lam. pyritic slst
S 6	P151	354.0	mixed py/slst
S 7	P151	353.5	slts/f.g. slst/py CUs
S 8	P151	353.0	slst with react. py band
S 9	P151	335.1	slst/sh CUs with thin py bands
S 10	P151	294.8	large slst/sh CU
S 11	P151	260.0	several slst/mst/py CUs
S 12	P151	276.8	several thin slst/mst CUs
S 13	P151	181.5	mst/mnr slst/py bands
P114 - 1	P114	301.8	slst?
P114 - 2	P114	321.6	slst?
P114 - 3	P114	340.0	slst?
P114 - 4	P114	350.0	slst?

Appendix II: Analyses of Lady Loretta siltstones and shales

Lady Loretta Assays October '92

	SAMPLE	SAMPLE	SAMPLE	SAMPLE	SAMPLE	SAMPLE	SAMPLE	SAMPLE	SAMPLE	SAMPLE	SAMPLE	SAMPLE	SAMPLE	SAMPLE
	1	2	3	4	5	6	7	8	9	10	11	12	13	14
	E	E	E	E	H	H	H	H		I	I	I	J	J
	1	2i	2ii	2ii	1	3	3	4	20495	1	2	4	1	2
ELEMENT														
Cu	20	25	25	30	20	20	10	25	15	20	20	30	25	20
Pb	30	50	55	55	25	35	30	190	200	50	110	250	75	35
Zn	8600	2.54%	1.61%	1.55%	1.41%	2.27%	2.22%	170	165	1600	250	530	2800	7300
Ag	<1	<1	<1	1	<1	<1	<1	<1	2	<1	<1	1	<1	1
Bi	<5	<5	<5	<5	<5	<5	<5	<5	<5	<5	<5	<5	<5	<5
Sb	<5	<5	<5	5	<5	<5	<5	<5	5	<5	<5	<5	<5	<5
Ba	620	550	520	540	810	670	740	360	50	380	570	460	480	105
Cd	<5	<5	<5	<5	<5	<5	<5	<5	<5	<5	<5	<5	<5	<5
Co	25	40	40	35	25	25	30	35	10	20	20	15	20	35
Cr	45	60	40	40	25	40	50	15	40	20	25	25	30	15
Mo	<5	<5	<5	<5	<5	<5	<5	<5	<5	<5	<5	<5	<5	<5
Ni	20	35	40	40	20	20	20	10	15	30	15	20	20	20
S	2700	6600	7900	7800	4100	2400	2500	3750	2.53%	5100	4350	5600	5750	1.51%
V	70	50	60	50	30	50	60	30	30	50	60	120	50	20
Zr	110	100	100	100	120	90	100	120	70	190	130	140	110	100
Ca	450	1550	940	970	1300	1200	1400	190	6.97%	980	230	260	290	250
Fe	5.29%	10.9%	8.51%	8.50%	11.6%	13.6%	14.5%	1.01%	5.93%	3.90%	1.50%	1.41%	3.51%	7.98%
Mg	7600	1.01%	9100	9250	9700	8750	1.04%	4150	4.23%	7550	7900	6750	6100	6850
Mn	1650	3150	2450	2450	4100	4150	4250	10	2500	60	10	10	680	1700
Ti	2000	1200	1550	1150	540	960	890	1500	620	1250	2700	3050	1850	600
Al	5.66%	5.35%	6.22%	6.35%	4.13%	5.09%	6.60%	3.92%	3.05%	4.70%	7.30%	7.09%	5.27%	3.81%
K	2.86%	2.84%	3.22%	3.44%	2.23%	2.59%	2.31%	2.37%	2.73%	1.97%	3.25%	3.60%	2.79%	1.75%
Na	1700	2100	980	1400	570	1350	870	1050	500	970	820	1250	1150	250
P	350	290	240	230	340	340	360	380	370	170	430	310	220	140
Sn	<20	<20	<20	<20	<20	<20	<20	<20	<20	<20	<20	<20	<20	<20
Sr	50	30	40	40	40	220	250	280	20	90	360	210	120	110
Tl	1.0	1.5	1.5	2.0	0.5	1.0	1.0	1.5	6.5	0.5	1.0	1.0	1.5	4.5

1

Lady Loretta Assays October '92

	SAMPLE	SAMPLE	SAMPLE	SAMPLE	SAMPLE	SAMPLE	SAMPLE	SAMPLE	SAMPLE	SAMPLE	SAMPLE	SAMPLE	SAMPLE	SAMPLE
	15	16	17	18	19	20	21	22	23	24	25	26	27	28
	J	K	L	L	L	L	L	L	L	L	L	L		M
	9	1	2	4	5	7	14	15	21	25	21/27	31	20509/1(	1
ELEMENT														
Cu	15	20	20	20	15	40	15	15	15	15	25	15	10	20
Pb	35	30	15	35	15	400	85	40	30	15	70	50	3950	50
Zn	220	3.63%	1200	4000	9450	270	4950	4900	100	55	60	50	390	490
Ag	<1	<1	<1	<1	<1	1	<1	<1	<1	<1	<1	<1	8	<1
Bi	<5	<5	<5	<5	<5	<5	<5	<5	<5	<5	<5	<5	<5	<5
Sb	5	<5	<5	<5	<5	<5	<5	<5	<5	<5	<5	<5	30	<5
Ba	310	490	400	390	420	450	105	90	175	200	130	170	35	280
Cd	<5	<5	<5	<5	<5	<5	<5	<5	<5	<5	<5	<5	<5	<5
Co	20	40	10	15	25	20	15	10	20	20	25	20	10	15
Cr	5	30	40	35	25	40	25	45	30	30	60	45	30	70
Mo	<5	<5	<5	<5	<5	<5	<5	<5	<5	<5	<5	10	<5	<5
Ni	<5	25	10	10	20	20	10	10	15	10	20	20	10	15
S	5350	3050	3700	7750	2650	4650	5400	1.41%	7100	4700	1.60%	1.45%	3.74%	2000
V	20	30	70	70	20	60	30	60	30	30	50	60	20	70
Zr	30	90	110	130	90	120	180	160	140	140	130	150	100	110
Ca	140	1550	1450	850	1150	130	440	420	4.43%	5.21%	3.93%	3.43%	5.87%	1200
Fe	4250	18.6%	4.41%	5.83%	11.7%	5050	8.49%	5.18%	2.43%	2.47%	3.43%	2.35%	5.88%	3.47%
Mg	1300	9000	1.16%	8500	9350	540	8200	8600	2.43%	2.52%	2.29%	1.95%	2.93%	1.28%
Mn	10	6850	420	1750	4100	<10	2050	1200	840	840	700	410	3650	320
Ti	640	890	2200	1750	740	2850	800	1700	1400	1150	1550	1850	760	2100
Al	4.01%	3.69%	7.50%	8.13%	4.08%	7.24%	6.03%	6.83%	4.75%	4.16%	6.22%	6.29%	3.80%	8.91%
K	9450	1.67%	2.00%	1.39%	1.87%	3000	1.65%	1.50%	1.56%	1.69%	2.49%	3.04%	3.64%	2.37%
Na	510	1000	1150	1100	360	1050	700	460	460	430	450	760	840	600
P	220	210	570	630	360	220	230	330	400	340	590	710	260	630
Sn	<20	<20	<20	<20	<20	<20	<20	<20	<20	<20	<20	<20	<20	<20
Sr	50	140	10	170	30	110	130	180	30	30	20	20	20	60
Tl	1.0	0.5	2.5	2.5	2.0	1.0	0.5	1.5	1.0	<0.5	3.0	1.0	35.5	2.0

2

Appendix II: Analyses of Lady Loretta siltstones and shales — cont.

Lady Loretta Assays October '92

	SAMPLE	SAMPLE	SAMPLE	SAMPLE	SAMPLE	SAMPLE	SAMPLE	SAMPLE	SAMPLE	SAMPLE	SAMPLE	SAMPLE	SAMPLE	SAMPLE
	29	30	31	32	33	34	35	36	37	38	39	40	41	42
	M	M	M		N	N	N	N	N	N	N	N	N	N
	4	7	14	20517	1	1	2	2	4	5	7	10i	10ii	14
ELEMENT														
Cu	10	30	20	10	15	15	15	20	5	10	5	10	15	10
Pb	30	125	50	2200	25	25	20	25	20	25	25	40	55	20
Zn	9500	280	2550	1100	1250	1250	620	890	145	7350	8100	200	145	90
Ag	<1	1	<1	5	<1	<1	<1	<1	<1	<1	<1	<1	<1	<1
Bi	<5	<5	<5	<5	<5	<5	<5	<5	<5	<5	<5	<5	<5	<5
Sb	<5	<5	<5	<5	<5	<5	<5	<5	<5	<5	<5	<5	<5	<5
Ba	410	240	95	65	250	260	200	260	230	310	240	580	770	1000
Cd	<5	<5	<5	<5	<5	<5	<5	<5	<5	<5	<5	<5	<5	<5
Co	25	15	25	5	10	10	5	10	5	10	25	15	15	15
Cr	45	70	20	20	45	40	40	55	30	45	20	35	30	30
Mo	<5	<5	<5	<5	<5	<5	<5	<5	<5	<5	<5	<5	<5	<5
Ni	25	15	20	10	20	20	15	20	5	20	15	10	10	15
S	5250	5450	1.17%	2.51%	4600	4650	2950	3950	4100	4900	3150	3850	3700	1550
V	50	40	20	10	70	70	60	90	50	50	30	40	50	50
Zr	100	130	100	90	110	110	90	120	50	80	90	100	100	90
Ca	1150	110	160	5.58%	1300	1150	870	1400	8.29%	2650	420	5.50%	3.81%	4.70%
Fe	7.88%	8400	3.74%	4.39%	5.83%	5.89%	2.25%	3.31%	3.80%	14.0%	8.52%	4.20%	2.62%	2.92%
Mg	9650	3450	7350	2.32%	1.19%	1.23%	7850	1.26%	4.06%	1.15%	8800	2.80%	2.04%	2.45%
Mn	2200	<10	430	3850	1650	1600	260	380	2250	5800	2250	1500	830	960
Ti	1050	1750	910	660	1800	1750	2200	2050	1050	760	610	1000	1350	1400
Al	6.79%	9.77%	6.58%	4.34%	7.67%	8.17%	6.03%	10.1%	4.90%	6.12%	4.75%	5.56%	6.98%	6.67%
K	3.03%	2.39%	1.81%	4.65%	3.53%	3.75%	3.39%	1.63%	1.84%	1.37%	1.05%	2.93%	3.90%	2.02%
Na	360	460	260	580	970	740	730	590	300	360	220	430	460	460
P	480	130	190	210	540	530	520	760	410	400	160	440	450	430
Sn	<20	<20	<20	<20	<20	<20	<20	<20	<20	<20	<20	<20	<20	<20
Sr	90	100	140	20	50	50	40	70	60	40	90	70	60	70
Tl	1.0	<0.5	4.0	18.5	2.0	2.0	1.5	1.5	1.0	1.0	1.5	1.5	1.5	1.0

3

Lady Loretta Assays October '92

	SAMPLE	SAMPLE	SAMPLE	SAMPLE	SAMPLE	SAMPLE	SAMPLE	SAMPLE	SAMPLE	SAMPLE	SAMPLE	SAMPLE	SAMPLE	SAMPLE
	43	44	45	46	47	48	49	50	51	52	53	54	55	56
	N	N	N	O	O	O	O	P	P	P	P	Q	Q	Q
	22	23	26	2	3	4	5	2i	2ii	4i	4ii	2	2	3
ELEMENT														
Cu	5	10	15	<5	10	<5	10	25	45	170	110	10	10	10
Pb	15	35	20	5	20	10	20	95	145	1.01%	1.12%	25	15	20
Zn	5700	230	95	90	3850	65	1000	280	500	5.91%	2.95%	3500	3450	4850
Ag	<1	<1	<1	<1	<1	<1	<1	3	6	34	28	<1	<1	<1
Bi	<5	<5	<5	<5	<5	<5	<5	<5	<5	<5	<5	<5	<5	<5
Sb	<5	<5	<5	<5	<5	5	<5	15	20	25	35	<5	<5	<5
Ba	170	220	120	170	350	360	540	960	960	280	15	470	430	370
Cd	<5	<5	<5	<5	<5	<5	<5	<5	<5	95	45	<5	<5	<5
Co	20	15	40	10	20	10	15	15	15	55	80	15	15	15
Cr	20	40	25	40	25	40	35	40	30	20	50	35	50	50
Mo	<5	<5	<5	<5	<5	<5	<5	<5	<5	10	10	<5	<5	<5
Ni	20	15	15	5	10	15	10	20	10	25	35	35	30	25
S	3300	1.24%	1.39%	2000	1200	6300	3800	4300	3250	7.43%	8.81%	4250	4300	6850
V	20	60	30	40	30	60	60	60	50	30	60	70	70	60
Zr	110	140	190	40	20	110	130	110	90	140	110	110	100	100
Ca	390	510	450	9.89%	2550	3.19%	650	2100	2800	570	510	500	550	430
Fe	8.10%	2.96%	2.13%	4.12%	7.61%	2.60%	1.68%	5.73%	9.24%	12.7%	10.3%	4.50%	4.62%	4.81%
Mg	7200	8200	4400	4.70%	8900	2.14%	9000	1.03%	1.16%	4950	5850	1.20%	1.26%	8450
Mn	1600	290	30	2750	2250	660	150	860	1550	2550	880	640	650	950
Ti	440	1150	1000	960	750	1450	2200	1400	900	410	500	2150	1100	910
Al	3.96%	8.24%	5.14%	3.97%	4.88%	7.72%	8.29%	7.67%	6.44%	3.48%	5.75%	7.77%	8.41%	7.24%
K	1.04%	4.16%	2.14%	1.79%	1.14%	1.77%	1.96%	3.43%	3.24%	2.22%	3.43%	4.24%	2.34%	2.76%
Na	220	500	430	250	320	440	400	450	370	460	320	1000	440	480
P	130	510	510	320	440	480	220	470	420	330	620	360	370	270
Sn	<20	<20	<20	<20	<20	<20	<20	<20	<20	<20	<20	<20	<20	<20
Sr	40	10	10	60	40	40	110	10	10	130	200	50	50	70
Tl	0.5	1.0	3.0	0.5	2.0	1.5	1.5	2.5	1.5	20.5	19.5	1.0	1.0	1.0

4

Appendix II: Analyses of Lady Loretta siltstones and shales — cont.

Lady Loretta Assays October '92

	SAMPLE	SAMPLE	SAMPLE	SAMPLE	SAMPLE	SAMPLE	SAMPLE	SAMPLE	SAMPLE	SAMPLE	SAMPLE	SAMPLE	SAMPLE	SAMPLE
	57	58	59	60	61	62	63	64	65	66	67	68	69	70
	Q	Q	Q	Q	Q	Q	Q		R	R	R	R	R	R
	4	6	8	9	11i	11ii	16	20521	1	3	4	5i	5ii	8
ELEMENT														
Cu	15	10	10	20	20	15	10	15	5	10	10	10	10	25
Pb	20	10	15	20	60	60	200	280	20	40	25	25	20	45
Zn	5650	6200	4100	1850	185	135	80	155	25	30	25	35	25	25
Ag	<1	<1	<1	<1	<1	<1	<1	1	<1	<1	<1	<1	<1	<1
Bi	<5	<5	<5	<5	<5	<5	<5	<5	<5	<5	<5	<5	<5	<5
Sb	<5	<5	<5	<5	<5	<5	<5	<5	<5	<5	<5	<5	<5	<5
Ba	380	470	480	320	300	910	340	40	195	55	270	310	370	430
Cd	<5	<5	<5	<5	<5	<5	<5	<5	<5	<5	<5	<5	<5	<5
Co	15	10	15	15	15	15	15	<5	10	15	15	10	10	15
Cr	30	35	60	35	25	20	20	15	40	35	30	40	25	25
Mo	<5	<5	<5	<5	<5	<5	<5	<5	<5	<5	<5	<5	<5	<5
Ni	30	25	20	20	15	15	10	10	15	20	15	10	10	25
S	2850	1700	5900	7550	5900	3600	640	3.16%	4400	2.63%	5800	6750	6700	5750
V	70	60	60	60	70	80	50	20	60	40	40	60	60	60
Zr	100	110	100	110	120	110	110	90	90	60	100	100	100	100
Ca	310	1100	350	230	90	100	140	3.60%	5.12%	8.28%	3.33%	4.14%	3.57%	2.60%
Fe	4.00%	5.70%	5.74%	3.07%	1.33%	1.33%	1.15%	4.18%	2.76%	5.65%	2.95%	3.05%	2.64%	2.18%
Mg	9600	1.13%	7900	6850	5550	7050	7700	1.54%	2.85%	3.69%	1.94%	2.16%	1.90%	1.67%
Mn	870	1250	1450	570	10	10	<10	1800	980	2300	830	1100	920	550
Ti	1300	1050	840	2250	1400	1750	1400	480	1300	430	760	1150	1800	940
Al	7.92%	7.79%	7.59%	6.62%	8.77%	9.18%	7.62%	4.38%	6.99%	3.67%	6.11%	6.45%	6.31%	6.99%
K	3.38%	2.67%	3.71%	3.00%	2.86%	2.46%	3.08%	4.44%	1.04%	2.51%	1.46%	2.28%	2.84%	3.94%
Na	450	430	380	1050	430	400	300	470	470	290	460	490	940	650
P	340	500	380	420	130	130	330	220	480	370	500	560	530	510
Sn	<20	<20	<20	<20	<20	<20	<20	<20	<20	<20	<20	<20	<20	<20
Sr	90	50	390	350	70	70	110	10	30	40	40	40	40	50
Tl	0.5	0.5	1.0	1.5	0.5	1.0	<0.5	34.5	<0.5	8.0	3.5	1.0	1.0	2.0

5

Lady Loretta Assays October '92

	SAMPLE	SAMPLE	SAMPLE	SAMPLE	SAMPLE	SAMPLE	SAMPLE	SAMPLE	SAMPLE	SAMPLE	SAMPLE	SAMPLE	SAMPLE	SAMPLE
	71	72	73	74	75	76	77	78	79	80	81	82	83	84
	S	S	S	S	T	T	T	T	T	V	W	W	W	W
	1	2	7	10	1	1	3	4	5	9	3	4	5	7
ELEMENT														
Cu	15	5	50	10	10	10	15	25	10	10	10	<5	<5	5
Pb	30	10	35	5	15	10	20	25	15	120	10	15	15	40
Zn	30	45	45	15	1800	1900	1700	1000	155	125	2800	35	40	35
Ag	<1	<1	1	<1	<1	<1	<1	<1	<1	<1	<1	<1	<1	<1
Bi	<5	<5	<5	<5	<5	<5	<5	<5	<5	<5	<5	<5	<5	<5
Sb	<5	<5	<5	<5	<5	<5	<5	<5	<5	<5	<5	<5	<5	<5
Ba	600	490	140	470	360	380	440	360	185	80	35	70	70	145
Cd	<5	<5	<5	<5	<5	<5	<5	<5	<5	<5	<5	<5	<5	<5
Co	10	15	10	10	5	5	20	20	10	10	5	<5	5	10
Cr	25	15	30	25	30	30	25	25	<5	10	20	15	20	30
Mo	<5	<5	<5	<5	<5	<5	<5	<5	<5	<5	<5	<5	<5	5
Ni	10	<5	15	10	10	10	20	30	<5	<5	10	<5	<5	15
S	4100	1950	1.94%	3950	3100	3200	4800	6500	3750	1.70%	2700	2500	2700	2.25%
V	60	20	40	70	60	60	40	70	20	50	10	20	20	60
Zr	110	140	90	110	110	120	120	110	130	80	20	30	30	120
Ca	3.10%	5.57%	4.46%	1.39%	1100	800	770	260	190	90	3450	11.4%	12.8%	3.00%
Fe	2.17%	2.08%	3.77%	1.63%	6.73%	7.19%	7.99%	3.41%	1.43%	7750	31.4%	2.81%	3.30%	2.91%
Mg	1.97%	2.88%	2.26%	1.37%	9550	1.01%	8250	6850	6700	3650	1.50%	5.97%	6.81%	2.03%
Mn	620	1050	900	240	2150	2250	2400	840	50	20	6250	2300	2450	510
Ti	2050	960	1150	2750	1500	2050	1150	2250	1150	1750	260	480	410	1800
Al	7.68%	3.56%	4.99%	8.84%	7.09%	7.57%	7.22%	5.99%	7.34%	6.02%	1.41%	2.07%	1.84%	6.81%
K	3.39%	1.50%	2.82%	1.54%	1.45%	2.06%	1.61%	3.71%	4.05%	2.64%	6850	1.24%	8450	2.43%
Na	820	480	730	1450	950	1050	1050	1100	940	730	140	190	170	540
P	520	300	410	480	400	400	620	200	160	440	50	260	210	770
Sn	<20	<20	<20	<20	<20	<20	<20	<20	<20	<20	<20	<20	<20	<20
Sr	20	30	40	20	10	10	10	60	<10	500	10	20	30	20
Tl	0.5	0.5	5.0	0.5	1.5	2.0	3.0	3.5	3.5	3.0	1.0	1.5	2.0	6.5

6

Appendix II: Analyses of Lady Loretta siltstones and shales — cont.

Lady Loretta Assays October '92

	SAMPLE	SAMPLE	SAMPLE	SAMPLE	SAMPLE	SAMPLE	SAMPLE	SAMPLE	SAMPLE	SAMPLE	SAMPLE	SAMPLE	SAMPLE	SAMPLE
	85	86	87	88	89	90	91	92	93	94	95	96	97	98
	W	W	W	W	W	W		X	X	X	Y	Y	Y	Y
	7	8	9	12	16	19	20524	1	7	8	2	3	4	4
ELEMENT														
Cu	10	5	10	<5	10	10	10	25	10	10	10	15	10	10
Pb	40	20	10	15	20	20	170	110	20	15	60	40	20	20
Zn	40	35	25	25	340	40	65	3050	510	290	1.95%	1.40%	1000	1000
Ag	<1	<1	<1	<1	<1	<1	2	3	<1	<1	1	<1	<1	<1
Bi	<5	<5	<5	<5	<5	<5	<5	<5	<5	<5	<5	<5	<5	<5
Sb	<5	<5	<5	<5	<5	<5	25	<5	<5	<5	<5	<5	<5	<5
Ba	125	155	150	70	165	120	50	570	280	280	190	550	400	450
Cd	<5	<5	<5	<5	<5	<5	<5	5	<5	<5	<5	<5	<5	<5
Co	10	10	10	10	10	15	5	20	15	20	30	20	10	10
Cr	30	10	10	15	40	10	30	60	25	30	25	40	60	45
Mo	5	<5	<5	<5	<5	<5	<5	<5	<5	5	<5	<5	<5	<5
Ni	15	5	<5	5	20	5	10	80	10	10	15	15	10	10
S	2.27%	9450	6100	1850	6250	2350	6.02%	5600	5350	4900	8350	6750	7050	7050
V	60	20	20	10	50	20	30	60	50	50	20	60	70	70
Zr	130	80	70	50	110	80	120	110	180	190	60	110	120	120
Ca	2.88%	4.62%	1.89%	11.3%	2450	1.49%	4.34%	750	750	470	1500	1100	500	530
Fe	2.88%	2.38%	1.36%	3.44%	5.32%	9550	7.58%	1.92%	3.63%	2.40%	11.4%	5.34%	1.94%	1.97%
Mg	1.97%	2.60%	1.29%	5.58%	7950	1.20%	2.39%	9650	6650	5100	8100	7550	7050	7450
Mn	480	940	350	2250	2750	280	2800	60	640	530	4000	1700	190	190
Ti	1650	780	1000	330	2000	1350	1200	2500	1850	1950	680	2000	2700	2750
Al	6.89%	6.10%	5.82%	1.69%	7.28%	6.34%	5.10%	7.58%	6.19%	5.27%	3.74%	6.84%	6.93%	7.40%
K	3.73%	1.64%	1.54%	8750	2.36%	2.90%	4.70%	2.65%	3.51%	2.61%	2.80%	3.49%	3.39%	2.80%
Na	910	600	480	200	520	380	530	470	640	470	290	650	780	900
P	800	260	320	180	500	360	400	420	760	490	490	450	470	480
Sn	<20	<20	<20	<20	<20	<20	<20	<20	<20	<20	<20	<20	<20	<20
Sr	20	20	<10	30	10	10	10	130	10	10	60	40	40	40
Tl	6.5	4.5	3.5	<0.5	2.0	0.5	31.5	3.0	2.0	1.0	9.0	2.0	2.5	2.0

7

Lady Loretta Assays October '92

	SAMPLE	SAMPLE	SAMPLE	SAMPLE	SAMPLE	SAMPLE	SAMPLE	SAMPLE	SAMPLE	SAMPLE	SAMPLE	SAMPLE	SAMPLE	SAMPLE
	99	100	101	102	103	104	105	106	107	108	109	110	111	112
	Y	Y	Y	Z	Z	Z	Z	Z	Z	Z				
	5	6i	6ii	3	5	7i	7ii	12	14	26	114-1	114-2i	114-2ii	114-3
ELEMENT														
Cu	10	<5	<5	10	45	20	30	15	10	10	25	15	15	10
Pb	10	5	10	15	115	140	65	270	300	85	5	20	20	<5
Zn	1.52%	85	70	6600	1.02%	1.16%	9300	2500	4200	60	35	25	35	25
Ag	<1	<1	<1	<1	2	2	2	<1	<1	<1	<1	<1	<1	<1
Bi	<5	<5	<5	<5	<5	<5	<5	<5	<5	<5	<5	<5	<5	<5
Sb	<5	<5	<5	<5	<5	<5	<5	<5	5	<5	<5	<5	<5	<5
Ba	240	75	175	800	330	130	160	360	140	2100	210	185	195	220
Cd	<5	<5	<5	<5	<5	<5	<5	<5	10	<5	<5	<5	<5	<5
Co	35	5	5	15	30	30	35	25	20	10	10	10	10	10
Cr	15	30	40	50	35	40	40	35	30	15	55	55	60	55
Mo	<5	<5	<5	<5	<5	<5	<5	<5	<5	<5	<5	<5	<5	<5
Ni	15	<5	<5	15	35	30	35	20	5	<5	10	10	15	10
S	3550	5050	7200	1750	1.11%	1.34%	1.09%	6050	7500	720	2400	1.01%	8400	6700
V	20	30	40	60	50	50	50	50	40	10	70	50	70	60
Zr	50	40	90	90	90	130	120	210	280	20	90	110	110	90
Ca	1100	9.86%	6.35%	1650	690	670	340	220	240	20	1.88%	4.37%	3.53%	4.46%
Fe	9.66%	2.93%	2.36%	6.32%	7.74%	8.45%	8.45%	2.77%	1.35%	1050	1.42%	3.33%	3.11%	3.09%
Mg	9100	5.12%	3.39%	8700	8300	1.13%	1.33%	6950	4650	30	1.22%	2.24%	2.08%	2.32%
Mn	3400	1750	1100	1450	2250	1600	1550	250	10	<10	380	1350	1100	1450
Ti	590	720	1600	1700	1750	1450	1500	2150	1850	370	2550	2100	2300	2150
Al	3.32%	2.61%	4.32%	7.06%	6.69%	6.44%	6.82%	5.16%	4.85%	4.37%	5.19%	5.88%	7.05%	6.53%
K	1.83%	1.89%	2.03%	2.50%	2.78%	2.91%	3.10%	1.87%	1.85%	320	2.65%	2.26%	2.80%	2.85%
Na	210	200	350	500	470	300	630	750	600	210	1150	1100	1300	670
P	290	270	390	110	270	430	100	380	570	90	470	480	460	440
Sn	<20	<20	<20	<20	<20	<20	<20	<20	<20	<20	<20	<20	<20	<20
Sr	30	20	20	40	170	160	30	350	450	60	20	30	20	30
Tl	3.0	6.5	3.5	1.5	3.5	7.5	5.0	2.5	0.5	<0.5	0.5	4.0	1.5	1.0

8

Appendix II: Analyses of Lady Loretta siltstones and shales — cont.

Lady Loretta Assays October '92

	SAMPLE	SAMPLE	SAMPLE	SAMPLE	SAMPLE	SAMPLE	SAMPLE	SAMPLE
	113	114	115	116	117	118	119	120
	114-3	114-4	20528	155-1	155-2	155-3	155-4	155-5
ELEMENT								
Cu	10	25	15	15	15	15	10	10
Pb	<5	<5	220	<5	15	<5	15	<5
Zn	25	30	240	30	35	20	25	20
Ag	<1	<1	1	<1	<1	<1	<1	<1
Bi	<5	<5	<5	<5	<5	<5	<5	<5
Sb	<5	<5	10	<5	<5	<5	<5	<5
Ba	220	230	130	300	170	190	195	130
Cd	<5	<5	<5	<5	<5	<5	<5	<5
Co	10	5	<5	25	15	15	20	15
Cr	55	40	25	50	40	25	25	30
Mo	<5	<5	<5	<5	<5	<5	<5	<5
Ni	10	10	5	20	10	10	15	15
S	6750	2050	2.95%	1.03%	4550	5350	3950	6750
V	60	70	20	60	40	30	20	50
Zr	90	100	110	150	100	180	50	130
Ca	4.57%	2.31%	4.74%	5600	6.23%	4.17%	5.64%	5.07%
Fe	3.16%	2.11%	4.69%	1.82%	2.46%	2.09%	2.05%	1.87%
Mg	2.35%	1.71%	2.18%	9350	3.41%	2.37%	3.13%	3.21%
Mn	1500	680	3050	130	770	500	620	400
Ti	2200	2550	940	2800	1750	1700	750	1850
Al	6.56%	8.84%	5.42%	7.69%	5.10%	4.89%	2.96%	5.12%
K	2.68%	2.62%	1.76%	3.38%	1.64%	2.21%	2.24%	2.33%
Na	850	740	590	840	430	450	300	880
P	450	550	250	620	330	330	250	450
Sn	<20	<20	<20	<20	<20	<20	<20	<20
Sr	30	20	10	20	30	20	30	30
Tl	1.0	0.5	24.5	0.5	<0.5	<0.5	<0.5	<0.5

9

Appendix III: Quality assessment of assay results

Table III-1 present my estimate of the accuracy and precision of the commercially obtained analyses report herein. The accuracy of the determinations was assessed by hiding six samples previously analysed at the University of Melbourne by a combination of XFR and radiochemical NAA. One of these was run twice thus generating a set of seven 'knowns'. The results for these samples are presented in Table III-2. As a gauge of precision nineteen of the analyses of 'unknowns' were duplicated (including nine 'hidden' duplicate samples). Clearly, the results for some elements are not satisfactory; these include Ba, Cr, K, Na, and Ti. While others need further checking. Of the elements determined by ICP-ES Al, Fe, Mg, Mn, P, S, Zn and Zr are acceptable. No assessment could be made of Ag, Bi, Cd, Mo, Sb and Sb because they were present at levels at or near the detection limit for the technique.

Element	Precision (19 duplicates)	Accuracy (7 'knowns')
Ag	na*	na (5/6 ok)
Al	fair-poor	**good**
Ba	fair	poor (all v. low)
Bi	na	na
Ca	fair-poor	**good-fair**
Cd	na	na
Co	**good**	na
Cr	poor	fair
Cu	fair	poor
Fe	**good**	**good**
K	poor	poor
Mg	**good**	**good**
Mn	**good**	**good-fair**
Mo	na	na
Na	poor	poor
Ni	**good**	poor (all low)
P	**good**	**good**
Pb	**good-fair**	poor (2 high, 4 low)
S	**good**	**good** (1 low)
Sb	na	fair (2 low)
Sn	na	na
Sr	**good**	na
Ti	fair-poor	poor
Tl	**good-fair**	poor (all low)
V	**good-fair**	fair
Zn	**good**	**good** (1 v. high)
Zr	fair-poor	**good**

*na - most analyses at or near detection limit

Appendix III: Quality assessment of assay results — cont.

Sample #	I.D.	Cu meas	Cu exp	Pb meas	Pb exp	Zn meas	Zn exp	Ag meas	Ag exp	Sb meas	Sb exp	Ba meas	Ba exp
9	20495	15	55	200	355	165	134	2	6.91	5	41	50	233
27	20510	10	65	3950	428	390	415	8	8.97	30	41	35	305
32	20517	10	43	2200	236	1100	108	5	5.81	5	25	65	591
64	20521	15	65	280	437	155	182	1	2.36	5	15	40	582
91	20524	10	66	170	311	65	74	2	3.22	25	38	50	958
115	20528	15	54	220	311	240	272	1	1.72	10	15	130	833
9 (qc)	20495	10	55	195	355	155	134	2	6.91	10	41	60	233

		Cd meas	Cd exp	Co meas	Co exp	Cr meas	Cr exp	Ni meas	Ni exp	S meas	S exp	V meas	V exp
9	20495	5	0.45	10	14	40	11	15		2.53	4.24	30	40
27	20510	5	1.40	10	6	30	23	10	20	3.74	4.10	20	31
32	20517	5	4.05	5	4	20	5	10	20	2.51	2.49	10	18
64	20521	5	0.47	5	3	15	7	10	20	3.16	3.42	20	22
91	20524	5	0.12	5	5	30	19	10	20	6.02	6.34	30	45
115	20528	5	0.77	5	3	25	9	5	26	2.95	3.42	20	27
9 (qc)	20495	5	0.45	10	14	20	11	15		3.99	4.24	30	40

		Zr meas	Zr exp	Ca meas	Ca exp	Fe meas	Fe exp	Mg meas	Mg exp	Mn meas	Mn exp	Ti meas	Ti exp
9	20495	70	64	6.97	9.43	5.93	6.01	4.23	4.48	2500	2880	620	1220
27	20510	100	99	5.87	6.53	5.88	6.14	2.93	3.25	3650	4210	760	1130
32	20517	90	85	5.58	5.75	4.39	4.39	2.32	2.53	3850	4410	660	821
64	20521	90	92	3.6	3.91	4.18	4.46	1.54	1.80	1800	2180	480	929
91	20524	120	118	4.34	4.64	7.58	7.87	2.39	2.63	2800	3180	1200	1710
115	20528	110	102	4.74	5.19	4.69	4.78	2.18	2.42	3050	3450	940	1100
9 (qc)	20495	80	64	8.9	9.43	5.82	6.01	4.14	4.48	2400	2880	500	1220

		Al meas	Al exp	K meas	K exp	Na meas	Na exp	P meas	P exp	Sr meas	Sr exp	Tl meas	Tl exp
9	20495	3.05	3.15	2.73	3.92	500	430	370	354	20	8	6.5	42.9
27	20510	3.8	4.04	3.64	4.94	840	1020	260	253	20	37	35.5	56.9
32	20517	4.34	4.51	4.65	5.31	580	831	210	201	20	21	18.5	52.8
64	20521	4.38	4.97	4.44	5.81	470	660	220	231	10	16	34.5	59.8
91	20524	5.1	5.40	4.7	5.96	530	734	400	415	10	20	31.5	70.6
115	20528	5.42	5.50	1.76	6.81	590	846	250	253	10	16	24.5	64.8
9 (qc)	20495	3.09	3.15	3.3	3.92	1000	430	370	354	20	8	5.5	42.9

DEPOSIT HALOS

2. Sulphur isotopes: status report

Peter McGoldrick
Centre for Ore Deposit and Exploration Studies

LADY LORETTA

At the time of writing no S isotope analyses have been carried on Lady Loretta samples, however, material collected for geochemical analysis (esp. pyrite samples) will be used for future work. Sulphur isotopes may reveal the source of S in the ores and the bedded pyrite, and also provide insights into the mechanisms involved in generating the sulphide needed for ore formation (e.g. Davidson's abstract in this volume).

Carr (1981, 1986) reports a small number of S isotope determinations from the Ore Horizon and from bedded pyrite in the Cyclic Unit above the ores. His work demonstrates a variation in $\delta^{34}S$ values from 4 to 22‰ in the ores and up to a 10‰ variation in individual pyrite beds. Only limited inferences can be made from these data, but they suggest both closed and open system sulphate reduction processes were operating on a small scale.

For the planned work at Lady Loretta the new laser ablation S isotope facility in the Central Science Laboratory at the University of Tasmania will be used to analyse individual 100 μm sized areas. This capability should help resolve the sampling difficulties inherent in using conventional techniques on isotopically variable samples and lead to new insights into.the ore forming process. It is worth noting that the conflicting interpretation of a large set of conventional S isotopic analyses from HYC was not resolved until the ion microprobe was used to analyse individual mineral generations *in situ* (Eldridge, Econ. Geol., in press).

SULPHUR ISOTOPES ELSEWHERE IN THE MCNAMARA GROUP

As reported in the July Quarterly report CRA/Newmont drill core from the Gunpowder Creek and Paradise Creek Formation on the southern flank of the Kamarga Dome (fig. 1) were sampled for S isotope determinations. These samples cover several hundred metres of mainly sparsely pyritic stratigraphy. Again the laser probe will be used for isotopic determinations on samples that would not yield enough (ca. 10 mg of pyrite) sulphide for conventional analysis.

Request have been made to sample core drilled by the Geological Survey of Queensland and Amoco in the late 70s and early 80s. The core is reposited with the GSQ in Brisbane and will be examined in December or early next year (this core will also be used for sedimentological studies). Samples from these holes should provide a complete S isotope profile for the McNamara Group in the northern part of the Lawn Hill Platform.

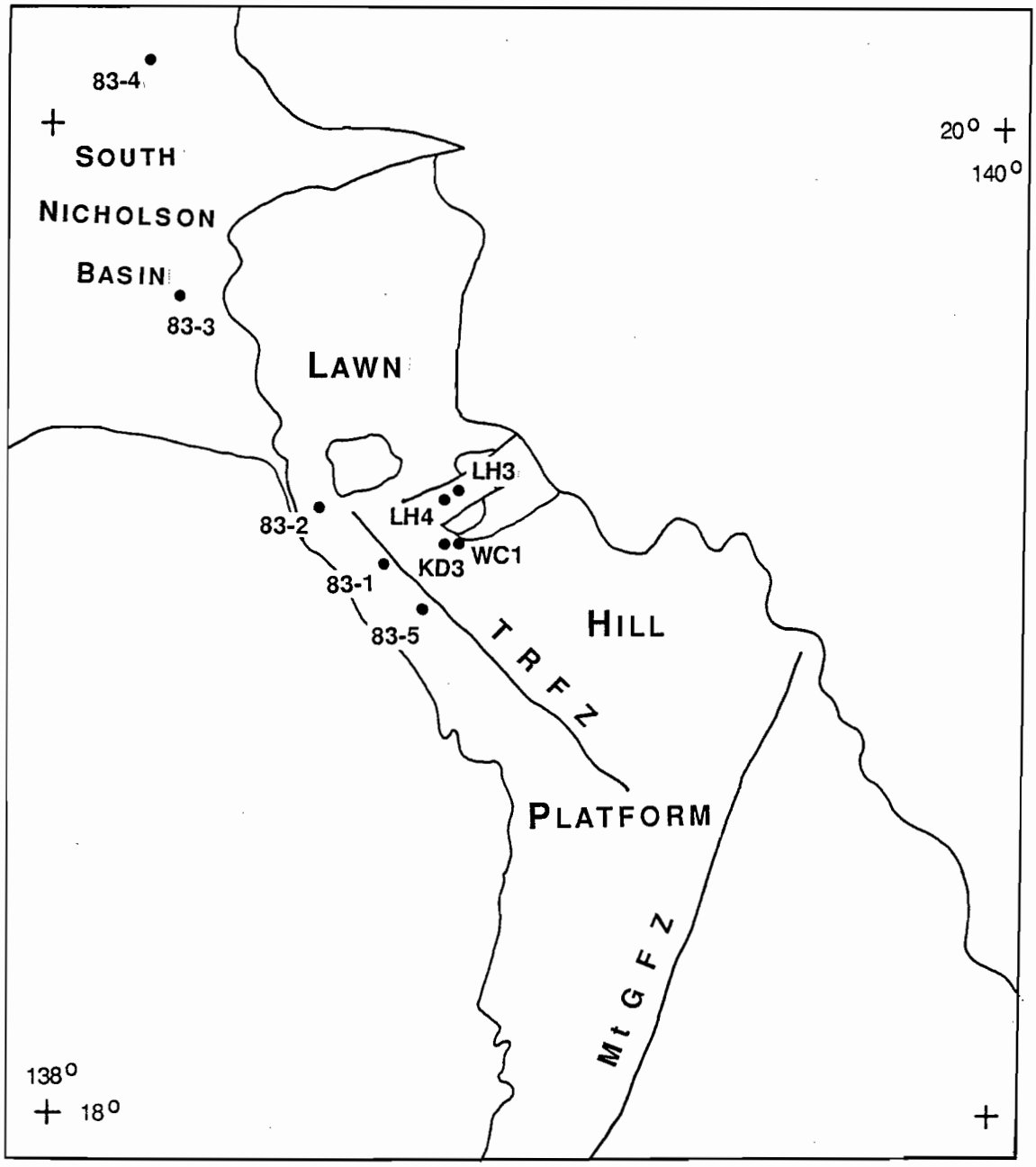

Figure 1 — General outline of the Lawn Hill Platform showing the location of diamond drill holes mentioned in text (Amoco holes 83-1 to 5, CRA/Newmont holes WC1 and KD3).

SEDIMENTOLOGY/BASIN ANALYSIS

Peter McGoldrick
Centre for Ore Deposit and Exploration Studies

1. UPDATE ON THE RESEARCH FELLOW APPOINTMENT

Over thirty applications were received for the Basin Analysis/Sedimentology Research Fellow position. From these a short list of seven was selected. At the time of writing an offer is about to be made to the most suitable of these and we hope to have confirmation of acceptance by the November meeting.

As a result of this years field work in both the McArthur basin and north west Queensland that there are a number areas for the new appointee to contribute to.

Prior to the next NT field season sedimentological studies are planned for Lady Loretta (see below) and assistance is needed to constrain stratigraphic sampling of Lawn Hill Platform core. In the southern McArthur Basin several areas mapped by Richard Keele and Jamie Rogers need sedimentologic work.

2. LADY LORETTA SEDIMENTOLOGY PhD PROPOSAL — The sedimentary setting of the Lady Loretta Zn–Pb–Ag deposit, northwest Queensland

Recent detailed investigations of the sedimentary host rocks of the Mount Isa and HYC deposits (Neudert, 1983 (PhD, RSES-ANU) reprinted 1986; Logan, var) have contributed to a fundamental re-interpretation of the geological setting and genesis of these deposits. Similar work has not been carried out at Lady Loretta, although, following a short visit in 1987, M. Neudert recommended that detailed sedimentological work should be undertaken.

Research work is being carried out at Lady Loretta as part of the AMIRA Project 384, and with mining activity "on hold", an opportunity exist for a detailed sedimentological analysis of the Lady Loretta Formation in the vicinity of the deposit. Drill core from the last twenty years is stored on site, and is, for the most part, reasonably well preserved and accessible. Costeans and surface exposure in the vicinity of the mine have been mapped at quite large scales. These materials provide an excellent background for detailed sedimentologic studies.

The work proposed has the potential to add substantially to our understanding of Proterozoic sediment hosted base metal deposits, and provide important background information to the geochemical halo studies currently underway at Lady Loretta. The project would address a number of questions with important exploration implications. These include, on a local scale:

- is there a small scale facies control on the position of the ore horizon (OH) in the Small Syncline?
- was the OH in the Big Syncline deposited in the same sedimentary environment as in the Small Syncline?
- what was the palaeogeography of the Lady Loretta sub-basin?
- can a plausible palinspastic reconstruction combining the Big Syncline and Small Syncline sequences be deduced?

and more regionally:

- can the sedimentary facies observed in proximity to the mine be recognised elsewhere in the Lady Loretta Formation?
- what elements of the sedimentary package mandatory for base metal mineralisation?
- can the Lady Loretta OH be identified regionally?
- can a sequence stratigraphy approach (i.e., interpreting sedimentary rocks in terms of basin scale events and cycles) be applied to the Lady Loretta Formation and/or McNamara Group?

- what are the tectonic controls on these sequences and how do these relate to the geological evolution of the Lawn Hill Platform, and what do these imply for basin scale fluid movements?

The initial work for this project would be twofold:

(i) detailed logging of underground and surface drill-core with the emphasis on sedimentary features; this would be complimented by lab studies of sample mineralogy and geochemistry
(ii) mapping of nearby measured sections and costeans to relate surface outcrop to the data from core.

The field work would require a three or four month field season in 1992.

Pending logistic support and availability of suitable drill-core material, later work would extend beyond the immediate Lady Loretta area.

BRINE CHEMISTRY

Sulfide solubilities and depositional processes in sedimentary brines: preliminary modelling results

David R. Cooke
Centre for Ore Deposit and Exploration Studies

INTRODUCTION

Geological and geochemical controls on ore transport and deposition in Proterozoic stratabound/stratiform environments are currently being investigated using thermodynamic computer modelling techniques. Preliminary work has involved updating and modifying the thermodynamic database SOLTHERM for use in this project. Initial calculations are now focusing on the metal-carrying capacity of reduced and oxidised sedimentary brines under a variety of geologically reasonable conditions. These calculations are an essential prerequisite for investigations of fluid–rock and fluid–fluid interactions in sedimentary/hydrothermal environments. Preliminary examples of fluid-buffered depositional processes are also presented to demonstrate what is planned upon completion of the solubility calculations.

SULFIDE SOLUBILITIES IN SEDIMENTARY BRINES

Key variables that can influence metal solubilities in hydrothermal solutions include temperature, total sulfur and dissolved gas concentrations, pH, salinity and the redox state of the fluid. To undertake the thermodynamic study, the following parameters have been selected to represent likely conditions for metalliferous brines immediately prior to their entry into the environment of mineral deposition:

- Temperature: 100°, 150°, 200°, 250°C
- Salinity: ≈ 5, 10, 15, 20 eq. wt. % NaCl (NaCl + KCl + $CaCl_2$)
- pH: K-feldspar–muscovite & muscovite–kaolinite buffers
- ΣS: 0.01, 0.001 and 0.0001 molal
- Redox state: reduced (pyrite field), oxidised (pyrite–hematite boundary, hematite field)
- Dissolved CO_2: 0.1 molal

As sophisticated thermodynamic software packages now enable detailed studies of complex multiphase systems, a 19-component chemical system has been selected that contains most of the important major and trace elements present in sediment-hosted base metal deposits. The component species considered are:

- H^+ H_2O Cl^- HCO_3^- SO_4^{-2} $SiO_{2\,(aq)}$
- Al^{+3} Ca^{+2} Mg^{+2} Fe^{+2} Na^+ K^+
- Zn^{+2} Cu^+ Pb^{+2} Ag^+ $AuCl_2^-$ Ba^{+2}
- HS^- (reduced fluid) or $O_{2\,(aq)}$ (oxidised fluid)

Total concentrations of unknown component species are calculated using computer program SOLVEQ (Reed, 1982; Reed and Spycher, 1984, 1985) to force mineral equilibration between the brine and any appropriate sulfide, oxide, silicate, carbonate and sulfate phases (e.g. Zn^{+2}–sphalerite; Pb^{+2}–galena). Initial calculations have been conducted at 250°C with the pH of the fluids buffered by K-felspar–muscovite equilibrium. To date, a total of eight brines have been constructed (table 1). This preliminary data provides some insights into the chemical nature of 'high' temperature high salinity fluids in the sediment-hosted environment (discussed below), in addition to testing some of the assumptions outlined above.

Salinity estimates

It has been assumed that the sedimentary brines are dominated by NaCl, with approximately one order of magnitude less KCl and $CaCl_2$. Initial calculations (Brines 1–6) were conducted with the following salt concentrations:

CODES: AMIRA/ARC Project P.384 — Proterozoic sediment-hosted base metal deposits. November 1992

- 5 wt. % NaCl (Brines 1 & 4) 0.5 wt. % KCl 0.5 wt. % $CaCl_2$
- 10 wt. % NaCl (Brines 2 & 5) 1.0 wt. % KCl 1.0 wt. % $CaCl_2$
- 20 wt. % NaCl (Brines 3 & 6) 2.0 wt. % KCl 2.0 wt. % $CaCl_2$

Note that Cl^- is the dominant ion in these brines. To maintain charge balance in the fluid, Cl– concentrations are adjusted during each forced mineral equilibration step. Initial calculations have revealed that this process results in increased chloride concentrations when other major elements are added to the system. For example, because iron becomes more soluble at high salinities, brines 3 and 6 have a significant component of $FeCl_2$, which adds to their total dissolved salt concentrations. To reduce the effects of 'salinity creep', lower initial salt concentrations have been selected as starting parameters for all subsequent brine calculations:

- 4 wt. % NaCl (Brine 7) 0.5 wt. % KCl 0.5 wt. % $CaCl_2$
- 8 wt. % NaCl (Brine 8) 1.0 wt. % KCl 1.0 wt. % $CaCl_2$
- 12 wt. % NaCl 1.5 wt. % KCl 1.5 wt. % $CaCl_2$

Dissolved CO_2

A value of 0.1 molal was selected to represent dissolved CO_2 concentrations in the modelled sedimentary brines. This was considered a reasonable starting assumption because higher CO_2 concentrations are more typical of metamorphic or proximal magmatic environments. However, the low CO_2 content has prevented carbonate saturation in any of the brines modelled to date. For example, even in the oxidised brines, talc (rather than dolomite) is the stable Mg-bearing phase. This situation is unlikely if the brines have interacted with carbonate-bearing horizons in the subsurface. Carbonate saturation in the mineralising brines requires either increased CO_2 concentrations (possibly caused by progressive dissolution of dolomite) or more alkaline fluids. Either scenario may be feasible, providing the mineralised brines are derived from a carbonate-dominated (rather than clastic-dominated) basin.

Zinc, lead and silver

The maximum amount of zinc and lead that can be transported in hydrothermal brines is normally controlled by the solubility of sphalerite and galena. For example, under reduced saline conditions at 250°C, maximum zinc concentrations can be calculated from the following reactions (Ruaya and Seward, 1986):

$$ZnS + 2H^+ + Cl^- \leftrightarrow ZnCl^- + H_2S \quad (1)$$
$$ZnS + 2H^+ + 2Cl^- \leftrightarrow ZnCl_2 + H_2S \quad (2)$$
$$ZnS + 2H^+ + 4Cl^- \leftrightarrow ZnCl_4^{-2} + H_2S \quad (3)$$

Similarly, galena solubilities are controlled by the following equilibria at 250°C (Seward, 1984):

$$PbS + 2H^+ + Cl^- \leftrightarrow PbCl^- + H_2S \quad (4)$$
$$PbS + 2H^+ + 2Cl^- \leftrightarrow PbCl_2 + H_2S \quad (5)$$
$$PbS + 2H^+ + 3Cl^- \leftrightarrow PbCl_3^- + H_2S \quad (6)$$

Examination of these equations reveals that galena and sphalerite are most soluble under high salinity, low pH and low total sulfur conditions in reduced fluids. Under oxidised conditions ($\Sigma SO_4^{-2}/\Sigma H_2S > 1$), galena and sphalerite solubilities become very high and independent of pH. High solubilities are also favoured by higher temperatures.

Silver is somewhat more problematical. In sediment-hosted base metal deposits, silver commonly occurs within argentiferous galena, sphalerite or tetrahedrite. However, there is currently no data available to allow modelling of silver substitution in base metal sulfides or sulfosalts. To calculate silver concentrations, equilibrium has been forced between the brines and Ag_2S. At 250°C and at high salinities (> 5 wt %), silver chloride complexes predominate over bisulfide complexes (Gammons and Barnes, 1989). Consequently, acanthite/argentite solubility is controlled by the same variables that affect galena and sphalerite (salinity, temperature, ΣS, pH and redox state).

Figure 1 and table 2 demonstrate that zinc, lead and silver behave in a similar fashion in neutral saline brines at 250°C. As predicted, greater sulfide solubilities are favoured by high salinities, oxidised conditions and low total sulfur concentrations, with the highest solubilities coinciding with the highest chloride concentrations. At any given salinity, highest galena, sphalerite and argentite solubilities occur in the more oxidised brines, with reduced, sulfide-rich brines having the lowest capacity for transporting base metals.

Fluids 1 to 8 are zinc-rich and relatively lead-deficient, with consistently high zinc ratios (100 Zn/Zn + Pb; table 2). If these saturated brines were responsible for base metal mineralisation in the sediment-hosted environment, the resultant orebody would contain abundant zinc and minor lead. The zinc-rich nature of these fluids is a consequence of metal speciation at 250°C. Under the conditions modelled for fluids 1 to 8, the dominant zinc chloride species is $ZnCl_4^{-2}$, whereas $PbCl_2$ and $PbCl_3$ are the major transporting agents for lead. Higher-order chloro complexes (such as $ZnCl_4^{-2}$) are stabilised at high chloride concentrations, allowing the fluids to transport greater quantities of the complexed metal

	1	2	3	4	5	6	7	8
pH	5.4	5.1	4.8	5.4	5.1	4.8	5.4	5.1
Salinity	6.0 wt %	12.0 wt %	24.5 wt %	5.9 wt %	11.1 wt %	25.4 wt %	5.50 wt %	11.1 wt %
ΣS	0.01	0.01	0.01	0.001	0.001	0.001	0.001	0.001
log $f_{(O_2)}$	-38.5	-38.5	-38.5	-37.8	-37.8	-37.8	-34.4	-34.3
H^+	0.0212	0.0223	.0264	0.0239	0.0262	0.0300	0.0238	0.0252
H_2O	1 kg	1 kg	1 kg	1 kg	1 kg	1 kg	1 kg	1 kg
Cl^-	1.085	2.341	5.588	1.081	2.150	5.883	0.996	2.143
SO_4^{-2}	-0.00609	-0.00651	-0.00660	-3.41E-04	-3.53E-04	-3.03E-04	0.001	0.001
HCO_3^-	0.0242	0.0259	0.0299	0.0242	0.0263	0.0299	0.0239	0.0253
HS^-	0.01	0.01	0.01	0.001	0.001	0.001	-	-
$SiO_{2\,(aq)}$	0.00643	0.00643	0.00643	0.00643	0.00643	0.00643	0.00643	0.00643
Al^{+3}	1.85 E-08	3.13 E-08	1.85 E-07	1.83 E-08	2.99 E-08	1.61 E-07	1.80 E-08	3.00 E-08
Ca^{+2}	0.0482	0.103	0.233	0.0480	0.0103	0.238	0.0475	0.100
Mg^{+2}	9.42 E-04	0.00843	0.00813	8.85 E-04	0.00718	0.00832	8.15 E-04	0.00704
Fe^{+2}	6.32 E-05	3.14 E-04	0.0404	9.38 E-05	0.00312	0.220	2.69 E-05	0.00151
K^+	0.0713	0.166	0.456	0.0691	0.157	0.357	0.0681	0.160
Na^+	0.913	1.949	4.526	0.912	1.948	4.512	0.722	1.523
Zn^{+2}	4.98 E-06	1.03 E-04	0.0150	1.23 E-05	4.06 E-04	0.0387	4.14 E-05	0.00212
Cu^+	9.30 E-08	4.05 E-07	1.20 E-05	6.58 E-08	4.72 E-07	1.31 E-05	4.11 E-07	3.52 E-06
Pb^{+2}	1.83 E-07	1.51 E-06	5.59 E-05	5.56 E-07	6.44 E-06	1.42 E-04	2.10 E-06	3.66 E-05
Ag^+	5.74 E-07	3.04 E-06	6.45 E-05	9.12 E-07	5.72 E-06	1.00 E-04	1.59 E-06	1.30 E-05
$AuCl_2^-$	5.90 E-07	3.74 E-07	2.41 E-07	2.55 E-08	1.91 E-08	1.87 E-08	1.02 E-08	4.83 E-09
Ba^{+2}	0.00151	0.00161	0.00186	0.00151	0.00161	1.86 E-03	5.50 E-05	2.52 E-04
$O_{2\,(aq)}$	-	-	-	-	-	-	-3.16E-04	-2.37E-03

Table 1 — Modelled brine compositions at 250°C. Unless otherwise stated, component species concentrations are in molal units. Brines 1 to 6: reduced fluids (pyrite stability field). Brines 7 & 8: oxidised fluids (pyrite-hematite boundary). Brine compositions are based on initial assumptions of ΣS, NaCl, KCl, and $CaCl_2$ concentrations and pH (K-feldspar-muscovite equilibrium). Total concentrations of component species have been calculated by forcing equilibration between the brines and the following minerals: $SiO_{2\,(aq)}$–quartz; Al^{+3}–K-feldspar; Mg^{+2}–talc; Fe^{+2}–pyrite; K^+–muscovite; Zn^{+2}–sphalerite; Cu^+–chalcopyrite; Pb^{+2}–galena; Ag^+–acanthite; $AuCl_2^-$–gold; Ba^{+2}–barite (brines 7-8); $O_{2\,(aq)}$–hematite (brines 7–8). Ba^{+2} concentrations for brines 1–6 are set at 194 ppm, based on measured concentrations from the Salton Sea brines (McKibben and Williams, 1989).

Brine	ΣZn (ppm)	ΣPb (ppm)	ΣAg (ppb)	ΣAu (ppb)	ΣCu (ppb)	ΣFe (ppm)	Zn ratio
1	0.305	0.0356	58.08	108.9	5.543	0.331	89.5
2	5.874	0.275	287.2	64.55	22.55	15.37	95.5
3	733.0	8.666	5207.6	35.60	570.8	1689.7	98.8
4	0.754	0.108	92.23	4.718	3.920	4.915	87.5
5	23.48	1.180	545.6	3.333	26.53	154.3	95.2
6	1867.2	21.680	7993.4	2.719	616.4	9088.9	98.9
7	2.557	0.411	161.5	1.894	24.67	1.420	86.2
8	123.6	6.740	1247.5	0.847	199.2	75.13	94.8

*Table 2 — Total mass of selected component species per kg of water in modelled brines at 250°C. Zinc ratios calculated using the formula 100*Zn/(Zn+Pb) from Huston and Large (1987). Brines 1, 2 & 3: reduced fluids (pyrite stability field), ΣS = 0.01 molal. Brines 4, 5 & 6: reduced fluids (pyrite stability field), ΣS = 0.001 molal. Brines 7 & 8: oxidised fluids (pyrite-hematite boundary), ΣS = 0.001 molal. Brines 1, 4 & 7: salinity ≈ 6 eq. wt % NaCl. Brines 2, 5, & 8: salinity ≈ 11 eq. wt % NaCl. Brines 3 & 6: salinity ≈ 24 eq. wt % NaCl. pH and log $f_{(O_2)}$ values are presented in table 1.*

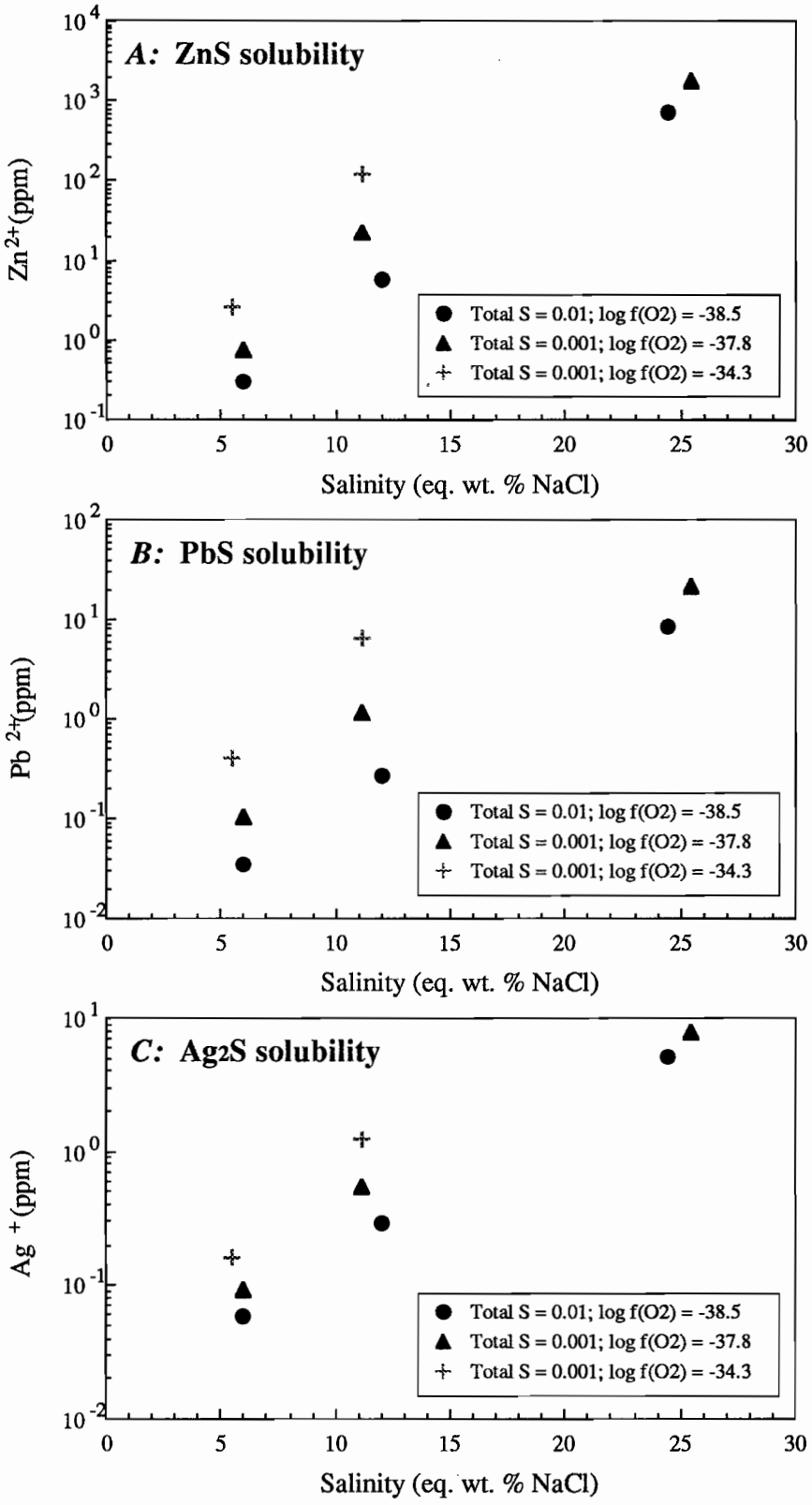

Figure 1 — Sulfide solubilities as a function of salinity in sedimentary brines at 250°C. A: Sphalerite. B: Galena C: Acanthite. The pH is buffered by K-feldspar-muscovite. For the oxidised brine ('+' symbols), oxygen fugacity is buffered by hematite-pyrite equilibria. For the reduced brines, oxygen fugacities are constrained to the pyrite field (just above the upper stability limit for graphite).

(in this instance zinc) than the metals that undergo lower-order chloro-complexing (e.g. lead).

Copper

In neutral saline brines, chalcopyrite solubility is mostly controlled by the same variables that influence galena, sphalerite and argentite. This causes copper to mimic the behaviour of the other base metals in these solutions (compare figs 1 and 2). However, the *amount* of copper that can be transported at 250°C under the modelled conditions is significantly less than the corresponding amounts of lead and zinc (generally 1 to 3 orders of magnitude lower; table 2). It is therefore unlikely that sedimentary brines with compositions similar to those modelled here would have the potential to form a significant copper resource. These results are in agreement with the four scenarios outlined in Large (1991), where copper-rich sediment-hosted deposits require oxidised brines as the metal-transporting agency.

Gold

Gold is transported primarily as a bisulfide complex at temperatures below 300°C under near-neutral pH conditions, whereas lead, zinc, silver and copper are transported as chloro complexes. High gold solubilities are favoured by high total sulfur concentrations, low salinities and neutral pH conditions. Furthermore, oxygen fugacities must be confined approximately between the pyrite–hematite and pyrite–pyrrhotite buffers for high gold solubility. Consequently, the behaviour of gold is markedly different to silver, lead, zinc and copper in the modelled brines (compare figs 1 and 2). Highest gold solubilities occur in low salinity sulfur-rich reduced fluids (table 2). When gold is compared to silver (table 2), the highest concentrations of silver (and lead and zinc) are found to correlate with the lowest gold values at any given salinity (i.e. in high salinity sulfur-deficient oxidised brines).

To date, there are no known examples of gold-enriched sediment-hosted Pb–Zn–Ag deposits. This could mean either:

(1) The mineralising brines responsible for sediment hosted Pb–Zn mineralisation are not capable of carrying sufficient gold to form economic gold mineralisation.
(2) Even though the fluids are capable of carrying significant amounts of gold (≈ 1 ppb or more), they remained undersaturated because of a paucity of gold in the source regime
(3) The fluids carried significant gold but did not undergo processes conducive for effective gold precipitation (e.g. boiling, oxidation, etc.).

The first scenario is considered most likely — solubility calculations have demonstrated that even at neutral pH (the most favourable conditions for gold transport as a bisulfide complex), certain brines have the capacity to transport significant zinc, lead and silver with very little gold (e.g. Brines 4 to 8; table 2).

The second scenario is considered unlikely because even though the sediments and volcanics in any given basin may have very low background gold, connate brines have the potential for prolonged residence times (millions to tens of millions of years) prior to their eventual release into the ore-forming environment. Such prolonged repose times should favour highly efficient scavenging of chalcophile elements, resulting ultimately in saturation (or near-saturation) of precious and base metals in the connate brines.

If the third scenario were true, gold would most likely form a dispersion halo around the mineralised system (if syngenetic or hydrothermal/diagenetic models of ore formation are correct). This possibility will hopefully be tested in the dispersion halo module by analysing selected samples from Lady Loretta to see if they have elevated gold values. It will also be tested in the brine chemistry module by numerical simulations of potential ore-forming processes in the sediment-hosted environment.

Conclusions

The brines modelled to date do not have the potential to form economic copper mineralisation, although some may have the capability to form a zinc-rich orebody. The brines capable of transporting significant gold are not likely to be representative of mineralising brines in sediment hosted systems. If pH is buffered by K-feldspar–muscovite equilibrium and the fluids are reduced, total sulfur contents of the mineralising brines in Pb–Zn–Ag systems must be low (0.001 or lower), implying that sulfur is most likely incorporated at the site of ore deposition.

The metal solubility calculations will be extended to lower temperatures and lower pH conditions, allowing us to compare and contrast a variety of solution compositions, in order to establish the most favourable conditions for metal transport (within the constraints of the available thermodynamic data).

DEPOSITIONAL PROCESSES IN SEDIMENT-HOSTED ENVIRONMENTS

Whereas the speciation calculations outlined above provide information on metal *transport* in sedimentary brines, investigations into fluid–rock and fluid–fluid interactions test the likelihood and relative efficiency of various *depositional* processes in sediment-hosted environments. The computer program CHILLER will

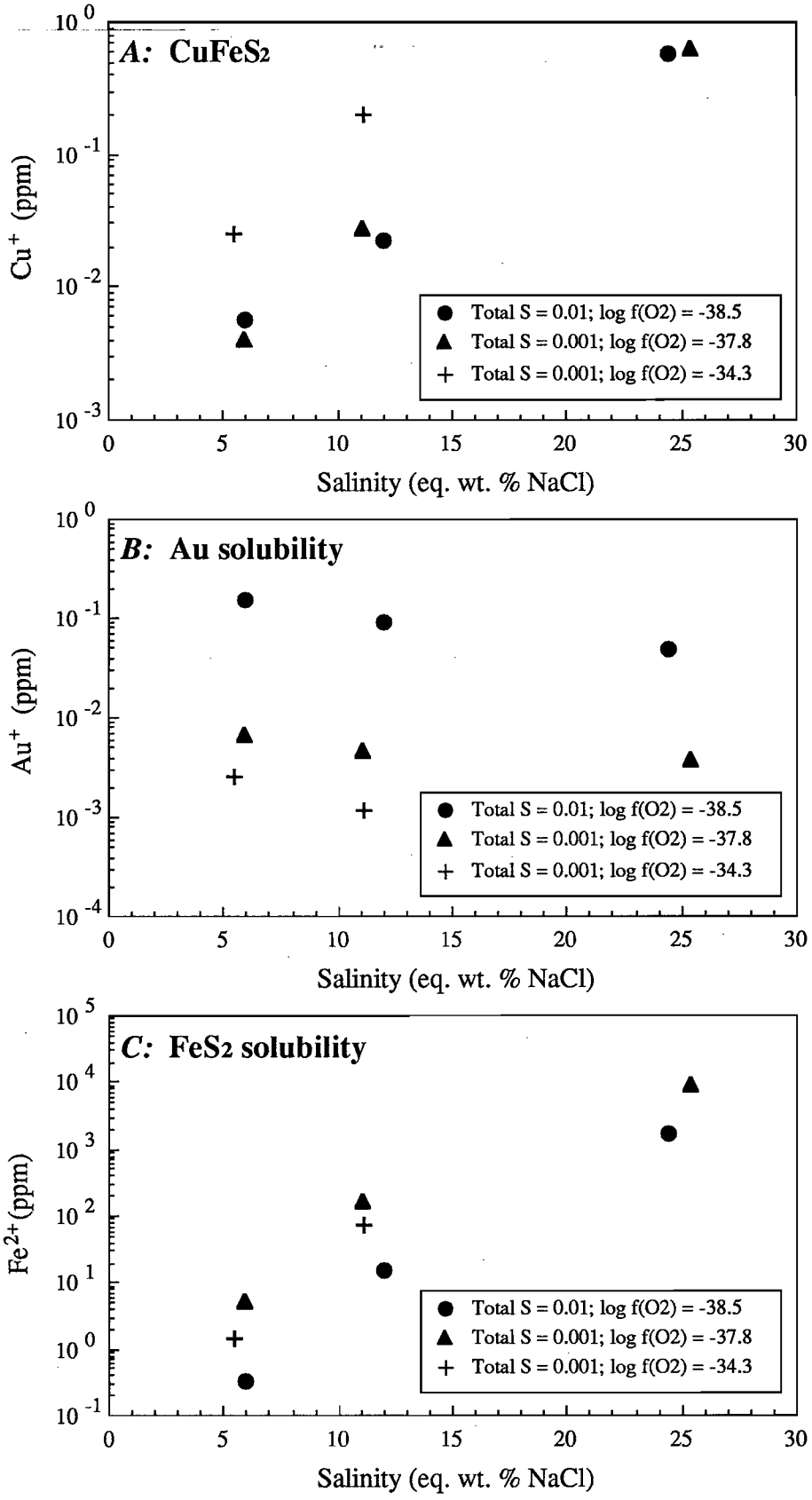

Figure 2 — Sulfide and gold solubilities as a function of salinity in sedimentary brines at 250°C.
A: Chalcopyrite. B: Gold. C: Pyrite. The pH is buffered by K-feldspar-muscovite. For the oxidised brine, oxygen fugacity is buffered by hematite-pyrite equilibria. For the reduced brines, oxygen fugacities are constrained to the pyrite field (just above the upper stability limit for graphite).

be used to test the four hypotheses for sediment-hosted deposit formation outlined in Large (1991), taking selected brines from the speciation calculations, mixing them with various types of seawater, and subjecting them to a variety of water–rock interactions to establish likely mechanisms of ore deposition. Much of this work is still to be done, however, preliminary examples of the types of calculations that can be undertaken (mixing, cooling boiling, etc.) are presented below, using a modified version of brine 4 (table 3).

Brine compositions

Brine 4 was selected as a likely candidate for a reduced fluid that might be responsible for sediment-hosted Zn (± Pb ± Ag) mineralisation. The composition of this brine was modified so that it was only saturated with quartz, pyrite, muscovite and K-feldspar. Other component species that had originally been calculated using forced mineral equilibration techniques were decreased by one order of magnitude to allow the various depositional processes to be tested for their relative efficiency in precipitating base and precious metal mineralisation, and to test whether sedimentary brines can be initially undersaturated by such a large amount and still precipitate economic base metal mineralisation. The modified brine composition is listed in table 3, along with an analysis of modern seawater used in the mixing simulation.

Cooling

The first simulation involves cooling of the mineralised brine from 250°C to 25°C. Throughout this simulation, pressures were kept above liquid–vapour saturation to prevent boiling. Cooling without boiling is a likely scenario for the subsurface feeder zone, provided the overlying basin is deep enough to maintain single fluid phase conditions. Minerals that precipitated during this simulation include quartz, pyrite, sphalerite, galena, acanthite and graphite (figs 3, 4 and 5). Quartz predominates the cooling-only assemblage (fig. 4), precipitating over the entire temperature range of interest at a relatively constant rate (fig. 5). Pyrite is also precipitated over a large temperature interval, although more than 50% (by mass) of all pyrite mineralisation is precipitated in the first 40° of cooling (fig. 5). Graphite precipitation began after the fluid had cooled to 165°C, with over half of all graphite precipitated in the next 15°C of cooling (fig. 5).

Sphalerite, galena and acanthite all show similar behaviour, initially precipitating at temperatures of 165°C (sphalerite) and 145°C (galena and acanthite; figs 3 and 5). After the initial onset of precipitation, more than half of the total mass of both galena and sphalerite were precipitated during the next 25°C of cooling (fig. 5). In contrast, acanthite had a slower initial precipitation rate, requiring 40°C of cooling to precipitate 50% (by mass) of total acanthite (figure 5). Overall, the proportions of sulfides to gangue minerals (fig. 4) suggests that cooling of a undersaturated brine of this nature is highly unlikely to result in the accumulation of an economic Pb–Zn resource.

Boiling

To demonstrate what would happen if confining pressures were not sufficient to prevent subsurface brines from boiling, a single stage isoenthalpic boiling simulation was conducted from 250°C to 100°C. Figures 6 and 7 demonstrate that the resultant mineral assemblage is not consistent with the mineralogy of sediment-hosted base metal deposits (note the presence of hydrothermal magnetite, biotite, calcic amphibole, calcic garnet and gold). Boiling is therefore considered an unlikely process in the subsurface environment of sediment-hosted systems.

The unusual mineralogy precipitated during this simulation is mostly a consequence of the relatively low gas contents of the system (H_2S and CO_2). Higher gas concentrations would result in a more typical 'boiling' assemblage, with abundant calcite, pyrite and/or chlorite, and no hydrothermal garnet, amphibole, magnetite or biotite.

Mixing with modern-day seawater

A large number of fluid mixing scenarios could be envisaged for the sediment-hosted environment. In this simulation, modified brine 4 has been mixed with modern day seawater (table 3) to demonstrate the effects of mixing a reduced brine with oxidised seawater. The minerals precipitated during this simulation are (from most to least abundant) barite, quartz, pyrite, sphalerite, galena, acanthite, muscovite and K-feldspar (figs 8 and 9). Whereas barite was never precipitated during the cooling or boiling simulations, it was found to dominate the mixing assemblage. Furthermore, almost 90% of all barite precipitated during the first 15°C of mixing-induced cooling (fig. 10). Quartz and pyrite are the dominant gangue minerals that occur in association with barite (fig. 9). Whereas quartz is precipitated at a relatively constant rate throughout the mixing simulation, pyrite is precipitated almost entirely during the first increment of mixing (fig. 10).

Sphalerite, galena and acanthite commenced precipitating at higher temperatures compared to the cooling and boiling simulations, suggesting that fluid mixing is more efficient at initiating sulfide deposition. Base metal sulfides are not, however, major components of the mixing assemblage, comprising

	Modified Brine 4	Modern Seawater *
T	250°C	5°C
pH	5.41	8.02
Salinity	5.9 wt %	2.5 wt %
ΣS	0.001	0.029
log $f_{(O_2)}$	-37.8	-2.71
H^+	0.0239	1.04 E-06
H_2O	1 kg	1 kg
Cl^-	1.079	0.442
SO_4^{-2}	-3.41 E-04	0.0292
HCO_3^-	0.0242	0.00241
HS^-	0.001	-
$SiO_{2\ (aq)}$	0.00643	8.63 E-06
Al^{+3}	1.83 E-08	3.42 E-09
Ca^{+2}	0.0480	0.00311
Mg^{+2}	8.85 E-05	5.05 E-04
Fe^{+2}	9.24 E-05	7.79 E-13
K^+	0.0688	0.0106
Na^+	0.912	0.485
Zn^{+2}	1.23 E-06	3.17 E-08
Cu^+	6.58 E-09	8.16 E-09
Pb^{+2}	5.56 E-08	1.50 E-10
Ag^+	9.12 E-08	3.84 E-10
$AuCl_2^-$	2.55 E-09	2.11 E-11
Ba^{+2}	0.00151	1.51 E-08
$O_{2\ (aq)}$	-	3.24 E-06

*Table 3 — Brine and seawater compositions used in the cooling, boiling and mixing simulations. Unless otherwise stated, component species concentrations are in molal units. Modified brine 4 is saturated with respect to quartz, pyrite, muscovite and K-feldspar. It is also undersaturated by one order of magnitude with respect to talc, sphalerite, chalcopyrite, galena and gold (compare with Table 1). The composition of modern-day seawater is taken from Drever (1984). * - Note that the seawater analysis as originally published is supersaturated with respect to muscovite, hematite, calcite and dolomite at 5°C. Consequently, the concentrations of K^+, Fe^{+2}, Ca^{+2} and Mg^{+2} have been reduced to 90% of saturation levels, to ensure no phases are saturated at the start of the mixing simulation.*

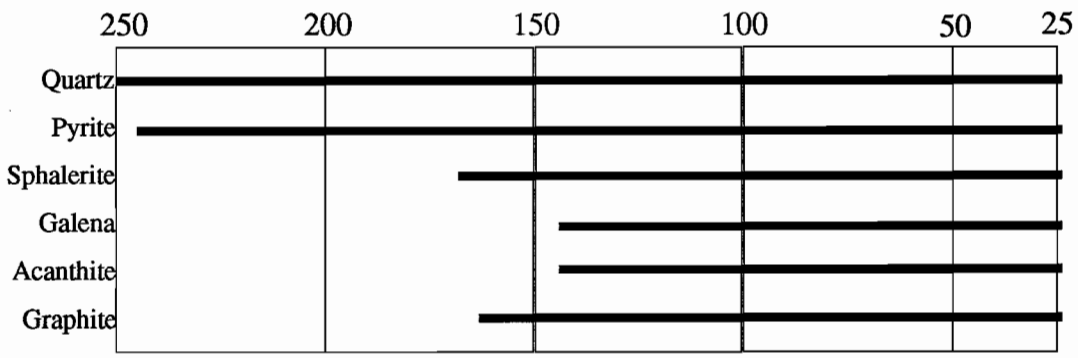

Figure 3 — Temperature ranges of minerals precipitated during the cooling simulation.

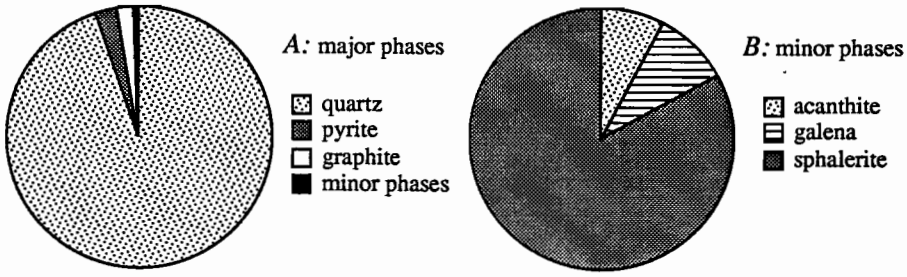

Figure 4 — Relative proportion of minerals precipitated during cooling of modified Brine 4. A: Major mineral phases. B: Minor phases. The proportion of all minor minerals relative to the major phases is illustrated by the thin black wedge on figure A.

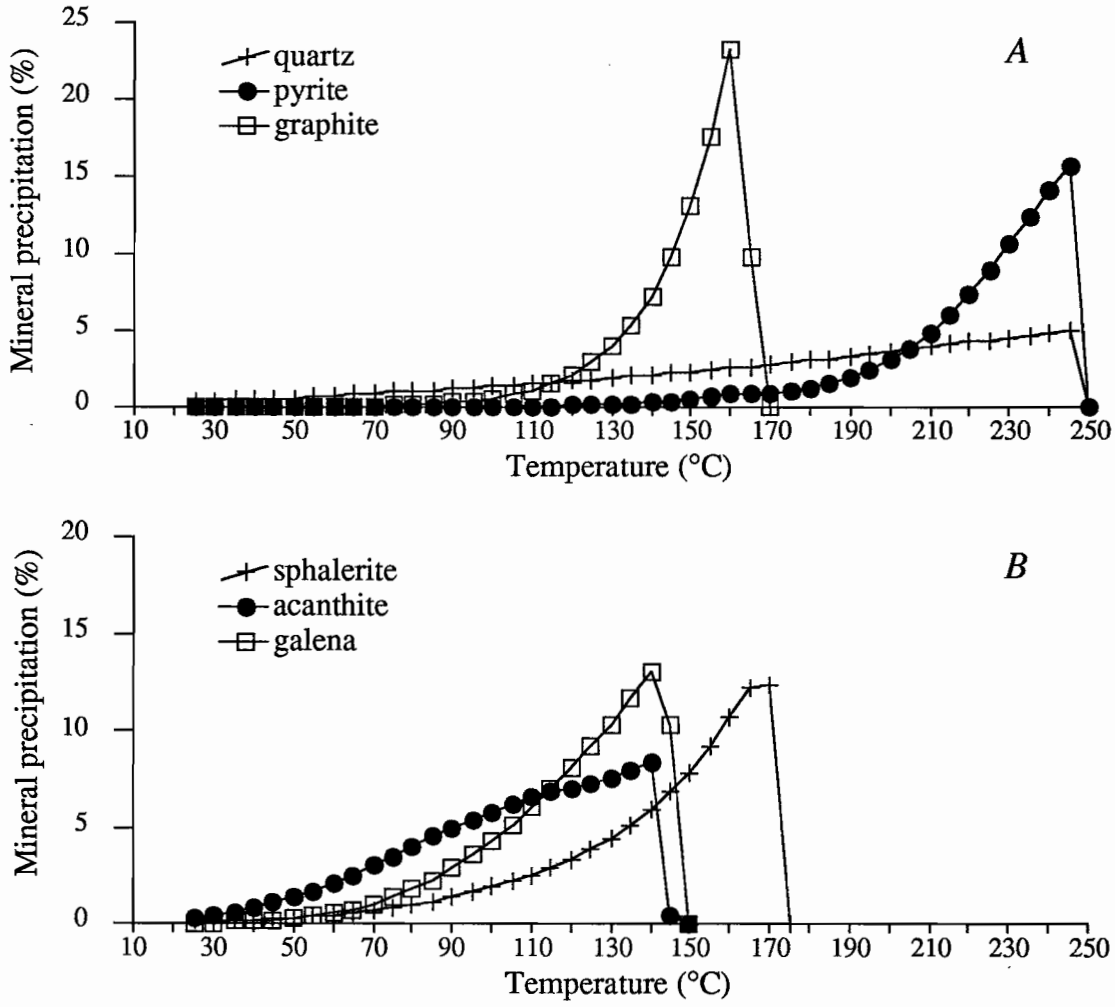

Figure 5 — Proportions of individual minerals precipitated per increment ofcooling relative to the total amount of each mineral deposited during the entire cooling simulation. The fluid was cooled progressively in 5°C increments.

less than 1% in total of all minerals precipitated (fig. 9). Sphalerite dominates the base metal assemblage (as predicted from the metal solubility studies), yet even it is not precipitated in sufficient quantities to form an economic zinc resource (fig. 9). These results suggest that a reduced brine undersaturated by one order of magnitude with respect to sphalerite, galena and acanthite is unlikely to form economic Pb–Zn–Ag mineralisation via fluid mixing with oxidised seawater. Higher concentrations of base metals are required in the fluid to enable significant precipitation of base metal sulfides. These ideas will be tested by further modelling using brines saturated with Pb, Zn and Ag.

Conclusions

Undersaturated, relatively low salinity reduced brines similar to modified brine 4 are unlikely to form economic Pb–Zn–Ag mineralisation via cooling, boiling or mixing with oxidised seawater. However, such brines may be capable of forming Pb, Zn-barren barite deposits similar to those in Arkansas and Nevada (Maynard, 1991) via mixing with oxidised sulfate-rich seawater.

During the mixing simulation, most mineral precipitation took place in the first four increments of mixing (approximately the first 20°C of mixing-induced cooling). Future mixing simulations will be conducted with smaller initial mixing increments, to allow the finer details of mineral precipitation within this interval to be investigated. Higher proportions of dissolved metals will be used in future simulations (saturated brines and 90% saturated), to establish whether base metal sulfides are precipitated in more appropriate proportions to gangue minerals. Future models will concentrate on fluid mixing processes (with oxidised and reduced seawater) and fluid–rock interactions (with carbonaceous, pyritic and hematitic shales, and pure and silty dolomites).

REFERENCES

Drever, J.I., 1984. *THE GEOCHEMISTRY OF NATURAL WATERS.* Prentice-Hall, N.J.: 234.

Gammons, C.H., and Barnes, H.L., 1989. The solubility of Ag_2S in near-neutral aqueous sulfide solutions at 25 to 300°C. *Geochim. Cosmochim. Acta* 53: 279–290.

Huston, D.L. and Large, R.R., 1987. Genetic and exploration significance of the zinc ratio (100 Zn/(Zn + Pb)) in massive sulfide systems. *Econ. Geol.* 82: 1521–1539.

Large, R.R., 1991. Geological and geochemical controls on Proterozoic sediment-hosted base metal deposits. AMIRA research proposal (unpublished): 16 pp.

Maynard, J.B., 1991. Shale-hosted deposits of Pb, Zn and Ba: syngenetic deposition from exhaled brines in deep marine basins. *In*: E.R. Force, J.J. Eidel and J.B. Maynard (Eds.) Sedimentary and diagenetic mineral deposits: a basin analysis approach to exploration. *Rev. Econ. Geol.* 5: 177–185.

McKibben, M.A., and Williams, A.E., 1989. Metal speciation and solubility in saline hydrothermal fluids: an empirical approach based on geothermal brine data. *Econ. Geol.* 84: 1996–2007.

Reed, M.H., 1982. Calculation of multicomponent chemical equilibria and reaction processes in systems involving minerals, gases and an aqueous phase. *Geochim. Cosmochim. Acta* 46: 513–528.

Reed, M.H. and Spycher, N.F., 1984. Calculation of pH and mineral equilibria in hydrothermal waters with application to geothermometry and studies of boiling and dilution. *Geochim. Cosmochim. Acta* 48: 1479–1492.

Reed, M.H. and Spycher, N.F., 1985. Boiling, cooling and oxidation in epithermal systems: a numerical approach. *In*: B.R. Berger and P.M. Bethke (Eds.) Geology and geochemistry of epithermal systems. *Rev. Econ. Geol.* 2: 249–272.

Ruaya and Seward, T.M., 1986. The stability of chlorozinc(II) complexes in hydrothermal solutions up to 350°C. *Geochim. Cosmochim. Acta* 50: 651–661.

Seward, T.M., 1984. The formation of lead(II) chloride complexes to 300°C: A spectrophotometric study. *Geochim. Cosmochim. Acta* 48: 121–134.

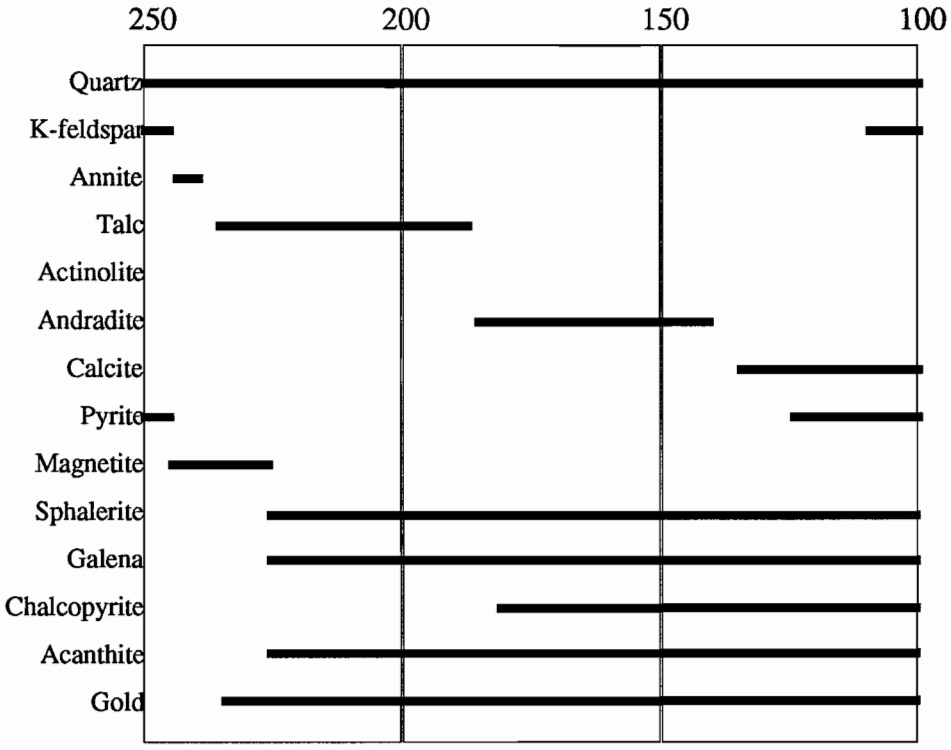

Figure 6 — Temperature ranges of minerals precipitated during the boiling simulation.

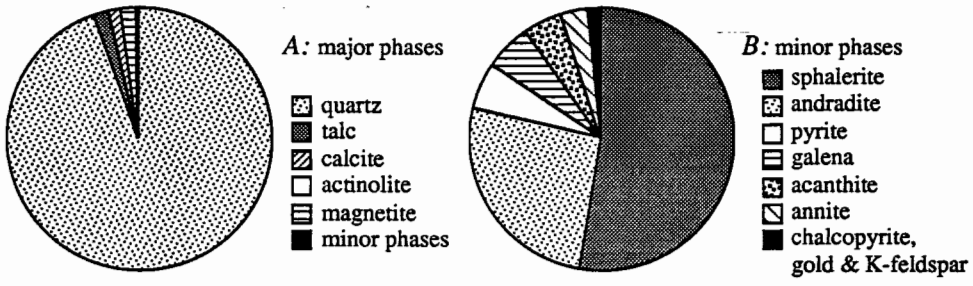

Figure 7 — Relative proportion of minerals precipitated during isoenthalpic boiling of modified Brine 4. A: Major mineral phases. B: Minor phases. The relative proportion of minor minerals compared to the major phases is illustrated by the thin black wedge in A. The fields for chalcopyrite, K-feldspar and gold are too small to distinguish individually. Their combined total is shown on B.

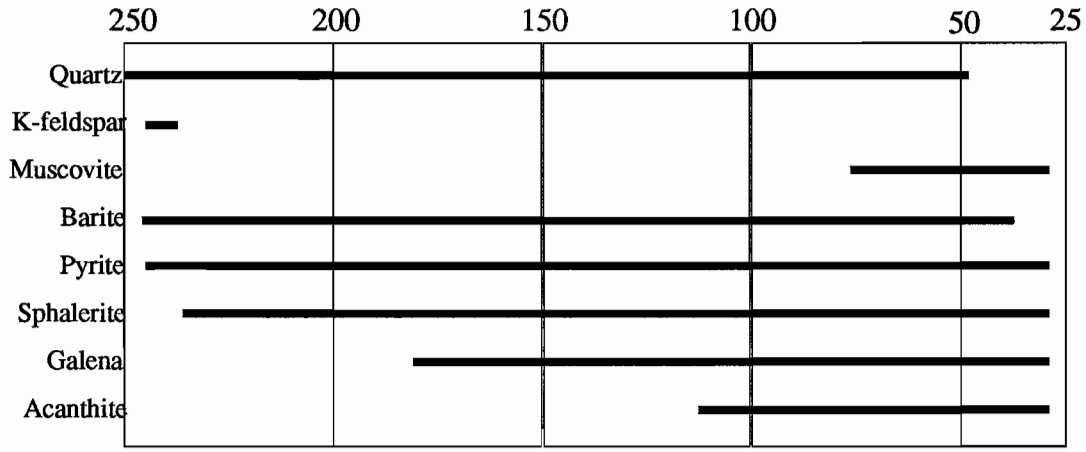

Figure 8 — Temperature ranges of minerals precipitated during mixing with oxidised seawater. Temperatures decreased from 250° to 29°C during this simulation.

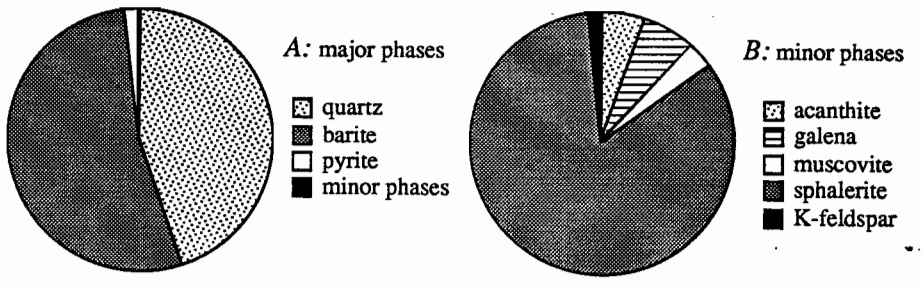

Figure 9 — Relative proportion of minerals precipitated during mixing of modified Brine 4 with seawater. A: Major mineral phases. B: Minor phases. The proportion of all minor minerals relative to the major phases is illustrated by the thin black wedge in A.

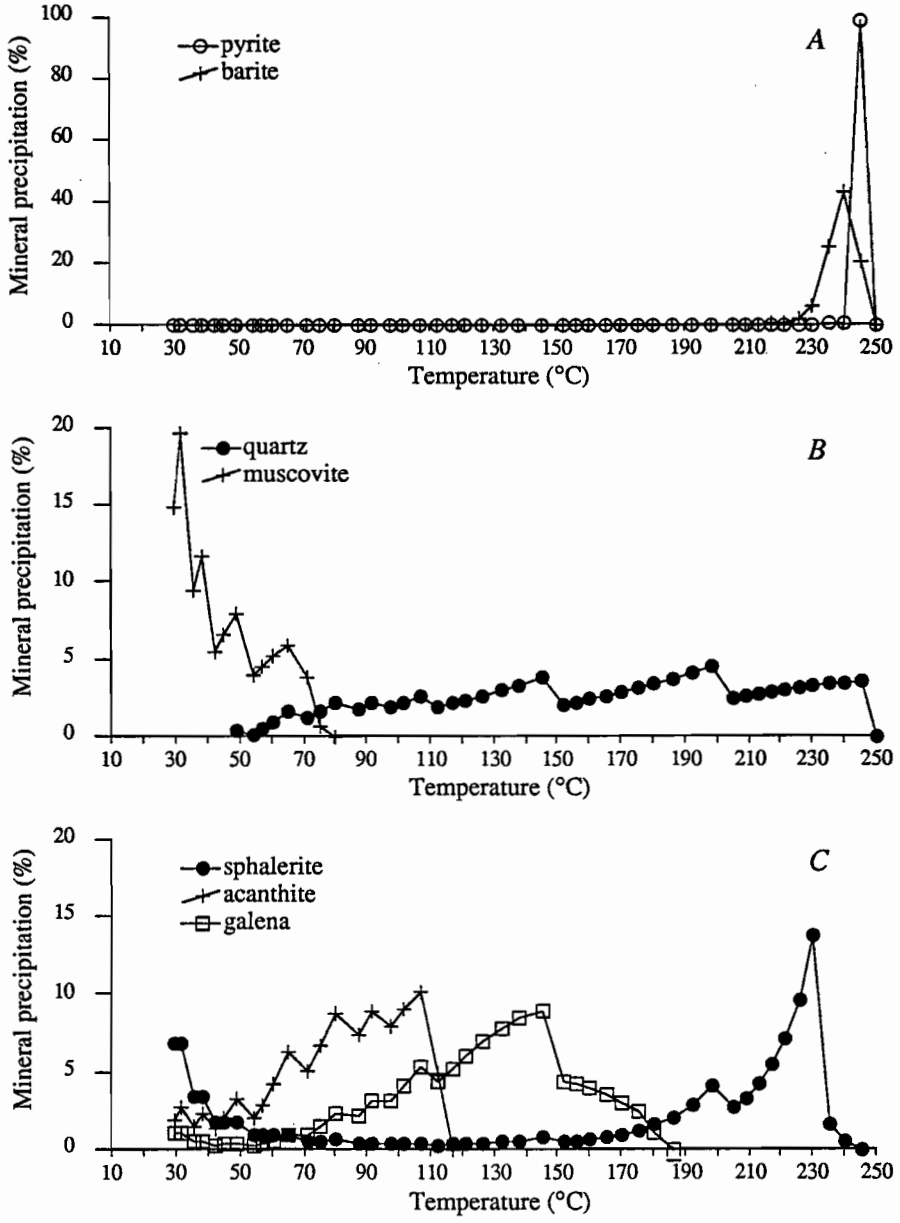

Figure 10 — Proportions of individual minerals precipitated per increment of mixing relative to the total amount of each mineral deposited during the entire mixing simulation. The magnitude of the mixing increments were increased at several temperatures during this simulation (e.g. 205°, 145°, 115°C), resulting in staggered profiles for the minerals shown in B and C.

A possible example of thermochemical sulfate reduction in a stratabound shale-hosted lead–zinc deposit: Dugald River, Australia

Grant Dixon and Garry J. Davidson
54 Marlyn Rd, South Hobart, Tasmania and Centre for Ore Deposit and Exploration Studies

Abstract of a manuscript submitted to Chemical Geology, September 1992

This study examines the along-strike and down-dip sulfur isotopic variation of the mid-Proterozoic Dugald River stratabound shale-hosted lead–zinc ore deposit, Australia. Although the metal grade of the Dugald River deposit has been substantially upgraded at its southern end by tectonism, petrographic textures and the large-scale distribution of metals indicate that mineralisation was emplaced during early diagenesis, probably in an organic carbon-rich, shallow, evaporitic, intracontinental setting. Cu, Cu/(Pb+Zn), Pb/(Pb+Zn), Ag, and Mn decrease in the mineralisation northwards independent of the main structural thickening, and so are likely to represent a type of primary geochemical dispersion that is also typical shale-hosted lead–zinc deposits globally.

d^{34}S in lode pyrite and sphalerite is zoned from averages of ~–1‰ in the south, coincident with highest copper content of the ores, to ~+8‰ in the north, accompanying lode thinning. In contrast, adjacent footwall and hangingwall biogenic pyrite does not exhibit isotopic zonation, and has a distinct mode at $\delta^{34}S$ = +3.5‰, average = 0.8‰ (n = 26), with some values as light as –14.5 ‰; limestones and dolomites throughout the sequence contain isotopically heavy disseminated pyrite, $\delta^{34}S$ = +5.5 to +17.5‰. Both host-rock populations are attributed to varying degrees of closed-system, biogenic, sulfate reduction. Carbon-isotopes ($\delta^{13}C$ = –15 to –25‰) indicate that carbonate in and adjacent to the ore formed by the oxidation of organic carbon.

Thermochemical fluid sulfate reduction by organic matter is preferred to explain the $\delta^{34}S$ zonation for three reasons: (1) mass-balance calculations (2) the $\delta^{13}C$ isotopic shift of ore and near-ore carbonate, and (3) the temperatures necessary for ore formation (150°C–250° C), which would have prevented biogenic but promoted abiogenic sulfur reduction. The proposed mineralisation model involves two sulfur sources. Sub-surface H_2S- and metal-bearing fluids with $\delta^{34}S$ ~–3 to 0‰ ascended into the Dugald basin in the south, and permeated laterally northward through carbonaceous sediments, reacting with organic matter and sulfate to form heavy sulfide by thermochemical reduction. Reaction was catalysed by the deep sourced H_2S, and H_2S from other sources such as biogenically-reduced pore-water sulfate and thermally-cracked organic matter. The sources of sulfate for the reaction were two-fold: (1) evaporites locally within the sequence; (2) sulfate diffusing from surface-waters into the diagenetic zone. The model has implications for fluid circulation during the diagenetic formation of shale-hosted ores. Mass balance relations allow (but do not require) heavy sulfur to be obtained from virtually the same area as the Dugald River deposit, hence there is only a minimal requirement of lateral advection of H_2S to the ore-site, and greater emphasis on downward supply of sulfate by diffusion from surface waters.

CODES: AMIRA/ARC Project P.384 — Proterozoic sediment-hosted base metal deposits. November 1992

The Kamarga Deposit: stratabound zinc–lead mineralization in the Middle Proterozoic McNamara Group, northwest Queensland

Douglas Jones
Pancontinental

Abstract from PhD thesis, University of New England, 1986

The Kamarga prospect is a Middle Proterozoic, stratabound, dolomite hosted zinc-lead deposit located 200 km north of Mount Isa, in northwest Queensland, Australia.

The mineralisation, which is currently sub-economic, displays many similarities to the discordant Ridge and Cooley deposits at McArthur River, Northern Territory, and the Carboniferous zinc-lead deposits of Ireland (Tynagh, Silvemines, Navan). The deposit occurs on the Lawn Hill Platform, a relatively stable cratonic platform to the west of a major rift structure, the Leichhardt River Fault Trough, which contains the Mount Isa, Hilton and Lady Loretta sediment hosted stratiform lead-zinc-silver deposits. The Kamarga mineralisation lies adjacent to, and to the east of, the Bream Fault, a spur of a major north-easterly trending basement lineament, the Baramundi Fault, on the southern flank of a large domal structure, the Kamarga Dome.

The Kamarga deposit is contained within the Gunpowder Creek Formation of the lower McNamara Group, which comprises a major part of the sedimentary cover of the Lawn Hill Platform. The lower McNamara Group on the Kamarga Dome consists of a basal terrestrial conglomerate and arenite sequence, the Torpedo Creek Quartzite, which is overlain by a shallow marine to paralic sequence of terrigenous and dolomitic lithologies, the Gunpowder Creek Formation. Two major transgressive-regressive cycles have been identified in the Torpedo Creek Quartzite–Gunpowder Creek Formation sequence, with the younger regression extending into the overlying dolomitic Paradise Creek Formation. Stratabound zinc–lead mineralisation is mainly restricted to dolomitic lithologies of the Gunpowder Creek Formation, which are characterised by dolomitised nodular and mush-textured evaporates, and intraclastic, algal-laminated, stromatolitic and oolitic dolomites indicative of shallow-subtidal to supratidal sabkha depositional environments.

The mineralisation occurs as coarsely crystalline, crustiform and colloform pyrite, sphalerite, galena and chalcopyrite deposited under open-space filling conditions in veins and breccias, and as disseminated to semi-massive and massive replacements of the host dolomites. The sulphides are associated with ferroan dolospar, quartz and minor fluorite, bitumen and baryte. The sulphide and gangue minerals were deposited sequentially in both space and time. In time, the paragenetic sequence of mineral deposition was from early to late, pyrite → pyrite + sphalerite + galena + chalcopyrite → sphalerite + pyrite + galena + baryte ± fluorite. This is reflected in a geochemical zoning pattern of Fe (Cu) → Fe Zn Pb(Cu) → Zn Fe Pb Ba. Sphalerite compositions also vary systematically, with Fe levels decreasing and Cd levels increasing, with increasing distance from the fault.

The discordant, cross-cutting character of the mineralisation strongly suggests that it formed epigenetically from fluids emanating from the Bream Fault, which flowed into, and reacted with, the adjacent dolomites. Mineralisation is believed to have occurred late in the diagenetic history of the sediments, when lithification was largely complete.

Fluid inclusion and mineral stability data indicate that the mineralisation was deposited from hot (~300°C), moderately saline (~20 wt % NaCl equivalent) moderately acid hydrothermal solutions under low-moderate oxygen and sulphur fugacities. The calculated oxygen and carbon isotope compositions

of the hydrothermal fluids ($\delta^{18}O_{H2O}$ = ~12.5 ‰, $\delta^{13}C_{H2CO3(ap)}$ = ~0.5 ‰) suggest derivation of the fluids from connate brines which have equilibrated with large volumes of marine carbonate at elevated temperatures. This is supported by the sulphur isotope composition of the sulphides ($\delta^{34}S_{\Sigma s}$ = 20 ‰) which suggests derivation of sulphur from evaporatic units within the McNamara Group. The bulk of this sulphur has been introduced in a reduced form with the hydrothermal solutions; however a relatively minor component of highly ^{34}S enriched sulphate sulphur may also have been introduced from the host dolomites during the early stages of mineralisation.

The galena lead isotope data indicate derivation of metals from well mixed crustal sources. The lead isotope composition of the Kamarga galena is indistinguishable from that of the sediment hosted stratiform lead–zinc–silver deposits of the Mount Isa–McArthur River province, suggesting a similar source and mechanism of metal extraction, and a similar age. This, and the presence at Kamarga of sideritic horizons containing anomalous base metal levels at a stratigraphic position broadly equivalent to the stratiform deposits, implies a depth of burial for the Kamarga mineralisation of 1.2 km. The non-radiogenic, homogenous galena lead contrasts with the radiogenic and in homogeneous lead in syndiagenetic pyrite. Epigenetic pyrite associated with the zinc–lead mineralisation falls on a line passing through both the galena leads and syndiagenetic leads, suggesting mixing of lead from these two sources, which is consistent with conclusions drawn from the sulphur isotope data.

The genetic model proposed for the Kamarga mineralisation envisages the incorporation of sulphate-rich, connate brines into a hydrothermal convection cell caused by an elevated geothermal gradient in a tensional tectonic regime. The brines were circulated through the base-metal enriched volcanic and granitic rocks underlying the McNamara Group, where, in high temperature reactions between the fluids and the basement rocks, the sulphate was reduced to H_2S and metals were extracted into solution as chloride-complexes. The fluids were subsequently expelled up the Bream Fault, possibly assisted b y seismic pumping. The most intense mineralisation occurs in the first dolomitic unit to be encountered by the ascending fluids, with neutralisation reactions providing the pH drive to deposit sulphides and dolospar, while declining temperatures during the later stages of mineralisation caused deposition of fluorite and baryte.

Although the Kamarga mineralisation shares many characteristics in common with the Mississippi Valley-type lead–zinc deposits, the higher temperatures of formation, and the lead isotope composition falling on the average lead evolution curve (growth curve), suggests a closer genetic association with the sedimentary exhalative affiliated Irish and McArthur River discordant deposits.

Regionally extensive, low grade, disseminated pyrite–chalcopyrite mineralisation in arenites of the Torpedo Creek Quartzite and lower Gunpowder Creek Formation, is genetically unrelated to the epigenetic zinc–lead mineralisation, and probably represents low temperature diagenetic deposition from pore water brines.

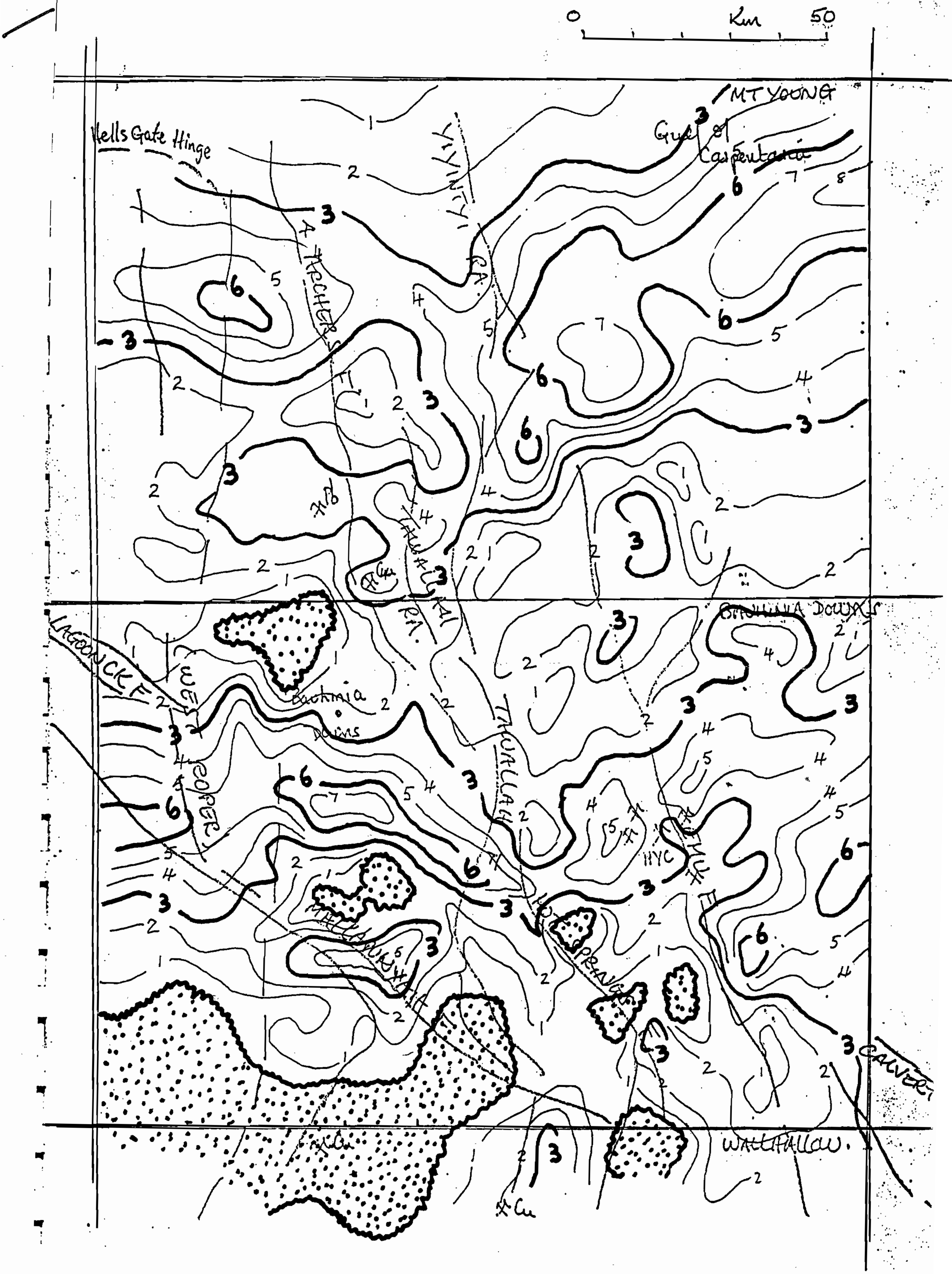

TON TROUGH
Thickness of Calcic Scatter Volcanics ... Contours in Km

Oct 92
PRELIMINARY

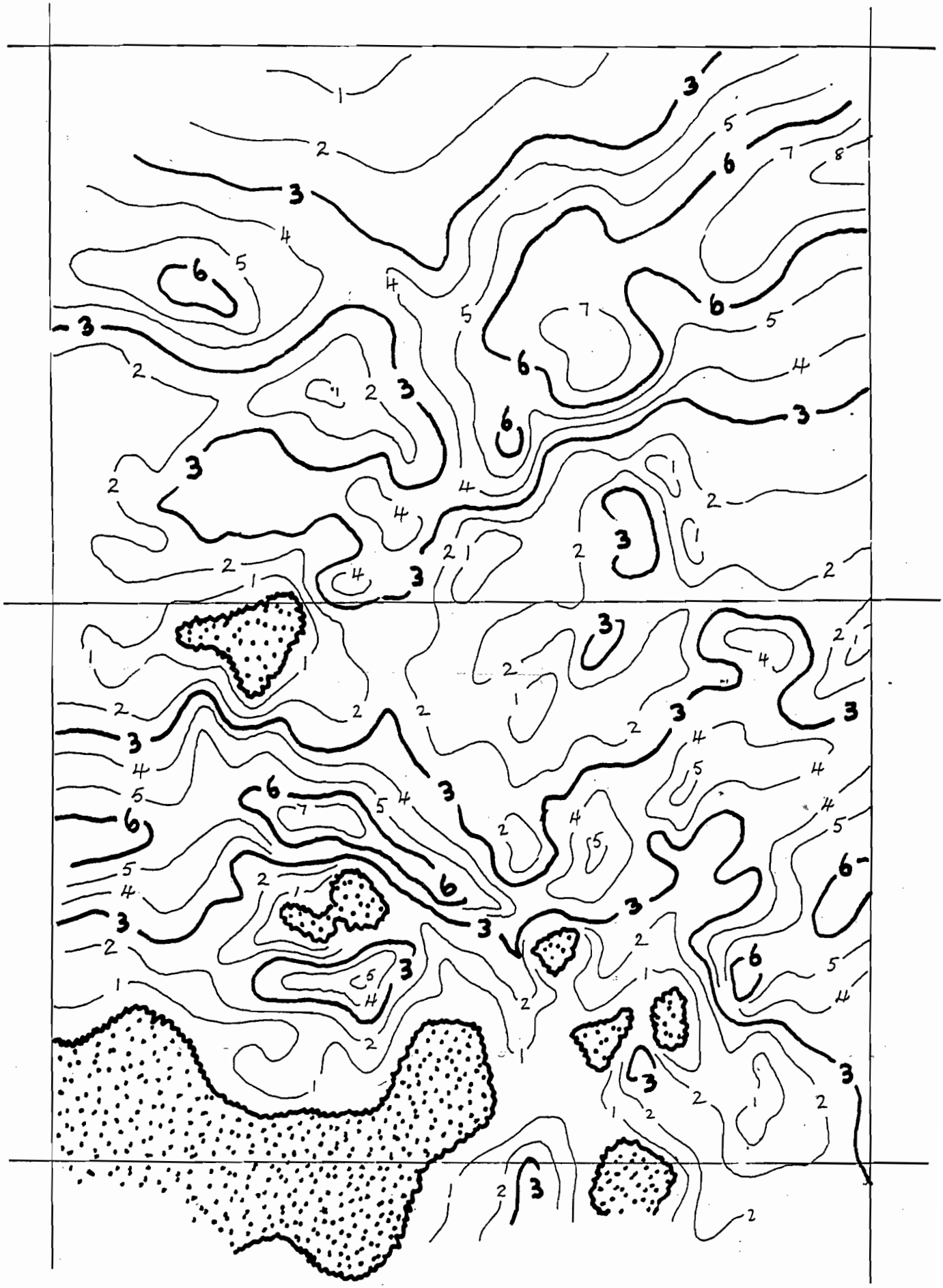

BATTEN TROUGH
Thickness of felsic Scrutton Volcanics . Contours in km.

DEL DEC '92
PRELIMINARY